HEPATIC STELLATE CELLS' INVOLVEMENT IN PROGENITOR CELL MEDIATED LIVER REGENERATION

By

DANA GABRIELA PINTILIE

A DISSERTATION PRESENTED TO THE GRADUATE SCHOOL
OF THE UNIVERSITY OF FLORIDA IN PARTIAL FULFILLMENT
OF THE REQUIREMENTS FOR THE DEGREE OF
DOCTOR OF PHILOSOPHY

UNIVERSITY OF FLORIDA

2009

To my beloved family, the rock that steadies me

ACKNOWLEDGMENTS

I thank my mentor Bryon E. Petersen for the scientific knowledge and ideals of perseverance towards understanding the unknown. I am also grateful to the other members of my committee, Drs. Maria Grant, Steven Ghivizzani, Edward Scott and Naohiro Terada for their continued support and scientific dialogue which helped me evolve into the scientist I am now. I would also like to extend my thanks to Drs. Seh-hoon Oh, Thomas Shupe, Susan Ellor, Houda Darwiche, Anna Piscaglia, Jennifer Williams and Liya Pi for sharing their research experience with me and for the friendship they have shown me throughout my time at the University of Florida.

I cannot explain the importance of my family which never told me I could not achieve any goal toward which I set my mind. Their love and unconditional support kept me going through thick and thin. I can never tell them enough how much they mean to me.

TABLE OF CONTENTS

page

LIST OF TABLES

LIST OF FIGURES

LIST OF ABBREVIATIONS

AA	Allyl alcohol
AAALAC	American Association for the Accreditation of Laboratory Animal Care
2-AAF	2-acetoaminofluorene
AFP	α-fetoprotein
Akt	Protein kinases B family
ALB	Albumin
AP-1	Activator protein 1
APS	Ammonium persulfate
bp	Base pair
BD	bile duct branch
BD1	Bile duct marker 1
BDS7	Bile duct specific marker 7
BrdU	Bromodeoxyuridine
C	Cytoplasm
CCC	Cholangiocellular carcinoma
CCl_4	Carbon tetrachloride
CDE	choline deficient ethionine
cDNA	Complementary deoxyribonucleic acid
Cdk2	Cyclin dependent kinase 2
Cdk4	Cyclin dependent kinase 4
CK	Cytokeratin
CK-19	Cytokeratin 19
CTGF	Connective Tissue Growth Factor

DAB	Diaminobenzidine
DAPI	4',6-diamidino-2-phenylindole
DAPM	Methylene dianaline
DEPC	Diethyl pirocarbonate
DHHS	Department of Health and Human Services
DMN	Dimethylnitrosamine
DNA	Deoxyribonucleic acid
DNase I	Deoxyribonuclease I
dNTP	Deoxynucleotide triphosphate
DTT	Dithiothreitol
ECM	Extracellular matrix
EDTA	Ethylenediaminetetraacetic acid
EC	Endothelial cell
EGF	Epidermal growth factor
Egr1	Early growth response protein 1
ERK	Extracellular-signal regulated kinase
ES	Embryonic stem cells
ET-1	Endothelin 1
FAK	Focal adhesion kinase
FBS	Fetal bovine serum
FDA	Food and Drug Administration
FGF	Fibroblast growth factor
FITC	Fluorescein isothiocyanate

G_0	Quiescent phase of cell cycle
G_1	Growth 1 phase of cell cycle
G_1/S	cell cycle checkpoint between growth 1 and synthesis phases
GAPDH	Glyceraldehyde-3-phosphate dehydrogenase
GFAP	Glial fibrillary acidic protein
GH-RH	Growth hormone releasing hormone
GGT	Gamma glutamyl transpeptidase
H	Hepatocyte
HA	Hepatic artery branch
HCC	Hepatocellular carcinoma
H&E	Hematoxylin and eosin staining
HES6	Hairy and enhancer of split 6
HGF	Hepatocyte Growth Factor
Hr	Hour
HSC	Hematopoietic stem cells
IACUC	Institutional Animal Care and Use Committee
IF	Immunofluorescence
IGF-2	Insulin-like growth factor 2
IHC	Immunohistochemistry
IL-1	Interleukin 1
i.p.	Intraperitoneal
JNK	c-Jun N-terminal kinase
M	Membrane
MAPK	Mitogen-activated protein kinase

MCP-1	Monocyte chemotactic protein 1
Me-DAB	3'-methyl-4-dimethylaminoazobenzene
min	Minute
MMP	Matrix metalloproteinase
MnSOD	Manganese superoxide dismutase
MODS	Multiple organ dysfunction syndrome
mTOR	Mammalian target of rapamycin
n	Number of animals included in an eperiment
N	Nucleus
NFkB	Nuclear factor kappa-light-chain-enhancer of activated B cells
NIH	National Institute of Health
NK	Natural killer cells
N-OH 2AAF	N- hydroxyl 2 acetylaminofluorene
NPC	Non-parenchymal cells
NRL	Normal rat liver
Nt	Nucleotide
OC	Oval cell
OCT	Optimal cutting temperature
OD	Optical density
oligodTs	oligodeoxythymidylic acid
OLT	Orthotopic liver transplant
O/N	Overnight
p	p value

PAS	Periodic acid Schiff staining
PBS	Phosphate buffered saline
PCR	Polymerase chain reaction
PDGF	Platelet derived growth factor
PDGFR-b	Platelet derived growth factor receptor beta
PHx	Partial hepatectomy
PHS	Public HealthServices
PI3-K	Phosphatidylinositol 3 – kinase
PT	Portal triad
PV	portal vein branch
Ras	Small GTPase involved in signal transduction
Rb	Retinoblastoma protein
RBC	Red blood cell
RNA	Ribonucleic acid
mRNA	Messenger RNA
ROS	Reactive oxygen species
RPM	Revolutions per minute
RT	Room temperature
rt PCR	Reverse transcription polymerase chain reaction
RT PCR	Real time quatitative polymerase chain reaction
RT-PCR	Real Time PCR
SC	Stellate cell
SCF	Stem cell factor
SDF1	Stromal derived factor 1

sec	Second
SHC	Small hepatocyte-like cell
α-SMA	Alpha- smooth muscle actin
Sp-1	Transcription factor
SREBP-1c	Sterol regulatory element-binding protein-1c
STAT3	Signal transducer and activator of transcription 3
TBE	Tris-Borate-Edta Buffer
TBS	Tris-buffered saline
TBST	Tris buffered saline with 0.1% Tween
TEMED	Tetramethylethylenediamine
TGF-α	Transforming Growth Factor α
TGF-β	Transforming Growth Factor β
TIMP	Tissue-specific inhibitor of matrix metalloproteinases
TNF	Tumor necrosis factor
v/v	Volume per volume
w/v	Weight per volume

Abstract of Dissertation Presented to the Graduate School
of the University of Florida in Partial Fulfillment of the
Requirements for the Degree of Doctor of Philosophy

HEPATIC STELLATE CELLS' INVOLVEMENT IN PROGENITOR MEDIATED LIVER REGENERATION

By

Dana Gabriela Pintilie

December 2009

Chair: Bryon E. Peteresen
Major: Medical Sciences

The close association between hepatic stellate cells and oval cells has been observed during 2-acetylaminofluorene/70% partial hepatectomy (2AAF/PHx) induced, progenitor mediated liver regeneration. Various interactions between these two cell populations have been proposed, including pro regeneration cytokine secretion and synthesis of a proliferation and differentiation conducive ECM (extracellular matrix).

Previous studies conducted by our laboratory have demonstrated that suppression of TGFβ (transforming growth factor-beta) mediated up-regulation of connective tissue growth factor (CTGF) by prostacyclin analogue iloprost resulted in a greatly diminished oval cell response to 2AAF/PHx in rats. We hypothesized that this effect is due to decreased activation of hepatic stellate cells. In order to test this hypothesis, we maintained rats on a diet supplemented with 2% L-cysteine as a means of inhibiting stellate cell activation during the oval cell response to 2AAF/PHx. *In vitro* Bromodeoxyuridine (BrdU) incorporation assay, reverse transcriptase polymerase chain reaction (rt-PCR), real time polymerase chain reaction (RT-PCR), Immunofluorescent staining (IF), immunohistochemistry (IHC) and quantitative computer image analysis

were utilized to analyze the involvement of hepatic stellate cells in liver injury and oval cell activation.

In vitro experiments demonstrated that L-cysteine did, indeed, prevent the activation of stellate cells while exerting no direct effect on oval cells. Desmin immunostaining of liver sections from 2AAF/PHx animals indicated that maintenance on the L-cysteine diet resulted in an 11.1-fold decrease in the number of activated stellate cells within the portal zones. The total number of cells proliferating in the portal zones of livers from animals treated with L-cysteine was drastically reduced. Further analyses demonstrated a four-fold decrease in the magnitude of the oval cell response in animals maintained on the L-cysteine diet as determined by immunostaining for both OV6 and AFP (alpha-fetoprotein). Global liver expression of AFP as measured by RT PCR was shown to be decreased 4.7-fold in the L-cysteine treated animals. These data indicate that the activation of hepatic stellate cells is required for an appropriate oval cell response to 2AAF/PHx.

CHAPTER 1
INTRODUCTION

1.1 Uncovering the Interactions between the Hepatic Stellate Cells and Oval Cells in Regenerating Liver

The first scientific data which started to shed light on the regenerating potential of stem cells emerged in the second half of 20th century. Once the scientific world learned about the mechanisms of graft rejection, it became clear that stem cells have a real therapeutic potential. Further characterization led to discovery of the existing differences between the embryonic and adult stem cells and to the development of the first successful stem cell therapy. The clinical results quickly exceeded the initial expectations and encouraged the attempts to characterize, cells with “stem potential” isolated from various organs. The emerging gene therapy studies made stem cells the ideal candidates for correcting inborn errors of metabolism, whilst regenerating the diseased organ. The progresses registered in the stem cell research are encouraging signals for scientist who believe that in the near future novel stem cell therapies would be available for clinical trial. Due to their tremendous therapeutic potential, the discovery of stem cells has proven to be one of the most important scientific advances of the last century.

Once the organ specific stem cells were identified and characterized from a morphological standpoint, the key to their therapeutical use became the understanding of the complex molecular processes governing their functions, differentiation and interactions with a particular site of origin. It quickly became evident that a thorough characterization requires a lot of time and effort, due to the tremendous heterogeneity of stem cell population and organ specific microenvironments. Several stem cell phenotypic markers have been proposed, but their use for cell labeling and lineage

tracing has its limitations. The alternative introduction of extraneous markers through genetic manipulation could potentially interfere with the cell's naturat fate. The isolation of stem cells takes them out of their natural environment and the chemical compunds able to manipulate their fate *in vitro* introduce variations in the cellular processes.

Although imperfect, the current techniques have uncovered a considerable body of evidence which can provide a better understanding of "stemness", differentiation, morphology, physiology and stem cell interactions with their environment. Currently scientists are striving to characterize the organ specific stem cells in relation with each step of their differentiation. In addition, effort is put in discovering the mechanisms responsible for maintaining the stemness versus promoting the differentiation toward a specific fate. A detailed characterization of the the patways and their specific molecular signals is a mandatory step for developing stem cell therapies.

Since its introduction in 1963, liver transplantation has become a widely accepted therapy, able to increase the life expectancy of patients suffering of terminal hepatic failure. Unfortunately, the donor shortage has limited its patient accessibility. The discovery of liver specific oval stem cell gave hope to terminally ill patients in dire need of a new liver. The perspective of an alternative stem cell therapy able to regenerate failing liver and correct the inborn metabolic diseases has accelerated the efforts toward understanding the hepatic stem cell. At this stage, the immediate goal is to expand the molecular characterization of various subpopulations in terms of stemness, differentiation fate, and *in vitro* manipulation toward a specific phenotype. Uncovering the mechanisms governing these processes would open the door to successfully develop an alternative stem cell therapy.

This project was designed to further understand the cell-cell interactions that govern oval cell proliferation, migration and differentiation toward a hepatic lineage. Previous work has demonstrated the close physical proximity between the oval and stellate cells during liver regeneration. Stellate cells are known to be activated early after injury and subsequent changes in ECM (extracellular matrix) and cytokine levels have been observed.

Through IHC, protein, and RNA analysis a correlation between the stellate cell activation and the specific profile of oval cell based liver regeneration was established. Chemical inhibition of stellate cell activation both *in vitro* and *in vivo* resulted in an abnormal profile of the regenerative process, delayed and blunted, involving phenotypic changes of regenerating cells.

This project outlined the requirement of certain intercellular interactions for achieving the effective amplitude of oval cell response. Without a robust contribution from stellate cells, oval cells' proliferation was reduced and delayed, failing to migrate towards the centrolobular area, differentiating instead into small hepatocyte-like cells. This study only opens the door to a better understanding of the intercellular interactions required by oval cell mediated liver regeneration. In addition, further studies would characterize the molecular and biochemical profile of the microenvironment created by the stellate – oval cell interactions.

CHAPTER 2
BACKGROUND AND SIGNIFICANCE

2.1 The Liver

2.1.1 Liver Anatomy

2.1.1.1 Structure of the hepatic organ

Human liver is the largest parenchymal organ in adults, functions as an annex gland for the digestive tract and is the site of a vast number of metabolic processes. Weighing between 1400 and 1600g, it represents approximatively 2% of the total body weight. Rat liver, although very similar functionally, weighs 7 to 8g which accounts for a greater percent of the body weight[1] (approximately 5%)

The complex hepatic functions are possible, in part, due to the particular dual blood supply of the liver. Almost 75% of the afferent circulation is supplied by the portal vein, carrying venous, poorly oxygenated blood loaded with nutrients absorbed in the gastro-intestinal tract[3]. The remaning 25% of the afferent blood supply is provided by the hepatic artery which brings oxygenated blood, with poor nutrient content, from the celiac trunk. Once reaching *porta hepatis*, these two main vessels subsequently divide into minor branches which ultimately reach the portal spaces. Both the portal and arterial blood enter the fenestrated sinusoids of the liver lobules, where an active exchange of metabolites takes place, mediated by the space of Disse (Figure 2-1). Sinusoidal blood converges toward the central venule of the liver lobule, to be further drained into the supralobular veins. It finally reaches the inferior vena cava, via the collecting and hepatic veins. Parallel to the blood vessels but opposing direction of flow, the biliary tree consists of excretory ducts that transport bile into the duodenum. The portal vein, hepatic artery and biliary tree form a central vascular bundle termed the

portal triad. The particular branching of hepatic vessels and biliary tree underlines the hepatic functional and surgical architecture. Human liver is formed by a right lobe (segments IVa, IVb, V, VI, VII and VIII), a left lobe (segments II and III), a quadrate lobe (segment IV), a caudate lobe (segment I), a caudate and a papillary process[4]. The rat liver is composed of five lobes (right lateral, left lateral, caudate and right medial incompletely separated from left medial) and a caudate process. Compared anatomy homologates left lateral lobe to human segments II, III, the right lateral lobe to segments VI, VII, the left medial to segments IV a, b the right medial lobe to segments V, VIII, whilst the caudate lobe together with the caudate process correspond to segment I[5].

2.1.1.2 Microarchitecture of the liver

There are three conceptual interpretations of the functional hepatic architecture (Figure 2-2): the classic hepatic lobule, based on endocrine function and structural parameters; the portal lobule, based on the exocrine function (bile drainage pathway from adjacent lobules toward the same bile duct); and the liver acinus concept, based on the gradient distribution of oxygen along the venous sinusoids in adjacent lobules[2]. The classic hepatic lobule is a hexagonal structure formed by cords of hepatocytes radiating from a central venule (which drains the sinusoids) toward the portal triad. At the angles of the hexagon are situated the portal triads: a bile duct together with terminal branches of portal vein and hepatic artery. A single portal triad forms the central axis of the portal lobule and drains bile from the surrounding hepatic parenchyma. The liver acinus concept is the most useful for understanding the liver regeneration patterns. It is defined as the parenchyma between two adjacent central veins, supplied by a terminal branch of hepatic artery. The flow of arterial and venous blood within the hepatic sinusoids creates gradients of oxygen and nutrients which

differentiate the three acinar zones of perfusion. Zone I, adjacent to the portal triad, is the richest in oxygen and nonmetabolized nutrients. Periportal hepatocytes specialize in glycogenolysis and gluconeogenesis and remove ammonia by producing urea. Zone III, closest to the central vein, is oxygen-poor, but rich in metabolism products. Centrolobular hepatocytes are active in glycolysis and glycogen synthesis and remove ammonia through glutamine synthesis. Zone II is intermediate in oxygen and nutrients. Within the liver acinus, blood flows through sinusoids from Zone I to Zone III, and the bile moves from Zone III to Zone I. Interestingly, hepatocytes within Zone III have an increased DNA (deoxyribonucleic acid) content (4N to 16N), predominant bi-nucleation, large size and can undergo centrilobular necrosis. Conversely, hepatocytes within Zone I are smaller and usually single nucleated (2N)[6]. Opposite to the blood, bile flows from the hepatocytes to the bile duct in the portal space. The smallest bile ducts lined by epithelium, named the canals of Hering, are situated at the periphery of the hepatic lobule.

There are about 800 million cells in the liver. Hepatocytes, which represent 70-90% of liver mass, are the functional exocrine and endocrine cells of the hepatic lobule. They have a life span of 180 - 400 days[7] and most of them are able to sustain about 69 - 86 doublings[8, 9]. Hepatocyte division results in compensatory hyperplasia, which restores the liver mass after injury. They form one cell thick anastomozing plates flanked by two sinusoidal spaces. The hepatocytes cord adjacent to the portal space forms the outer limit of the hepatic lobule and is therefore named the limiting plate. Gap and tight junctions on lateral surfaces of adjacent hepatocyte membranes enable the

intercellular functional coupling in the plates and separate the basolateral from the apical membrane domain.

The basolateral domain has abundant microvilli which protrude in the space of Disse and are actively involved in the exchange between hepatocytes and blood. The excess fluid in space of Disse is collected by the space of Mall, which is drained by lymph vessels piercing the limiting plate. The basolateral domain is responsible of both absorption of blood-borne substances and secretion of plasma proteins synthesized by the hepatocyte.

The apical domain is a membrane depression also lined by microvilli. Occluding junctions connect the apical domains of adjacent hepatocytes sealing the bile canaliculus which drains the exocrine product of hepatocytes. The abundant rough endoplasmic reticulum of hepatocytes synthesizes plasma proteins (albumin, fibrinogen, prothrombin, coagulation factors V, VII, IX), whilst the highly developed smooth endoplasmic reticulum is involved in cholesterol and bile salts synthesis, glucuronide conjugation of bilirubin, steroids and drugs, breakdown of glycogen into glucose, esterification of free fatty acids to triglycerides, removal of iodine from triiodothyronine and thyroxine hormones, detoxification of lipidsoluble drugs[2].

Associated with the hepatic microsomal membrane resides the cytochrome P450 (CYP 450) enzymatic complex which catalyzes a variety of reactions including monooxygenase reaction/hydroxylation, S-oxydation, epoxidation, N-dealkylation, O-dealkylation. This family of hemeproteins is responsible for hepatic biotransformation and detoxification of a large number of exogenous and endogenous substances,

ranging from drugs and toxic compounds to bilirubin[10], and also for cholesterol synthesis.

Bile produced by hepatocytes is secreted into the intercellular spaces known as bile canaliculi, hence flows into cholangioles, thin intralobular ductules which drain into the terminal ductules named canals of Hering. The later are lined by squamos-to-cuboidal simple epithelium and exit the lobule through the limiting plate to open into the bile duct of the portal triad. The cuboidal epithelium lines all the intrahepatic bile ducts and expresses CK-19 (cytokeratin 19) marker.

The liver sinusoids are lined by two cell types: fenestrated endothelium and Kupffer cells which are the liver resident macrophages. They lie in between or on top of endothelial cells but their cytoplasmic extensions allow direct cell-to-cell contact with the parenchymal hepatocytes. Kupffer cells are specialized mainly in phagocytosis of hepatic cellular debris and blood borne pathogens but their morphology and biocapacity is variable, depending on their location. The periportal ones are larger and more active in phagocytosis, whereas the smaller centrolobular ones are more active in cytokine synthesis[11].

Also adherent to the sinusoid endothelium reside the pit cells, hepatic NK-cells cytotoxic for metastatic tumor cells that reach the liver via the portal venous system. Their functions are dependent on Kupffer cells which control their immunity, adherence, viability and cytotoxicity[12] and together they are responsible of liver's immune defense. Containing the largest population of macrophages in the body, liver is a potent modulator of systemic immune response to severe infections[13]. Kupffer cells interact with neutrophils and T-cells being both antigen presenters and producers of TNF-α

(Tumor necrosis factor α), IL1 (Interleukin 1), IL6 (Interleukin-6) and cytokines which induce the expression of acute phase proteins[14]. There is definite proof of Kupffer cells' involvement in liver regeneration (*vide infra*) helped by the bioactive mediators they express: TGF-β1, 2, 3 (Transforming Growth Factor β1, 2, 3), latent TGF-β binding protein 1, 2[15], TGF-β receptors, MMPs 2, 9, 13, 14 (matrix metalloproteinases 2, 9, 13, 14), TIMP-1(Tissue-specific inhibitor of matrix metalloproteinase 1) [16] and TIMP-2 (Tissue-specific inhibitor of matrix metalloproteinase 2) [17].

2.1.1.1.3 Biology and clinical significance of hepatic stellate cell

Hepatic stellate cells, also known as the Ito cells, reside in the space of Disse in proximity to the hepatic sinusoids, in close contact with hepatic regenerating cells[18]. They are in contact with the blood stream and regulate the sinusoid vascular tone[19]. Hepatic stellate cells are in direct contact with endothelial cells and interact with parenchymal cells via microspines extending from their cytoplasmic processes[20].

Stellate cells account for one-third of the nonparenchymal cell population in normal liver[21]. They are spindle-shaped with oval or elongated nuclei and located in the space between the basolateral surface of hepatocytes and the ablumenual side of sinusoidal endothelial cells. Besides storing vitamin A, they are producing and secreting cytokines and fibers which form the hepatic ECM (extracellular matrix).

Stellate cells can recruit inflammatory cells through expression of adhesion molecules, secretion of chemokines and cytokines and hence play regulatory roles in liver inflammation. During tissue remodeling, quesicent stellate cells become activated and transdifferentiate into myofibroblast-like cells. They lose retinoids and become very proliferative, fibrogenic and contractile[22]. Activated stellate cells are also an important source of cytokines and synthesize a large amount of extracellular matrix components

including collagen, proteoglycan and adhesive glycoproteins. The production of ECM component is mediated through integrin-dependent signaling events including focal adhesion kinase, tyrosine kinase and ERK (Extracellular-signal regulated kinase)α activation. Transforming growth factor (TGF-β) is a major promoter of myofibroblast differentiation, which is characterized by the expression of α-SMA (Alpha- smooth muscle actin) and adhesive receptors and the increasing synthesis of extracellular matrix molecules such as fibronectin. Normally, activated stellate cells ensure a fine-tuning of the wound-healing response according to the duration, the type and the amount of damage, through extra cellular matrix production. However, overexpression of extracellular matrix components by these cells causes hepatic fibrosis.

Stellate cells express some phenotypic markers such as desmin and alpha smooth muscle actin, both specific for activated stellate cells. Interestingly, they also express neuroendocrine markers including glial fibrillary acidic protein, neural cell adhesion molecule, the class VI intermediate filament protein nestin and synaptophysin[23, 24]. Such characteristics raise the question of a possible neural crest origin of stellate cells.

These specialized hepatic pericytes of mesenchimal origin[25] contain fat and retinyl palmitate in their cytoplasm, storing 80% of vitamin A body reserves. Under physiological conditions SCs (stellate cells) are quiescent, exhibiting a star-like phenotype (Figure 2-3). Their activation is followed by proliferation and transdifferentiation into highly contractile myofibroblast-like cells. Stellate cell activation is an essential step in both liver regeneration and in the initiation of liver fibrosis. The resulting myofibroblastic phenotype is represented by lipid droplets and vitamin A

reduction, increased collagen, desmin and α-smooth muscle actin synthesis followed by actin cytoskeleton reorganization and ECM deposition.

Activated stellate cells proliferate and secrete cytokines and ECM proteins. They migrate to the liver injury site acting as specialized wound healing cells. Initially surrounding the hepatic necrotic areas, hepatic stellate cells appear enlarged; then they migrate amongst the oval cells and newly regenerated hepatocytes, emitting numerous extensions and preceding the migration of endothelial cells that will generate the sinusoidal walls.

The stellate cell activation is a sequential process. It is initiated by transcriptional events, paracrine stimulation by Kupffer or other neighboring cells and early ECM changes. Subsequent cytokine secretion, receptor tyrosine kinase upregulation and accelerated ECM remodeling ensure its perpetuation. Once the healing is complete, the activation stops. It is not clear yet if its resolution is a process of reversion or if the activated hepatic stellate cells undergo apoptosis (Figure 2-4).

Under pathological circumstances, the activation process perpetuates and the increased deposition of collagen fibers and ECM within the space of Disse is followed by a loss of fenestrations and gaps between sinusoidal endothelial cells. As the fibrotic process advances, increasing numbers of hepatic stellate cells transdifferentiate into myofibroblasts, constricting the sinusoids lumen and increasing the vascular resistance inside the liver lobules. Together with the dissecting fibrous bands that distort the lobular architecture, the abnormally high resistance to blood flow in the hepatic sinusoids leads to portal hypertension, a complication of advanced cirrhosis[19].

Almost 465 genes are highly expressed in activated stellate cells under various conditions[26]. Among the products synthesized by Ito cells, hepatocyte growth factor (HGF)[27] and its receptors[28], stem cell factor[29] (SCF), platelet derived growth factor[30] (PDGF), endothelin 1 (ET-1), transforming growth factor β1 (TGF-β1), connective tissue growth factor (CTGF) and its receptors, monocyte chemotactic protein 1 (MCP1) are effectors known to be involved in autocrine, paracrine and endocrine interactions which result in liver healing and regeneration. TGF-β1 is produced in an inactive form, bound to latent TGF-β binding protein and secreted into the ECM where it is activated and exerts its matricrine action[31].

Many ECM components are secreted by Ito cells: collagen type 1, 3, 4, 14, and 18[32], decorin and perlecan, fibronectin, dermatan and heparan sulfate, syndecan[33], entactin, tenascin, laminin and proteoglycans[34]. Hepatic stellate cells are also involved in a continuous process of ECM remodeling intermediated by their secretion products with antagonistic functions: matrixmetalloproteinases MMPs 1, 2, 3, 9, 10, 13, 14[17, 35] and tissue specific inhibitor of matrix metalloproteinases TIMP-1, 2[36]. These changes in protein expression are accompanied by a distinct phenotype and a specific migration pattern.

Either hepatocyte, or stem/oval cell mediated, liver regeneration is always accompanied or preceded by stellate cell activation. Closely associated with stellate cells and surrounded by their processes, the oval stem cells seem to be nurtured by the non-parenchymal cells. Trough direct cell-to-cell interactions, growth factors and cytokine secretion, stellate cells are thought to promote oval cell growth and differentiationetion [18].

ECM is composed of various macromolecules, including fibronectin, collagen, laminin, vitronectin, and proteoglycans. It functions as the physical support for epithelial and endothelial cells and modulates cell differentiation, migration, growth, and apoptosis. Liver ECM is distinct from other organs where ECM acts as a diffusion barrier between plasma and the epithelial cells and forms a basement membrane.

Lacking a true basement membrane, the liver has ECM in the perisinusoidal space of Disse, which separates the basolateral domain of the hepatocyte membrane from the blood circulating in the endothelium lined hepatic sinusoid. The specific organization of the 0.2 – 0.5 μm wide space of Disse is thought to facilitate a maximal exchange of proteins and other nutrients between circulating blood and hepatocytes. The ECM fibers of the perisinusoidal space are collagen (types I, III, and VI), laminin, entactin, perlecan, and the most abundant, insoluble fibronectin. Hepatocytes are the source of both soluble, circulating plasma fibronectin and insoluble, cellular, ECM form of fibronectin secreted during liver regeneration.

Laminin, consisting of three distinct chains, is normally detected in the perisinusoidal space, large blood vessels, and biliary ducts. Although there are several lines of evidence suggesting that the laminin sub-units are expressed in normal liver and regenerating liver, the exact composition of these laminin subunits in normal liver and in regenerating liver remains unclear[37]. The ECM components interact with cells through cell surface heterodimer integrin receptors, a family of transmembrane proteins composed of α and β chains[37].

During oval cell mediated liver regeneration there is a constant remodeling of the ECM, which becomes more permissive for migration and facilitates cell-to-cell

interactions. In this respect, ECM acts as a regulator of cell's dynamic behavior. ECM proteoglycans sequester a wide range of growth factors which are released and activated after protease cleavage[38].

2.1.2 Liver Physiology

2.1.2.1 Metabolic homeostasis

Liver is an annex gland of the digestive tract. It is also the site of multiple metabolic processes, thus playing a major role in homeostasis. Being the main site of protein synthesis, it maintains the colloid osmotic pressure of the blood by producing the most abundant protein in the plasma, albumin. Other important plasma proteins such as lipoproteins, glycoproteins, prothrombin, fibrinogen and coagulation factors V, VII, IX, X, XI and the non-immune α- and β-globulins are synthesized by the liver. Thus, liver is the major regulator of coagulation process in the body. It also catabolizes the aminoacids by deamination and conversion of resulting ammonia into urea[39].

Liver regulates the plasma levels of glucose: by converting it into its storage form, glycogen; thus reducing the glicemic level. When the energetic needs are increased, it cleaves the glycogen into glucose, inducing a rise of glycemia (*vide infra*).

2.1.2.2 Storage

Together with the muscular tissue, liver is the major deposit of glucose, stored in hepatocytes as glycogen. Whenever the energetic needs of human body increase, glycogen is cleaved and resulting glucose is oxidized to water, carbon dioxide and ATP. Also, the glucose released into the blood stream maintains the normal glycemic levels.

Several vitamins are stored and converted into metabolically active forms in the liver. 80% of vitamin A reserves are in the stellate cells' cytoplasmic lipid droplets. Vitamin B_{12}, copper and iron reserves are also located in the liver. By storing and

releasing the iron in a metabolically active form, liver is an important regulator of its homeostasis. Because of its involvement in iron metabolism, liver is the first organ affected in conditions associated with iron overloading.

As part of the metabolic chain resulting in synthesis of biologically active vitamin D, liver plays an important role in rickets and osteomalacia prevention. Vitamin D_3 is converted into its circulating form 25-hidroxy cholecalciferol, thus being available to the kidney for further transformation. Vitamin K absorbed in the colon is used by the liver for blood clotting factors synthesis, thus supplying the necessary proteins for a physiological coagulation cascade[39].

2.1.2.3 Blood reservoir

Hepatic particular capillary network and vascular supply associated with its large parenchymal mass make possible the storage of a large volume of blood. Liver has a dual afferent blood supply: 75% of hepatic blood comes from the portal vein, and 25% of it from hepatic artery. By receiving mixed (venous and arterial blood) the liver is able to store 25 – 30% of cardiac output and hold up to 1500 ml of blood[39].

2.1.2.4 Detoxification

Acting as a waystation between the splanchnic and systemic circulation, liver receives xenobiotics which are detoxified by its cytochrome – P 450 enzymes. The resulting water soluble products are excreted into urine by the kidney. Alcohol; dehydrogenase and isoforms of uridine diphosphoglucuronate glucuronosyltransferase (UGT) allow for the biotransformation of exogenous and endogenous toxic compounds. Conversion of ammonia into urea is such an example of endogenous waste product detoxification. Bilirubin degradation products and cholesterol are excreted through the bile into the small intestine.

2.1.2.5 Liver endocrine functions

Liver is considered a mixed gland. Its endocrine function cosists in synthesis and secretion of proteic products, as part of its metabolic homeostasis function. It has a significant impact on hormonal homeostasis by being part of the metabolic pathways of degradation of hormones produced by other glands, such as estrogens, insulin and glucagon. It also controls the hormonal functions by regulating their secretion and activation[3]. Liver is an important source of GH-RH (growth hormone releasing hormone) and converts thyroxine into triiodothyronine.

2.1.2.6 Liver exocrine function

Liver is described as an annex gland of the GI tract due to its bile secretion. Collected by the intrahepatic biliary ducts, it is stored in the gallbladder and reaches the duodenum during the meals. Acting as a detergent, bile emulsifies the intestinal lipids and contributes to their absorption. Cholesterol secretion into the bile is its only mechanism of excretion in the human body.

2.1.2.7 Immune defense

Being a way station between the splanchnic and systemic circulation, liver receives, via the portal blood, toxins and pathogens which escape the enteric barrier into the bloodstream. Rich in Kupffer cells (resident macrophages) and pit cells (hepatic NK lymphocytes) it is able to remove actively the antigens and act like a sieve for the portal blood. Kupffer cells are the hepatic resident macrophages responsible for phagocytosis of hepatocyte necrotic products and aged red blood cells. Pit cells, the Kupffer cell dependent NK (Natural killer) cells phagocytose neoplastic cells coming to the liver from the digestive tract.

2.1.3 Liver Regeneration

There are two distinct patterns of inducing hepatocyte proliferation: compensatory regeneration following liver mass loss and mitogen induced direct hyperplasia in the absence of significant cell loss[40]. Compensatory hyperplasia, generally and, in the absence of a liver blastema, improperly referred to as liver regeneration occurs after partial hepatectomy and hepatocellular necrosis. Direct hyperplasia is a process of hepatocyte proliferation triggered by various chemicals which do not cause liver necrosis (Figure 2-5).

Liver regeneration is the result of the interplay between two major sets of events: the adaptive changes elicited by the metabolic and vascular imbalance and the mitogenic changes which trigger the hepatocyte transition from a quiescent to a replicative state. This process requires the activity of multiple interacting pathways grouped into cytokines, growth factors and metabolic networks. Within minutes after a partial hepatectomy, hepatocytes exit G_0 and enter G_1. This so called “priming phase” governed predominantly by the cytokine network debuts with the enhanced expression of the early genes: c-fos, c-jun proteins (components of AP-1, activation factor 1), c-myc transcription factor, NFκB (Nuclear factor kappa-light-chain-enhancer of activated B cells), Egr-1 (Early growth response protein 1), STAT3 (Signal transducer and activator of transcription 3), HGF (Hepatocyte Growth Factor), TGF-α (Transforming Growth Factor α), IL-6 (Interleukin -6), transcribed in the first 30 minutes – 2 hours post injury.

However, the cell cycle progression requires growth factors, responsible for overriding the G_1/S checkpoint (between growth 1 and synthesis phases of cell cycle). High levels of EGF (Epidermal growth factor) and HGF (Hepatocyte growth factor) are associated with increased expression of cyclins D, E, A. Phosphorylation of overly

expressed Rb (Retinoblastoma protein), allows the formation of cdk4/cyclinD (Cyclin dependent kinase 4/cyclin D) and cdk2/cyclinE ((Cyclin dependent kinase 2/cyclin E) complexes.

Although it is difficult to identify the mechanisms modulating the liver growth in accordance to the needs of the whole organism, it is generally accepted that the increased metabolic demands imposed on the liver remnants post injury are activating the DNA replication. Amino acids are known to activate the mTOR pathway responsible of sensing the nutrient and energy status, integrating growth factor signals and regulating the cell growth[41]. This metabolic regulation is also responsible for controlling the hepatocyte mediated liver regeneration.

Compensatory hyperplasia is triggered by several damaging factors ranging from surgical resection to hepatotoxins and chronic viral infection. In response to the injury induced by these aggressors, the parenchymal loss is compensated by an active process of hepatocyte division. Despite their minimal replicative activity in the absence of injury, hepatocytes are able to restore the liver mass after hepatic necrosis. Figure 2-6 (adapted after the first depiction, by Higgins and Anderson, of the residual hepatic lobes growth after 70% partial hepatectomy[43]) shows the restoration of liver mass without the recovery of the original hepatic anatomy.

Compensatory hyperplasia progresses in a centripetal direction inside the liver lobule, first hepatocytes to exit G_0 (quiescent phase) and enter G_1 (Growth 1 phase) being situated in the periportal areas. Mediated by cyclin D_1 pathway activation[44, 45], hepatocyte proliferation spreads gradually towards the centrolobular vein[42, 46]. According to Michalopoulos[45] the DNA synthesis profile post 70% partial hepatectomy

has a camel back shape with an initial high peak after 1 day and a second small peak another day later. This particular pattern is caused by an initial hepatocyte proliferation in zones I and II, followed by non-parenchymal cells (NPC) and zone III hepatocytes division, as shown in Table 2-1. Whilst hepatocyte division is progressive, NPCs exhibit a simultaneous proliferation across the acinar zones. The original liver mass is usually restored within 2 weeks of the hepatectomy.

Several hepatotoxins have been used to study the mechanisms of compensatory hyperplasia in the liver, amongst them CCl_4 (carbon tetrachloride) and AA (allyl alcohol). Despite variations in necrotic area location[47, 48, 49, and 50], in both animal models the hepatocytes are responsible for regeneration, without any contribution from other cell populations. It was later discovered that hepatocytes are not the only regenerating resource for damaged liver. When hepatocytes are severely impaired by pathogens and toxins, making impossible their division, a facultative regenerating cell population is activated. The hepatic stem cell compartment reacts to the inability of liver to recover its mass loss by multiplying in an amplification compartment represented by the oval cells. Although several data about oval cells' origin have emerged lately, less in known about the molecular mechanisms which trigger oval cell proliferation and determine their lineage fate.

2.2 Stem Cells and Their Therapeutic Potential

The interest in regeneration has been present for quite some time in the scientific world, triggered by observations made in freshwater hydra and axolotl which are able to regenerate parts of their bodies. Although few recordings from the 1908 Congress of Hematologic Society in Berlin[51] have survived, we now know[52] that Alexander Maximov heralded the existence of stem cells and even coined the term of "stemzelle"[51]. As a

result of his studies on blood cell lineages he hypothesized the existence of a pluripotent white blood cell, able to differentiate into a different cell type[51]. The interest in stem cells soared after the devastating effects of atomic radiation on blood cells were discovered in the mid 20th century. The concept of stem cell therapy in the form of bone marrow transplantation dates from the same period, but the first results were utterly disappointing because of the little knowledge on immune compatibility.

The stem cells were first identified in blood and characterized by James Till and Earnest McCulloch[53, 54], work that has dubbed them the “fathers of stem cell research”. Discovering the proteins that enable stem cells to differentiate and mature, Till and McCulloch made possible the quantitative analysis of a single hematopoietic stem cell. Their researched revolutionized the success of bone marrow transplants. Further research[55, 56] showed that a single cell type was able to repopulate bone marrow and set the basis for the current research boom in the field of stem cell therapy. Based on the emerging research, stem cells were defined as multipotent cells able to self renew and differentiate into cells of various germ layers. They are located both in embryonic and adult tissues.Research data emerging in the early 1980’s shed light on the clonogenicity and totipotential nature of the embryonic stem cell and emphasized the differences between them and the adult stem cells. The only truly totipotent cells are found in the fertilized egg. To this date, many adult and embryonic stem cells were proven to be multipotent. However the differentiation capacity of stem cells is not fully described.

Embryonic stem (ES) cells isolated from the inner cell mass of blastocysts[58-60] are able to differentiate into cells originating from all three embryonic layers (ectoderm,

mesoderm and endoderm). Under specific culture conditions and *in vivo* ES were induced to differentiate into cells of mesoderma; origin: hematopoetic, hemangioblast, vascular, cardiac, skeletal muscle, chondrogenic, osteogenic, and adipogenic lineages[62-71]. Endodermal lineages like pancreatic and hepatic cells were derived from ES. Ectodermal lieage differentiation of ES into neurons suggests the tremendous versatility and potential of stem cells for treating degenerative diseases, organ failure and inborn errors of metabolism. Unfortunately, the ethicall issues and the formation of teratomas indicate that more research needs to be done in order to fully elucidate the nature of stem cells and pave the way for developing stem cell therapies. More data about the differential and self renewal capabilities, the nature of full lineage commitment of stem cells are needed. The discovery of murine embryonic stem cells represented a breakthrough in experimental medicine, offering the chance of isolating cells for replacement therapy. It became possible the development of a bone marrow transplantation protocol, which nowdays represents the greatest success of human stem cell therapy.

Adult stem cells proved to have a great plasticity, too. They can be manipulated to differentiate into endodermal, mesodermal and ectodermal cell lines[72- 74], similar to ES. Reversible differentiation of neural stem cells into hematopoietic lineages was demonstrated[75]. Human adult bone marrow stem cells were manipulated to differentiate into hepatocytes[76, 77] and endothelial cells[82], proving for the first time the value of murine models in development of human adult stem cell therapies. In addition, bone marrow stem cells have been shown to participate in neural development[83, 84]. Further research has uncovered the capacity of human bone marrow stem cells to differentiate into

neurons, intestine, pancreas, skin, skeletal and cardiac muscle cells in human recipients of bone marrow or organ transplants[79, 80]. Bone marrow mesenchymal cells have also been shown to be pluripotent[81]. These studies emphasize the broad differentiation spectrum adult stem cells possess.

2.3 Oval Cells Biology and Their Clinical Significance in Liver Regeneration

2.3.1 Origin and Morphology of Oval Cells

Liver mass restoration post injury requires the coordinate interaction of several cell types. In addition to hepatocytes and non-parenchymal cells the liver contains stem cells which can generate a transit compartment of precursor cells. Named oval cells by Farber[85] who described them in 1956, these tissue specific, liver adult stem cells are able to give rise to both hepatocytes and cholangiocytes[86].

Embryologically, they are suggested to derive from the ventral foregut endoderm and form the main component of the liver primordium[87]. Initially thought to reside only in the canals of Hering, the traditional liver stem cell niche, there are several lines of evidence proving that bone marrow is an alternative source for the oval cells[74,88]. Alternative origins for oval cells were reported, starting with Petersen[74] who has shown that some of them may actually arise from an extra-hepatic source within the bone marrow. Several other investigators have confirmed that bone marrow derived cells possess the ability to produce functioning hepatocytes and bile ductular cells[76, 88]. Although a number of studies suggest that the oval cells reside in the hepatic parenchyma in close association with bile duct epithelium, the exact oval cell niche has yet to be characterized.

Several recently published studies clearly demonstrate that stellate cells within the liver may, through a process of mesenchymal to epithelial transition, give rise to

hepatocytes[89]. It is possible that this phenomenon involves an intermediate cell type with oval cell properties. For the moment it is impossible to determine beyond any doubt if mesenchymal to epithelial transition contributes to the oval cell pool seen in the current experimental models. However, this possibility deserves mention.

It is believed that the oval cells constitute a heterogenic cell population which account for 1%-3% of the normal liver cell pool. Their morphological variability made Roskams *et al.*[90] differentiate them into three categories: oval cells, intermediate bile duct-like cells and intermediate small hepatocyte-like cells. The last two populations were described as progeny of the first.

Thought to be a reserve compartment activated only when hepatocytes fail to proliferate, the most common conditions involving oval cells in humans are: massive acute hemorrhagic necrosis, haemochromatosis, Wilson disease and chronic hepatitis C. During both acute necrosis and fibrotic reorganization stages of the disease a significant number of oval cells are present in the regeneration/proliferation areas of the human liver.Recent data suggest a correlation between the prevalence of oval cells and the fibrosis stage in pediatric patients with chronic hepatitis B[91].

Morphologically, the oval cell is small (5 – 10 μm) and has a large ovoid nucleus containing predominantly dense heterochromatin lining the nuclear envelope (Figure 2-7). The nucleus to cytoplasm ratio is very high compared to the hepatocyte and, in the electron microscopy the scanty cytoplasm appears slightly brighter due to the poorly developed organelles. The tonofilaments in the cytoplasm give them the flexibility and strength needed for their migration and attach on the desmosomes/macula adherens which connect their membranes to the neighboring hepatocytes and cholangiocytes.

This morphology corresponds mostly to the type I oval cell described by Roskams. The intermediate small hepatocyte-like cells are twice bigger than the progenitors, but half the diameter of a mature hepatocyte. Their nuclei, similar to the mature hepatocytes, have less heterochromatin and occasionally nucleoli were reported. Mitochondria, peroxisomes and rough endoplasmic reticulum are visible in the less dense cytoplasm as visible in the electron micrograms published by Sobaniec-Lotowska[91].

The intermediary bile duct-like cells have a rounder nucleus, more organelles and tonofilaments in the cytoplasm and microvilli at the apical pole. The small hepatocyte-like cells are intermediary in size between oval cells and hepatocytes, have a higher nucleus to cytoplasm ratio due to a larger volume of basophilic cytoplasm. They are very active metabolically and numerous vacuoles filled with lipids are present in the cytoplasm.

Oval cells express different combinations of phenotypic markers from both the hepatocyte and biliary lineage. Similar to cholangiocytes in their cytoskeletal proteins (CK-19) and isoenzymatic profile (gamma-glutamyl transpeptidase GGT), they also express alpha feto protein (AFP), OV6, OC2, A6 antigens[92]. Classical hematopoietic markers Thy-1, c-kit (SCF receptor) and CD34 expressed on the surface of oval cells strongly support their bone marrow origin. Table 2-2 shows a comparative expression of cell markers by various hepatic cell types.

2.3.2 Experimental Models and Mechanisms of Oval Cell Induction

Several models of oval cell induction have been developed in rodents, such as choline deficient/ethionine supplemented diet, 2-acetylaminofluorine/70% partial hepatectomy, galactosamine and dipin injection. They all have in common the association of liver injury with impairment of hepatocyte division, creating a

pathophysiological mechanism similar to the severe acute or chronic viral, toxic or drug induced liver pathology in humans. There are some differences though, regarding the onset, phenotype and location of the regenerating cells.

Activated oval cells observed in the above mentioned murine models migrate from the periportal region towards the centrolobular zone, forming primitive ductular structures with poorly defined lumena[93]. The origin of oval cells remains unclear. According to some reports[94] which analyze their involvement in periportal repair, some data suggest that the oval cell niche is located in the periportal area. Although the oval cell presence has not been observed in the regenerative response to PHx or CCl_4 injury, prior administration of 2AAF induces their proliferation in the periportal areas.

2AAF is converted into its N-hydroxylated active metabolite by the cytochrome P 450 enzymes in hepatocyte endoplasmic reticulum. After being translocated into the nucleus 2AAF metabolites form voluminous adducts with DNA, rendering it unable to be approached by the transcription apparatus. As a result, cyclin D_1 synthesis is inhibited and the hepatocytes are arrested in the cell cycle at the G_1/S checkpoint.

Once the hepatocyte proliferation comes to a halt, injured liver mobilizes the alternative regeneration mechanisms resulting in oval cell activation. As with allyl alcohol induced injury, oval cell proliferation in these models begins in the periportal region, followed by migration deeper into the acinar zone I as regeneration progresses. Depending on the site of injury, the migration may stop either in acinar zone II, or in the pericentral area.

2AAF/PHx model, developed after the Solt-Farber 1976 protocol[95] elicits a vigorous oval cell response which is associated with oval cell activation in the periportal

area where progenitor cells are proliferating[18, 96, 97]. The concomitant activation and close proximity between oval and stellate cells during the stem cell mediated regeneration led to the hypothesis that perisinusoidal stellate cells may control the developmental fate of the progenitor cells. The potential regulatory mechanisms are either direct by secreting growth factors, such as hepatocyte growth factor (HGF) and transforming growth factors (TGF), or indirect via urokinase induced extracellular matrix (ECM) remodeling[98]. Other studies emphasized the self reliance of oval cells, able to synthesize TGF-β, acidic fibroblast growth factor (FGF), or IGF-2 (insulin-like growth factor 2). All these factors are responsible for autocrine regulation of their differentiation fate[6]. To which extent are oval cells dependent on other resident cell population for creating the cytokine and growth factors microenvironment conducive to a certain lineage commitment remains to be found.

The proposed sequence of events for oval cell activation includes an initial immune response with a significant increase of cytokines secretion. These signals promote the infiltration of the damaged area by Kupffer and stellate cells which further produce cytokines and growth factors. If the hepatocyte regeneration is impaired, resident oval stem cells located in the canals of Hering are activated. Hepatic progenitor cells may also be recruited from the bone marrow by chemoattractants, such as SCF (stem cell factor) and SDF-1 (stromal derived factor 1) and further infiltrate the liver lobules in response to the cytokines produced by Kupffer and stellate (Ito) cells. TNF (tumor necrosis factor) stimulates oval cell proliferation. HGF, EGF and TGF-β regulate the plasminogen activators responsible for TGF-α and HGF activation. TGF-β can also trigger apoptotic pathways in oval cells, resulting in cessation of oval cell mediated liver

regeneration. The delicate balance between the various cytokines and growth factors at a definite time point is believed to dictate the amplitude and the duration of the oval cell response.

2.3.3 Oval Cell Plasticity

Although the oval cell potential to differentiate into hepatocytes was suggested over seventy years ago[99], it took almost two decades before the first supporting data emerged. Later research confirmed the hepatocyte differentiation and revealed a second fate commitment towards bile duct cells[100 - 103]. Initially the bipotentiality was attributed to the heterogeneity of oval population, but the increasingly consistent findings led to a consensus over the capacity of oval cells to differentiate into both hepatocytes and cholangiocytes.

More recent data[105, 106] have shown the oval cell potential to differentiate into several cell lines, ranging from hepatocytes and cholangiocytes, to intestinal and pancreatic acinus epithelium, or neural cells (Figure 2-8). It was also reported that hepatic oval cells express not only AFP (indicating their non-terminally differentiated status), but also hematopoietic cell markers like Sca-1[108] for mice and Thy-1[107] in rats. These data suggest that both oval cells and HSCs might share, to a certain extent, a common developmental pathway. An alternative explanation might be that they share a common stem progenitor located in the bone marrow. In this situation, the actual tissue specific environment might be the trigger which induces the development of oval cells towards hepatic parenchymatous cells. This interpretation is supported by the well established fact that the particular developmental program stem cells engage to reach a certain differentiation fate is dictated by the specific regulation of their gene expression. Various liver specific extracellular signals are believed to interfere with expression of

genes responsible for stemness, self renewal and differentiation. Describing these signals and their specific signaling pathways is the main goal for researchers striving to establish novel cell therapies. The roles of stellate and Kupffer cells are currently evaluated as part of cell-to-cell interactions able to influence oval cells' fate.

2.3.4 Oval Cell and Hepatic Neoplasms

From a pathophysiological standpoint, the neoplasm inducing mechanism is considered to trigger either the dedifferentiation of a terminally differentiated cell, or the maturation arrest of a non-fully differentiated one. Since liver is known to be populated essentially by two distinct cellular pools, the unipotential hepatocytes and the multipotential oval cell, it is reasonable to assume that both major populations can become the origin of neoplastic tumors. The ongoing debate regarding the carcinogenetic potential of oval cells was triggered by the fact that the non-terminally differentiated state of the oval cell is associated with their capacity of undergoing a large number of cell divisions. Since the likelihood of a preneoplastic mutation is proportional to the number of mitoses, oval cells became a candidate for being the cell of origin for neoplastic tumors. Early studies seemed to support this hypothesis[43], demonstrating that hyperplasia of small round cells, somewhat similar phenotypically to the oval cells is associated with subsequent development of hepatocellular carcinomas. Since the morphology was the only proof invoked by the authors, it is hard to affirm beyond any doubt the oval cell nature of all hepatocellular carcinomas. More recent data showed that the transitional duct cell, progeny of oval cell, might be implicated in initiation and progression of liver carcinogenesis[110]. One study[111] examining the cellular markers of primary HCC (hepatocellular carcinoma) tumors demonstrated that oval cells, hepatocyte nodules and malignant areas express both oval cell and hepatocyte

antigens, suggesting a precursor relationship between oval cells and HCC[111]. Subsequent examination of alternative oval cell markers in different models of HCC[112, 113] found these markers in HCC nodules.

The current histological grading, considers that the degree of differentiation of a malignant tumor is dictated by the differentiation status of the cell of origin. This would suggest that the highly differentiated hepatic tumors may not originate in an oval cell. There are published reports[109] documenting the existence of cancers with higher differentiated status, like hepatocellular carcinoma (HCC) and cholangiocarcinoma (CCC) - which originate in hepatocytes. A study examining HCC tumors developed in patients with hepatitis B found oval cells expressing both hepatocyte and bile duct markers[114, 115]. Although these data seem to support the hypothesis of oval cell origin of HCC, they are not able to eliminate the possibility of hepatocyte dedifferentiation as origin of the neoplastic process.

Proponents of both theories had to face criticism. Although it is assumed that various cell types are able to resist to a different extent to mutations and epigenetic transformations, it is not known yet if the oval cell is less resistant to carcinogens than the fully differentiated cells. For these reasons, it is hard to believe that the oval cell is the only cell type with carcinogenetic potential in the liver, but it is more probable to assume that at least some of the cancers originate in hepatocytes and cholangiocytes.

Whether the presence of cells with oval cell-like phenotype is due to the dedifferentiation of mature hepatocytes undergoing the carcinogenic process, or they are real oval cells engaged on a procarcinogenic pathway is not known. Experiments using oval and epithelial liver cells exposed to various carcinogens showed a chemical

dependent phenotype in the preneoplastic and neoplastic cells[116-119]. It was also impossible to replicate *in vitro* the exame sequence of events happening *in vivo* during the carcinogenetic process. Considering these conflicting data, until further proof, it is safe to conclude that any cell type in the liver, including oval cells, has the potential to undergo the neoplastic cascade.

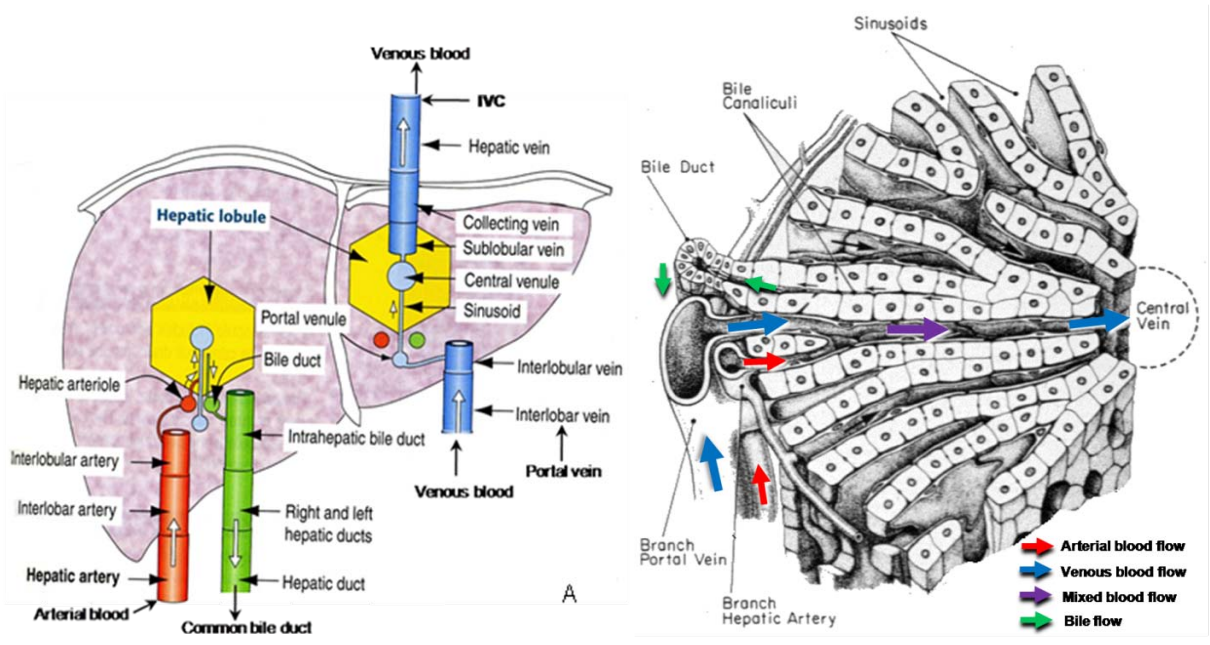

Figure 2-1. Diagrams of liver blood supply and microarchitecture. A) Representation of hepatic biliary flow and blood supply (flow direction indicated by arrows), B) Portal triad and intralobular blood flow (adapted after Kierszembaum[2]).

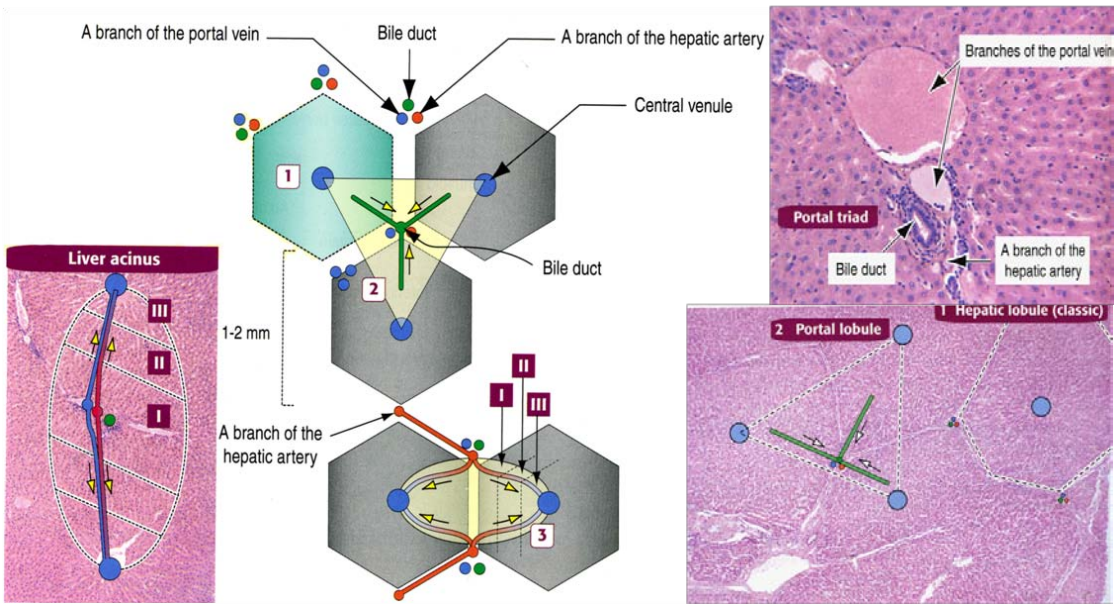

Figure 2-2. Conceptual interpretations of the functional hepatic architecture (adapted after Kierszenbaum 2002[2]). I – acinar zone I, II – acinar zone II, III – acinar zone III, dotted triangle – contour of a portal lobule, dotted hexagon – contour of a hepatic (classic) hepatic lobule, dotted diamond – contour of the liver acinus, color code: blue represents veins, red represents arteries, green represents bile ducts.

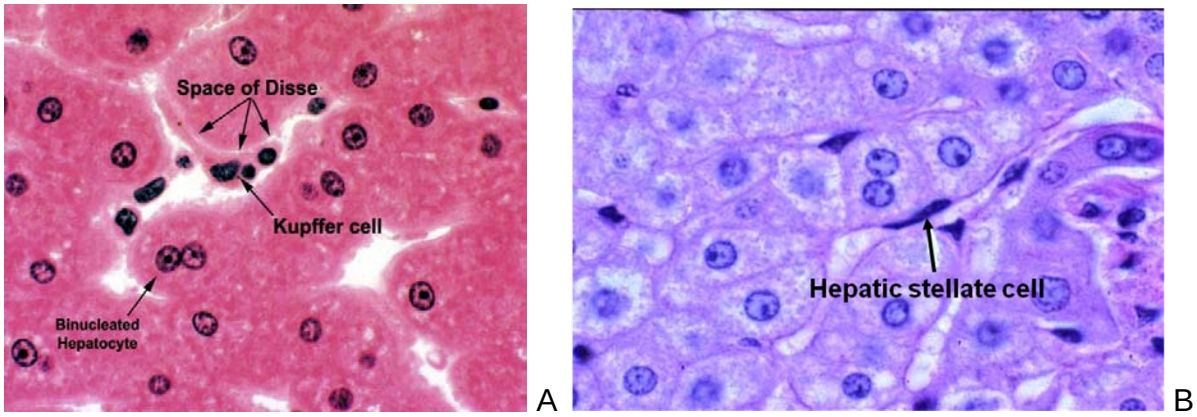

Figure 2-3. Histograms of Hematoxylin and Eosin (H&E) stained hepatic cell populations. A) Hepatocytes, Kupffer cells and the space of Disse, B) The intimate relationship between hepatic stellate cells and hepatocytes.

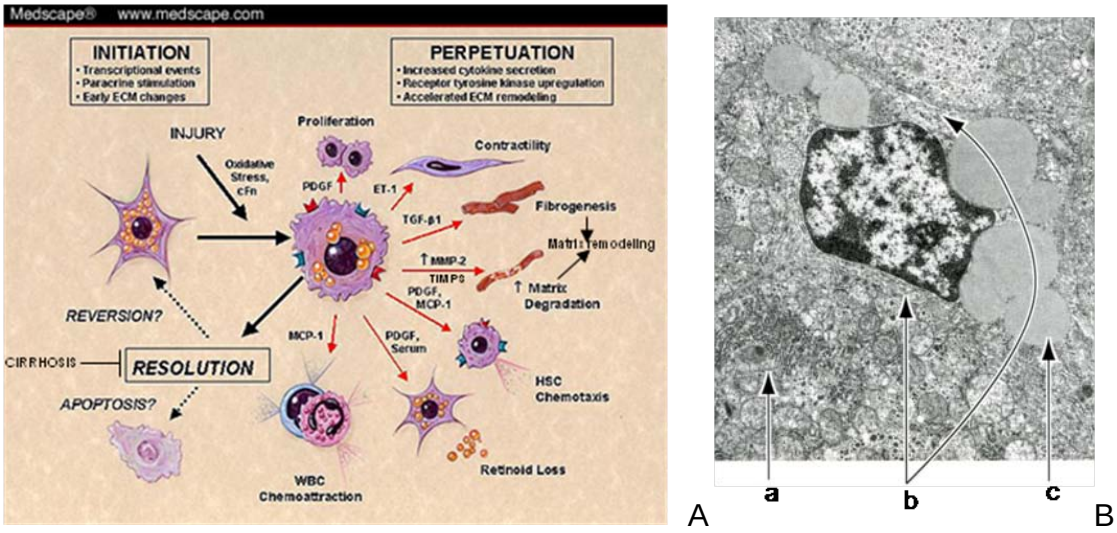

Figure 2-4. Hepatic stellate cell: morphology and activation diagram. A) Representation of hepatic stellate cell activation (adapted after www.medscape.com), B) Electron microscopy image of a quiescent hepatic stellate cell in the space of Disse (adapted after Kierszembaum[2]; a – hepatocyte, b – space of Disse, c – lipid droplets containing vitamin A).

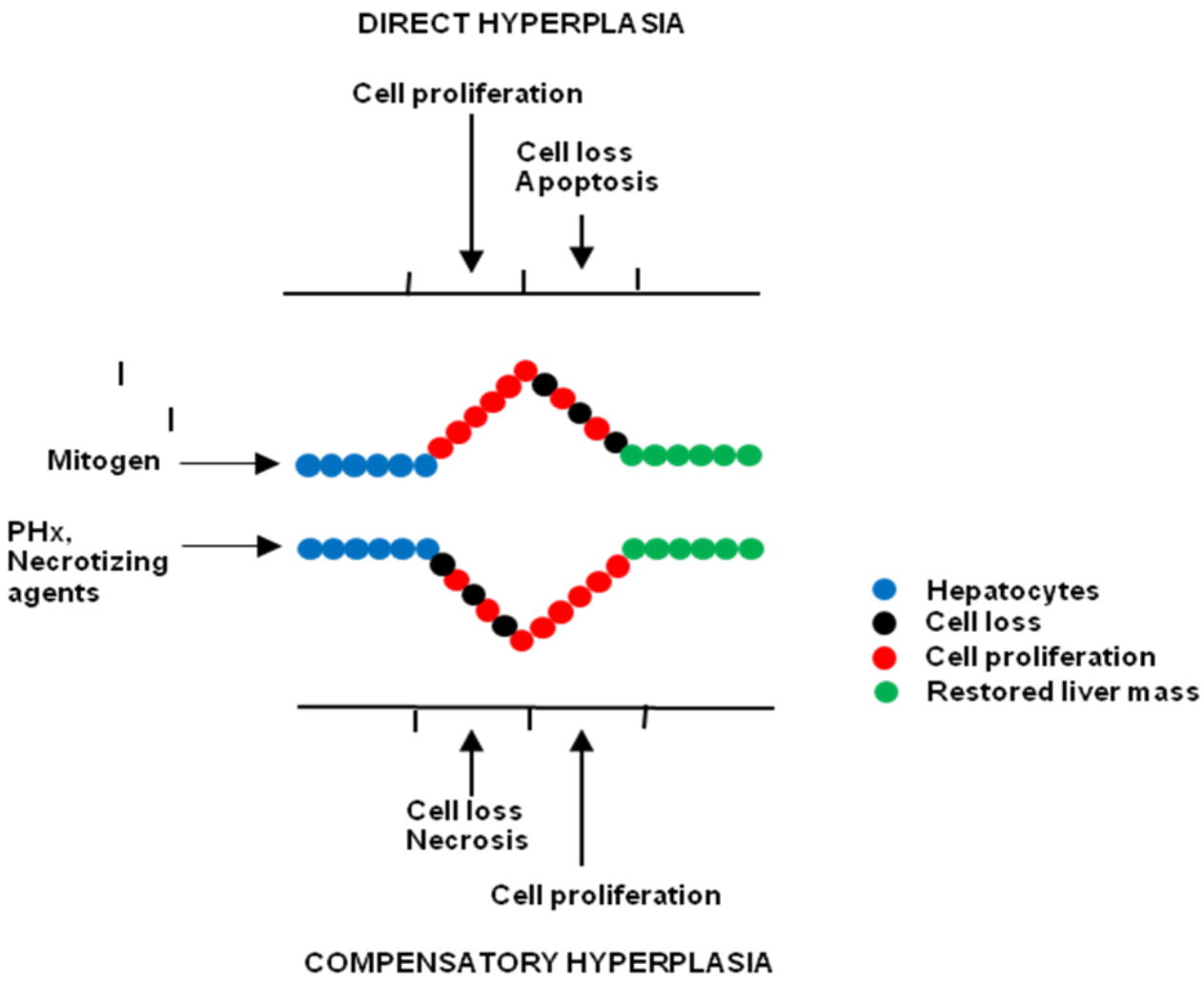

Figure 2-5. Diagrammatic representation of the specific mechanisms differentiating compensatory regeneration from direct hepatic hyperplasia (adapted after Columbano[40]).

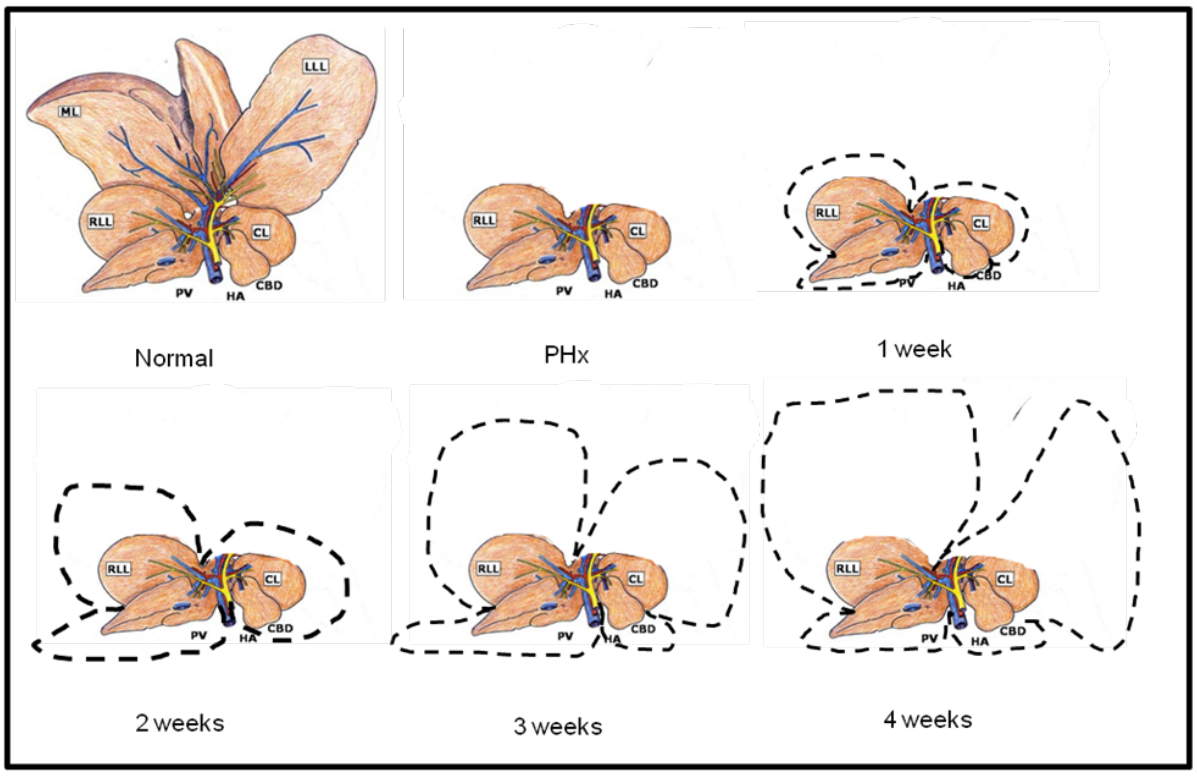

Figure 2-6. Diagrammatic representation of liver parenchyma growth after 70% partial hepatecomy in rat; compensatory hyperplasia is respomsible for restoring the original hepatic mass (adapted after Higgins and Anderson 1931[43]).

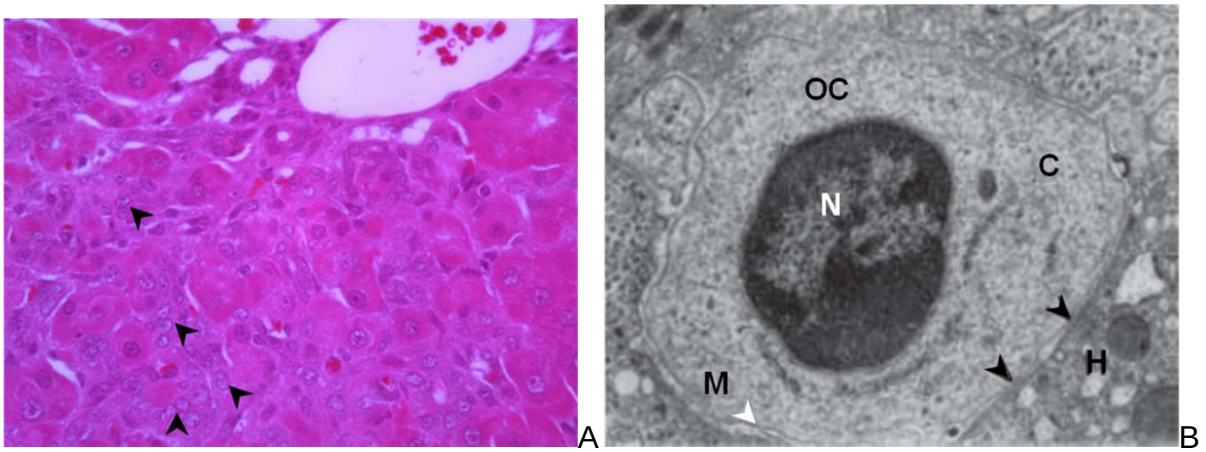

Figure 2-7. Oval cell phenotype: A) Light microscopy of Hematoxylin and Eosin (H&E) stained image of small ovoid cells with high nucleus/cytoplasm ratio (black arrow heads indicate the oval cells radiating from the periportal area into acinar zone I; magnification 40x). B) Electron microscopy histogram of an oval cell (OC), adjacent to a hepatocyte (H): N – nucleus, M – membrane, C – cytoplasm with scarce organelles, white arrowhead indicating the oval cell membrane and black arrowheads pointing to the desmosome junctions between the oval cell and the neighboring hepatocyte..

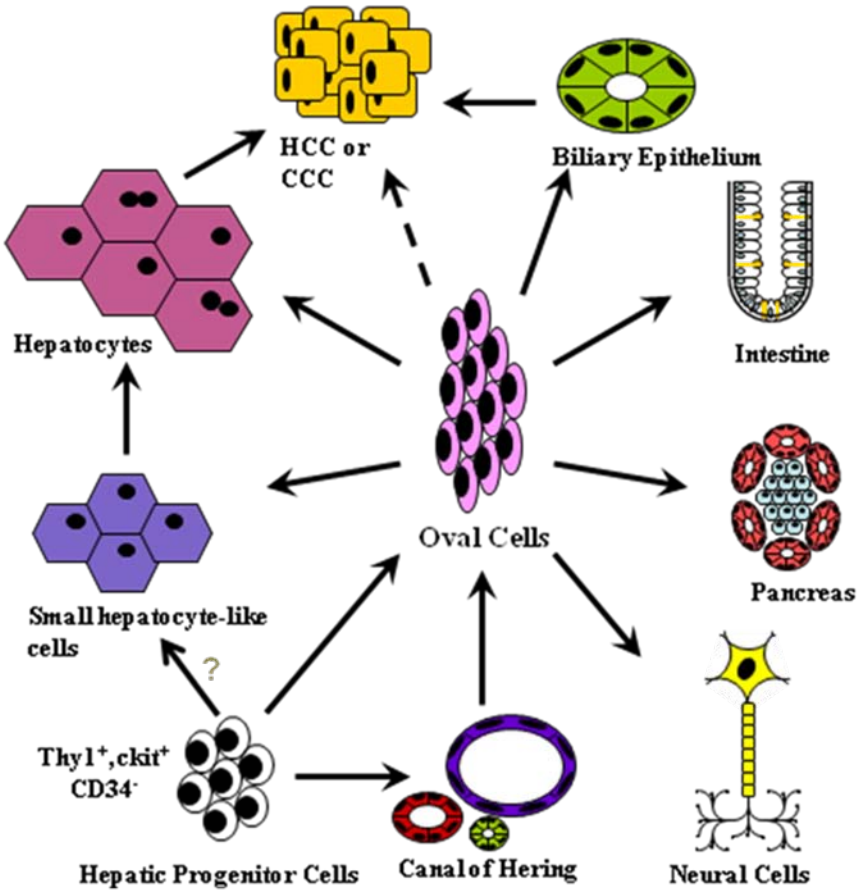

Figure 2-8. Oval cell plasticity: diagrammatic representation of hepatic progenitor cells differentiation fate under various experimental conditions, depicting their transformation into various normal cell lines, but also into hepatocellular and cholangiocarcinomas (modified after Williams 2007[104]).

Table 2-1. Liver regeneration post 70% hepatectomy reflected by DNA synthesis in various resident hepatic cells; chosen time points indicate the number of days after the acute liver injury (adapted after Michalopoulos[45]).

Cell type	Regeneration onset	Peak of regeneration	End of regeneration	Duration of regenerationr
Hepatocyte	Within 12 hrs posthepatectomy	Beginning of 2nd day post hepatectomy	End of 4th day posthepatectomy	4 days
Cholangiocytes	End of 1st day posthepatectomy	2nd day post hepatectomy	End of 4th day posthepatectomy	3 days
Nonparenchymal (Kupffer and Ito cell)	Beginning of 2nd day post hepatectomy	End of 2nd day post hepatectomy	End of 10th day post hepatectomy	9 days
Sinusoid endothelial cells	During the 2nd day post hepatectomy	End of 4th day post hepatectomy	End of 10th day post hepatectomy	8.5 days

Table 2-2. Molecular markers for several hepatic cell populations

Marker	Oval cell	Hepatocyte	Cholangiocyte	Stellate cell
AFP	+	-	-	-
ALB	-	+	-	-
A6	+	-	-	-
BD1	-	-	+	-
BDS7	-	-	+	-
c-kit	+	-	-	-
CK7	-	-	+	-
CK8	-	-	+	-
CK18	-	-	+	-
CK19	-	-	+	-
CD34	+	-	-	-
Desmin	-	-	-	+
GFAP	-	-	-	+
GGT	+	-	+	-
HES6	-	+	-	-
OC2	+	-	+	-
OC3	+	-	+	-
OV1	+	-	+	-
OV6	+	-	+	-
Thy-1	+	-	-	-

CHAPTER 3
SPECIFIC AIMS

The extraordinary regenerative capacity of the liver makes it one of the most resourceful viscera, able to restore its original mass during the next two weeks post injury. The first line of regeneration employed is represented by mature hepatocytes division, an ongoing process during the lifetime. Certain pathological contexts, such as massive acute hepatic necrosis and chronic long term injury result in impairment of hepatocyte division. Under these circumstances the liver stem cell compartment takes over, acting as a backup regenerative system.

The progenitor dependent compensatory hyperplasia takes place in the amplification compartment, composed of multiplying stem cells progeny known as oval "stem" cells and located traditionally in the canals of Hering[120]. Recent studies proved the bone marrow origin of at least one subpopulation of oval cells[107]. Their progenitor phenotype exhibits transitional features between hepatocytes and cholangiocytes and expresses markers evoking their bone marrow ancestry. Similar to the hepatocyte dependent compensatory hyperplasia, stem cell mediated liver regeneration is an orchestrated response induced by specific local and systemic stimuli which elicit sequential changes in gene expression, followed by growth factor production, cellular activation, proliferation, migration and differentiation.

The first and foremost question concerning oval cells is which signals are involved in oval cell activation and which cellular interactions are responsible for these signals? It is generally accepted that the different hepatic cell types influence the fate of oval cells by cell-to-cell interactions and also by creating an extracellular environment conducive for regeneration. The overarching question/hypothesis is in which interactions and to

what extent are hepatic stellate cells involved during oval cell activation, engraftment, and differentiation? The overall project goal is to explore the effects of stellate cell inhibition on oval cell activation, proliferation and differentiation. In order to test this hypothesis, two specific aims were designed:

Specific aim I: Test the hypothesis that stellate cells play a necessary role in facilitating oval cell proliferation in the liver. Several studies have shown that hepatic stellate cells are important in the early stages of oval cell proliferation[121, 122]. The complex interactions between these cell types are mediated both by cytokines and extracellular matrix proteins. Oval cells express many receptors for stellate cells-produced growth factors which may trigger regulatory molecular pathways for liver stem cell activation, growth and development. As a major source of ECM proteins, the stellate cells are involved in the recently described matricrine regulation[123]. They also remodel the extracellular environment, indirectly influencing the migration and the differentiating fate of oval cells. We hypothesize that stellate cell activation and proliferation is required for the oval cell mediated liver regeneration, being a major player in the complex cellular interactions which result in oval cell activation. To test the complex role of stellate cells we will utilize the well characterized 2-acetylaminoflourene/partial hepatectomy (2AAF/PHx) acute hepatic injury model associated with the L-Cysteine diet, a proven stellate cell inhibitor[124]. The specificity of L-cysteine inhibition was determined by in vitro treatment of stellate cells, portal fibroblasts and oval cells. Changes of oval cell activation were analysed for corresponding time points during the study.

Specific aim II: To test the hypothesis that in the absence of a robust stellate cell activation the oval cell activation is delayed. Liver regeneration is a very complex

process involving several cell-to-cell interactions. One of the histological features of diseased liver is the numeric imbalance between the hepatic cell types. In order to circumvent this issue and increase the chances of success for cell therapy, it might be necessary to inject more than one cell type. A potential mixture between oval cells and other hepatic cells (most likely stellate and Kupffer cells) might be necessary. Since the recruitment of monocytes is persisting to a certain extent in the ailing liver, it is possible to stimulate their hepatic homing by injecting monocyte specific chemoattractants. This chemokine mediated recruitment is not operating in the case of stellate cells and it might be necessary to isolate, expand and reinject them together with the oval cells. The exact speed of oval cell mediated liver regeneration is crucial for survival of patients with terminal hepatic failure. If too slow, the irreversible hepatic encephalopathy, coupled to the associated multiorgan dysfunction syndrome (MODS) could lead to a fatal outcome, despite of a promising onset of oval cell proliferation. For these reasons, even a delay in oval cell activation might prevent a successful outcome of oval cell therapy. There are several redundant mechanisms in the body and specifically in the liver. To determine if other hepatic cell types are compensating for the lack of adequate stellate cell contribution to oval cell mediated liver regeneration, the effects of stellate cell inhibition was analyzed quantitavely and also in terms of timing of the regenerative response. A general evaluation of regeneration was done comparatively for animals kept on the inhibiting diet comparative to control animals during the whole time course of the experiment. Samples collected at corresponding time points were immunostained for markers of stellate and oval cell activation and the positivity was assessed by quantitative analysis. Expression of AFP gene which is a hallmark for the regeneration

amplitude was assessed by real time PCR. A clearer picture of amplitude and timing of liver regeneration in the absence of robust stellate cell contribution emerged.

CHAPTER 4
METHODS AND MATERIALS

4.1 Animal Treatments

In order to test our hypothesis we combined an experimental model of oval cell activation with the stellate cell inhibition. The 2AAF/PHx protocol (a modern modification of the original Solt and Farber technique[95]) was utilized to induce the progenitor mediated liver regeneration, explore and characterize oval cell activation, proliferation and differentiation under various extraneous factors introduced in the experimental system. This well established model shown in Figure 4-1 makes possible the isolation of oval cells necessary for *in vivo* studies, but more importantly, overcomes the limitations of cell culture systems. Although informative, the *in vitro* studies can provide data limited to the proliferation and differentiation status of oval cell, but are not able to reproduce the complex molecular interactions which take place in the liver lobule. Our animal model reproduces in rats the pathological circumstances present in the liver of human patients suffering of chronic hepatic conditions which exhaust or inhibit the natural proliferative capacity of hepatocytes. 2AAF is a mitogen known to be metabolized by the cytochrome P 450 enxymes into its bgiologically active, N-OH derivatives. After entering the nucleus 2AAF metabolites form voluminous adducts with DNA, rendering it unable to be approached by the transcription apparatus. This results in cyclin D_1 and E inhibition, followed by G_1/S check point cell cycle arrest, as shown in Figure 4-2. The stellate cell inhibition was performed subjecting the laboratory animals to a diet supplemented with 2% L-cysteine, a non-essential amino acid. There are several proposed mechanisms for L-cysteine inhibition of stellate cells, as shown in Figure 4-3. Either by ROS (reactive oxygen species) inhibition of cyclin D_1, or PDGFRβ (platelet

derived growth factor receptor β) inhibition it suppresses the stellate cell activation in murine models of liver fibrosis[124].

4.1.1 Animals and Animal Housing Facilities

For this study we used Fisher 344 male rats obtained from Charles River Laboratories, Inc. (Wilmington, MA). Animals were housed in the Animal Care Services Facility in the Medical Science and Communicore Buildings. During the whole study, constant veterinary care was provided by the animal care facility: Animals were checked regularly and assistance with euthanasia decisions was provided.

The animal protocols used were approved by the University of Florida IACUC (Institutional Animal Care and Use Committee). The animal care program at University of Florida is accredited by AAALAC (American Association for the Accreditation of Laboratory Animal Care). University of Florida meets National Institutes of Health standards as described in DHHS publication #NIH 86-23. The PHS (Public Health Science) “Policy on Humane Care and Use of Laboratory Animals by Awardee Institutions” and the National Institute of Health “Principles for the Utilization and Care of Vertebrate Animals Used in Testing, Research and Training” are mandatory for the animal protocols at the University of Florida.

4.1.2 Animal Sacrifice and Tissue Collection

At determined time points a number of three animals were sacrificed for tissue collection. Each animal was euthanized by injection of 150 mg/kg Nembutal Sodium Solution (OVATION Pharmaceuticals, Inc., Deerfield, IL), according to Euthanasia D Special protocol. This procedure conforms to the recommendations of American Veterinary Medical Association and the Guide for the Use and Care of Laboratory Animals (US Department of Health and Human Services/NIH Publication #86-23).

Tissue samples were excised from various organs (brain, heart, lung, liver, pancreas, spleen, kidney and intestine) and collected for embedding in OCT compound, paraffin embedding, RNA and protein isolation. Tissue collected for cryosections was immersed in Tissue-Tek OCT Compound (Sakura Finetek USA Inc Torrance, CA), snap frozen in a 2-methylbutane histobath and stored at -80ºC until sectioning. Organ samples for paraffin embedding were fixed in 10% Neutral Buffered Formalin (Richard-Allan Scientific, Kalamazoo, MI) O/N (over night). After being transferred in PBS (phosphate buffered saline) the following day, the collected tissues were submitted to the University of Florida Molecular Pathology Core Facility for paraffin embedding. For histological analysis all samples used in our study were cut into 5 µm thick sections. Samples used for protein and RNA extraction were snap frozen in a 2-methylbutane histobath and stored at -80ºC until isolation was performed.

4.1.3 Oval Cell Induction in Rat

4.1.3.1 2AAF pellet implantation

2-Acetylaminofluorene (2AAF) is the DNA adducts forming mitogen used in our protocol to selectively inhibit hepatocyte proliferation. Its inhibitory activity on cyclins D_1 and E associated with the formation of voluminous DNA adducts blocks the cell cycle at the G_1/S checkpoint[125], as shown in Figure 4-2. It has been used for quite some time, administered by gavage to rats undergoing the 2AAF/PHx protocol. It has become commercially available in intraperitoneal slow release pellet (70mg/pellet over a 28 day release, Innovative Research of America Inc., Sarasota, FL, USA). In this form insures the quick absorption of an efficient dose of 2.5 mg/day.

The pellet is inserted seven days before the partial hepatectomy through a 0.5 cm long incision made in the left hind quadrant of the abdominal cavity. Prior to the

surgery, the animals were anesthetized with isofluorane. The abdomen was shaved and scrubbed in a centrifygal pattern three times with ethanol and three times with Betadine (Purdue Pharma L.P., Stamford, CT). After drapping the abdominal wall with a Steri-Drape (3M, St. Paul, MN) a 0.5 cm long incision was made in the lower left quadrant of the abdomen, ensuring a convenient distance from the liver. Midline incisions are discouradged, due to the post operatory fibrosis resulting in adhesions between the pellet and the hepatic tissue. The incision sectioned the skin, subcutaneous tissue, muscle and parietal peritoneum, allowing the pellet insertion into the abdominal cavity. The muscle was then sutured with 3-0 Vicryl (Ethicon, Inc., Cornelia, GA) and the skin was closed with the Autoclip Wound Closing System (Braintree Scientific Inc Braintree, MA). Post operatory the animals were housed in warmed cages and monitored every six hours until complete recovery. Ten days later the staples were removed. The potential complications, hemorrhage, dehydration and hypothermia, were absent.

4.1.3.2 Two-thirds partial hepatectomy

To induce compensatory hyperplasia, 70% partial hepatectomy is performed according to the protocol described by Higgins and Anderson[43]. Left lateral, left medial and right medial lobes of rat liver were removed. Prior to the surgery, the animals were anesthetized with isofluorane. The abdomen was shaved and scrubbed in a centrifygal pattern three times with ethanol and three times with Betadine (Purdue Pharma L.P., Stamford, CT).

The xyphoid process is palpated and after drapping the abdominal wall with a Steri-Drape (3M, St. Paul, MN) a 1.5 cm long midline incision was made. Skin, subcutaneous tissue and muscle are sectioned and the xyphoid process was removed. The three lobes were extruded through the incision and were tied off with silk. After

exposure, the lobes were removed and the stump hemostasis was performed. After carefully examining the abdominal cavity for signs of persisting hemorrhage, the abdominal wall was closed. Any post operatory bleeding is a fatal complication for animals. The muscle is sutured with 3-0 Vicryl (Ethicon Inc. San Angelo, TX). Autoclip Wound Closing System (Braintree Scientific, Inc.) was used for skin closure. Staples were removed ten days later. After surgery the animals were housed in warmed cages and monitored for post operatory complications until complete recovery. Dehydration, bleeding and hypothermia were not present. Animals were sacrificed at days 3, 5, 7, 9, 11, 13, 15, 17, and 20 days post-PHx.

4.1.4 2% L-cysteine Diet

The 6 week old Fisher 344 male rats (Charles River Laboratories, Wilmington MA) were maintained on standard laboratory chow supplemented with 2% L-cysteine (Dyets Inc. Betlehem, PA) for the duration of the experiment, according to a protocol established by Horie[124]. The diet was custom made by the manufacturer using standard rat food supplemented with laboratory purity standard L-cysteine (MP Biomedicals LLC, Cleveland OH). To identify any potential repulsion to the diet, which might incur unwanted consequences on the weight gain and introduce variables into the experiment, the animal reaction and feeding habits were monitored and their weight was measured daily. Since there were no differences in terms of food repulsion reactions and weight gain between the animals kept on diet and the control group kept on standard rat food, L-cysteine diet was offered *ad libitum* to the whole group of animals included in the experiment.

4.1.5 Animal Numbers

Several animal groups were included in this study. Besides normal liver, diet, 2AAF, diet/2AAF, diet/PHx controls, for each time point of animal sacrifice in the L-cysteine/2AAF/PHx group there was a corresponding 2AAF/PHx control. As table 4-1 shows, animals were sacrificed on days 1, 3, 5, 7, 9, 11, 13, 15, and 20 days after PHx. Animal numbers at the various time points and the experimental protocol they were subjected are shown in Table 4-1. All animals included in this study survived the experimental protocols performed on them.

4.2 BrdU Analysis – *In Vitro* Cell Response to L-cysteine

4.2.1 Maintenance of WB-F344, HSC T6 Cells and Portal Fibroblasts in Culture

WB-F344 oval stem cell line, graciously provided by Dr. William Coleman was cultured in chamberslides with RPMI-1640 medium (Mediatech Inc., Herndon VA) supplemented with 10% fetal bovine serum (Sigma Aldrich, St. Louis MO), 10 IU Penicillin/ml and 10 µg/ml streptomycin (Mediatech Inc., Herndon VA) in a 37°C humidified incubator containing 5% CO_2 and 95% air. The culture medium was changed every other day. Primary isolated portal fibroblasts, kindly provided by Dr. Rebecca Wells were maintained in chamberslides on DMEM medium (Hyclone Lab Inc., Logan UT) supplemented with 10% fetal bovine serum (Sigma Aldrich, St. Louis MO), 10 IU Penicillin/ml and 10µg/ml streptomycin (Mediatech Inc., Herndon VA) at 37°C, 5% CO_2 humidified incubator. Culture medium was replaced every other day. HSC T6 hepatic stellate cell line, kind gift from Dr. Robert Friedman, was cultured in chamberslides on DMEM F12 50/50 medium (Hyclone Lab Inc., Logan UT) supplemented with 10% fetal bovine serum (Sigma Aldrich, St. Louis MO), 10 IU Penicillin/ml and 10 µg/ml

streptomycin (Mediatech Inc., Herndon VA) in a 37°C humidified incubator containing 5% CO_2 and 95% air. The culture medium was changed every other day.

4.2.2 Cell Synchronization and BrdU Treatment

When each cell culture achieved 30% confluence, they were synchronized with 0.4 µg/ml Demecolcine (Sigma Aldrich, St. Louis MO), an inhibitor of mitotic spindle formation added to their respective culture media. When cell cycle was blocked in mitosis after 24 hours of exposure, demecolcine was washed and 100 µM L-cysteine (MP Biomedicals LLC, Cleveland OH) was added to the culture media, thus inhibiting the hepatic stellate cell activation. After a three day exposure to L-cysteine, the chamberslides were treated with 10 µM bromodeoxyuridine (BrdU) (Sigma Aldrich St. Louis, MO) and fixed in 4% paraformaldehyde.

4.3 Histology and Immunohistochemistry

4.3.1 Hematoxylin and Eosin Staining of Paraffin Embedded Tissue

5 µm thick tissue sections were cut and placed in a 42ºC water bath. After being mounted to a Superfrost Plus slide (Thermo Fisher Scientific Inc. Waltham, MA) the sections were air dried overnight (O/N) at room temperature (RT). The sections were deparaffinized by immersing them in xylene for 2 x 5 minutes. Further immersion in several baths of ethanol rehydrated the sections: 100% ethanol 2 x 2min, 95% ethanol 2 x 1min, and distilled H_2O for 1min. Nucleic acids were stained with hematoxylin 7211 (Richard-Allan Scientific, Kalamazoo MI) for 2min and rinsed with H_2O for 2 x1min. Consecutive baths of clarifier 1 (Richard-Allan Scientific, Kalamazoo MI) for 1min, distilled H_2O for 1min, bluing reagent (Richard-Allan Scientific, Kalamazoo MI) for 1min, distilled H_2O for 1min, and 80% ethanol for 1min intensified the hematoxylin color. For cytoplasm staining was used eosin-Y (Richard-Allan Scientific, Kalamazoo MI) for 1min

30 sec. Several baths of 2 x 1min 95% ethanol, 2 x 1min 100% ethanol, and 3 x 1min xylene dehydrated the sections before coverslipping with Cytoseal XYL (Richard-Allan Scientific, Kalamazoo MI).

4.3.2 Periodic Acid-Schiff Staining of Paraffin Embedded Tissue

5 µm thick tissue sections cut and mounted to a Superfrost Plus slide (Thermo Fisher Scientific Inc. Waltham, MA) air dried O/N at RT were deparaffinized and rehydrated according to the same protocol described above. They were immersed 5 min in Periodic Acid solution (Richard-Allan Scientific, Kalamazoo MI), rinsed in distilled H_2O, stained with Schiff Reagent (Richard-Allan Scientific, Kalamazoo MI) for 15 min and rinsed for 10 min in lukewarm tap H_2O. After 1 min hematoxylin staining, 30 sec rinsing in distilled H_2O, bluing for 1 min, rinsing for 30 sec in distilled H_2O, the sections were dehydrated 2x1 min in 100% alcohol. Sections cleared in 3x1 min baths of clearing reagent were mounted with with Cytoseal XYL (Richard-Allan Scientific Kalamazoo, MI).

4.3.3 Immunohistochemistry

4.3.3.1 Chromogen staining

Paraffin and frozen sections were incubated O/N at 4ºC for primary antibody and 30 min for secondary antibodies, then stained using Vector ABC, DAB (Diaminobenzidine) (Vector Laboratories Burlingame, CA) as per manufacturer's instructions. DAB slides were counterstained with Vector Hematoxylin QS (Vector Laboratories Burlingame, CA) and mounted with Cytoseal XYL (Richard-Allan Scientific Kalamazoo, MI). Aditional antigen retrieval methods are mentioned, together with the antibodies, in Table 4-2.

4.3.3.2 Fluorescent staining

5 µm thick frozen sections were cut and placed on Superfrost Plus (Thermo Fisher Scientific Inc. Waltham, MA). The sections were air dried for 5 min at RT and fixed for 10 min in ice cold methanol. After 5 min incubation in TBS plus 0.1% Tween (TBS-T) and 20 min serum block, the slides were incubated with the primary antibody for 1 hr at RT or O/N at 4ºC. Slides were then washed for 5min in 1X TBS-T at RT and incubated with a fluorochrome labeled secondary antibody for 30 min. After being washed again for 5 min in TBS-T at RT the slides were coverslipped with Vectashield Mounting Media with DAPI (Vector Laboratories).

5 µm thick paraffin sections were cut and placed on Superfrost Plus slides (Thermo Fisher Scientific Inc. Waltham, MA). Two xylene baths of 5 min each were used for deparafinization. The slides were then rehydrated by immersing in successive baths of 100% ethanol (2 x2 min), 95% ethanol (3 min), 70% ethanol (1 min) and H_2O (2 x 1 min). After antigen retrieval at 95°C using Dako Target Retrieval 1X (Dako, Carpinteria, CA - see table 4-2 for details) and serum block, the slides were exposed O/N to a mixture of rabbit anti rat Ki67 antibody (Novocastra - Leica, Bannockburn, IL) and mouse antihuman desmin clone D33 (Dako, Carpinteria, CA). The slides were washed in 1X TBST (Tris buffered saline with 0.1% Tween), incubated with fluorochrome conjugated secondary antibodies for 30 min at RT. After washing they were coverslipped with Vectashield Mounting Media with DAPI (4', 6-diamidino-2-phenylindole), (Vector Laboratories Burlingame, CA). Fluorescence was observed and photographed with a fluorescent microscope: BX51 Olympus Fluorescent microscope fitted with cubes for FITC (Fluorescein isothiocyanate), Texas Red, DAPI and dual pass FITC/Texas Red, and Optromic Digital Cemera with Image Pro 3.1 Software and

Magnafire 3.1. Computer image analyses of immunostained sections was performed using Aperio ScanScope Image Analysis Platform (Aperio, Vista CA) and MetaMorph software (MDS Technologies, Concord ON, Canada) for histological evaluation and quantitation.

4.4 RNA Analysis – Real Time Quantitative PCR

The mRNA (messenger RNA) levels were assessed by two-step quantitative real-time PCR (Polymerase chain reaction) reaction, using a DNA Engine Opticon 2 Continuously Fluorescence Detector (MJ Research Inc Waltham, MA). Total RNA was extracted using the RNA Bee isolation kit (Tell-Test Inc. Friendswood, TX), treated with Dnase I (Deoxyribonuclease I) (Ambion, Austin, TX) and reverse transcribed with the Superscript III First Strand Synthesis System for rt PCR (Reverse transcription polymerase chain reaction), (Invitrogen, Carlsbad, CA). Amplification was performed on a customized RT2Profiler PCR Array plate for the genes of interest (SA Biosciences, Frederick, MD) using iQ SYBR Green Supermix (Bio-Rad Laboratories, Hercules, CA).

4.4.1 RNA Isolation

4.4.1.1 Tissue homogenization and phenol-chloroform phase separation

50 mg liver tissue samples kept on ice were homogenized in 1ml of RNABee Reagent (Tel-Test, Inc. Friendswood, TX). Then 0.2 ml of chloroform per 1ml of RNABee Reagent was added and the tubes shaked for 30 sec and incubated on ice for 15 min. The samples were then centrifuged at 12,000 x g for 15 min at 4°C and, as a result, the lysate separated into a lower blue, phenolchloroform phase, a white opaque interphase, and a colorless upper aqueous phase. RNA remains exclusively in the aqueous phase which makes for approximately 50% of the mixture volume.

4.4.1.2 Precipitation, washing and redissolving of RNA

The aqueous phase is carefully aspirated and transferred to a fresh tube. Aspiration of interphase would result in RNA contamination and compromise its quality. RNA is precipitated from the aqueous phase by adding 600 µl isopropyl alcohol for each 1ml of RNABee Reagent used for the initial homogenization. The samples were then incubated at RT for 10 min and centrifuged at 12,000 x g for 5 min at 4°C. The RNA precipitates as a white gelatinous pellet on the side of the tube.

The supernatant was discarded, the pellet was resuspended and vortexed in 1 ml 75% ethanol, then centrifuged for 5 min at 7 500 x g at 4°C. For a better quality of extracted RNA, the washing step was repeated. The supernatant was decanted and the RNA pellet was air-dried for 5-10 min, avoiding it being dryed completely, as this would greatly decrease its solubility. The RNA was dissolved in RNase-free water and stored at -80°C.

4.4.1.3 Quantification of RNA by spectrophotometry

The RNA was diluted by mixing 1 µl of RNA sample with 99 µl of DEPC-treated H_2O (Diethyl Pyrocarbonate-treated H_2O). For this solution, the absorbance at OD (Optical density) of 260 nm and 280 nm was measured by a spectrophotometer. RNA purity was determined based on an OD 260/280 ratio and found between 1.6 – 1.9. The concentration of RNA was determined using the following formula:

RNA (ng/µl) = OD 260 × 40 ng/µl × dilution factor of 100

4.4.2 Real Time PCR (RT PCR)

4.4.2.1 First-strand cDNA synthesis from total RNA using rt PCR

First strand cDNA was synthesized using SuperScript III First-Strand Synthesis System (Invitrogen Carlsbad, CA) according to manufacturer's instructions:

- A volume of solution containing 5 µg RNA was mixed with
- 1µl 10 mM dNTPs (Deoxynucleotide triphosphate),
- 1µl oligodTs (oligodeoxythymidylic acid) and
- DEPC H2O was added up to 10 ml.

After a short spin, the mixture was incubated at 65°C and then kept on ice for 1 min. In the meantime the cDNA (Complementary DNA) synthesis mix was prepared by mixing:

- 2µl 10X RT buffer B,
- 4µl 25 mM MgCl2,
- 2µl 0.1M DTT (Dithiothreitol),
- 1µl Rnase OUT (40 U/µl) and
- 1µl Superscript III RT (200 U/µl).

10µl of cDNA synthesis mix was added to each RNA/primer mixture, mixed, briefly centrifugated and incubated for 50 min at 50°C. The reaction was terminated at 85°C for 5 min and then was chilled on ice. After a brief centrifugation, 1 µl of Rnase H was added to each tube and incubated for 20 min at 37°C.

4.4.2.2. PCR amplification of target cDNA

cDNA was amplified using GAPDH (Glyceraldehyde-3-Phosphate Dehydrogenase) primers as a loading control for the RT PCR reaction. The following reaction mixture prepared on ice was used:

- 2 µl 10X PCR buffer B,
- 0.6 µl 25mM MgCl2,
- 0.4 µl 10mM dNTP mix,
- 1 µl GAPDH forward primer,
- 1 µl GAPDH reverse primer,
- 13.81 µl H2O, 1 µl cDNA and
- 0.2 µl Taq polymerase (5 U/µl).

The GAPDH primers used for the reaction had an annealing temperature of 58°C and produced a 577 bp cDNA:

- Forward primer TGA GGG AGA TGC TCA GTG TT
- Reverse primer ATC ACT GCC ACT CAG AAG AC

Taq polymerase was added immediately before samples were placed in a thermocycler. The PCR reaction was run as follows:

1. 94°C for 10min
2. 31 cycles of
   - 94°C for 30 sec
   - Annealing temp 58°C for 30 sec
   - 72°C for 30 sec
3. 72°C for 10min
4. 4°C indefinitely

4.4.2.3 Agarose gel electrophoresis

The 0.7% w/v (wheight per volume) agarose gel for cDNA electrophoresis was prepared by microwaving agarose with 30 ml 0.5 X TBE. When the agarose was completely dissolved, 0.001% v/v (volume per volume) ethidium bromide was added. Then, the gel was poured into a gel poring apparatus and, after inserting the well comb, it was left to solidify. The comb was removed before placing the gel pouring apparatus in the gel electrophoresis chamber. 0.5X TBE was added to cover the gel and the wells were loaded with a mixture of 0.5 µl of 10X agarose gel loading buffer, 3.5 µl of Milli-Q H_2O and 1 µl of each cDNA sample. One well loaded with an appropriate base pair ladder was used to identify the cDNA of interest. The gel was run at 90 – 110 volts until the desired separation of bands was achieved. Pictures of cDNA bands were taken with a GelDoc XR (Bio-Rad Hercules, CA) apparatus.

4.4.2.4 Real-Time PCR analysis of AFP levels

To accurately assess the variations of AFP message levels after L-cysteine exposure at day 9 post hepatectomy in animals subjected to 2AAF/PHx protocol, Real Time PCR quantitative analysis was performed using an $RT^2Profiler^{TM}$ PCR array produced by SA Biosciences (Frederick, MD). The PCR microarray plate used had

primers for beta-actin, rat genomic DNA contamination, AFP, RT PCR control and rt PCR control. The amplification conditions were:

1. 94°C for 10min
2. 40 cycles of
   - 95°C for 15 sec
   - 55°C for 30 sec
   - 72°C for 30 sec
3. 72°C for 10min
4. 4°C indefinitely

The comparative Ct threshold cycle method was used to assess the expression level, normalized to β-actin mRNA expression.

4.5 Statistical Analysis

Values were expressed as mean +/- standard deviation (SD). Statistical significance was determined by ANOVA, and student t- test performed in Microsoft Excel. p values <0.05 were considered statistically significant.

4.6 Solutions

10X Agarose Gel Loading Buffer

1. 15.0 mg bromophenol blue
2. 15.0 mg xylene cyanol
3. 8.0 g sucrose
4. Milli-Q H_2O qs to 10 ml

10X PBS (Phosphate buffered saline)

1. 80.0 g NaCl
2. 2.0 g KCl
3. 11.5 g $Na_2HPO_4 \times 7H_2O$
4. 2.0g KH_2PO_4
5. Milli-Q H2O qs to 1 L

5X TBE (Tris-Borate-EDTA Buffer)

1. 54 g Tris base.
2. 22.5 g Boric acid,
3. 4.7 g EDTA (Ethylenediaminetetraacetic Acid),
4. Milli-Q H2O qs to 1 L

10X TBS

1. 80.0 g NaCl
2. 2.0 g KCl
3. 30.0 g Tris base
4. 800 ml H_20
5. Milli-Q H_2O qs to 1L

Adjust pH to 7.4 using 1M HCl

DEPC water

1. Diethylpirocarbonate 1ml
2. Milli-Q H2O 999ml

After being mixed well and let set at RT for 1 hour, it was autoclaved at 121°C for 60 min and let cool at RT before use.

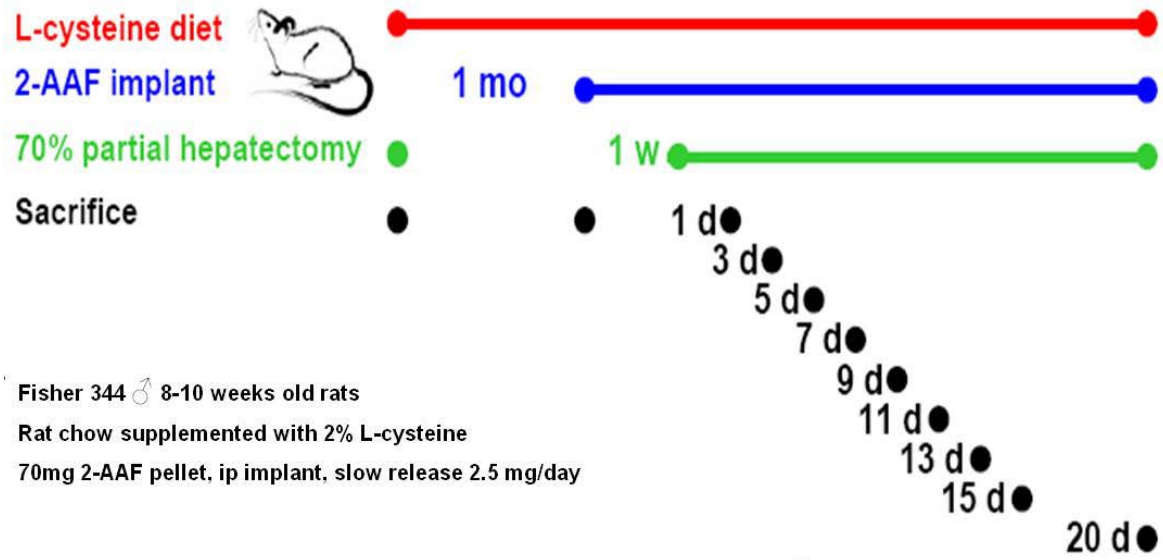

Figure 4-1. Diagrammatic representation of the 2% L-cysteine diet/2AAF/PHx experimental protocol, combining chemical inhibition of hepatic stellate cells and oval cell activation.

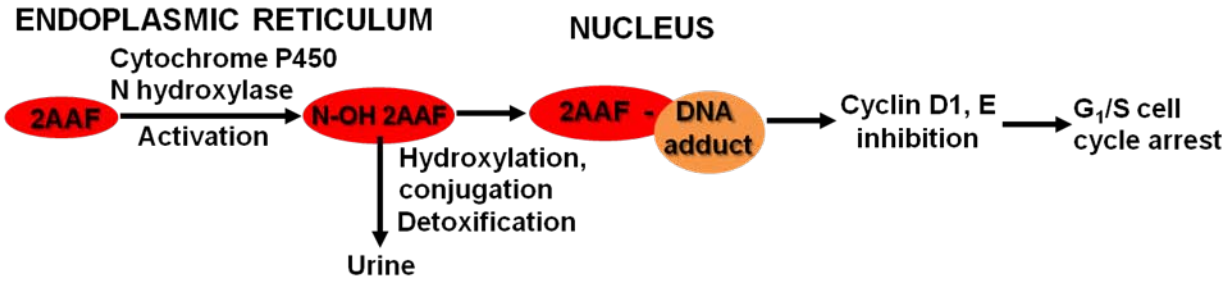

Figure 4-2. Mechanism of action, metabolic activation and detoxification of 2AAF (2-acetylaminofluorene), N-OH 2AAF (N hydroxyl 2AAF), G_1/S – checkpoint between G_1 and S phase of cell cycle.

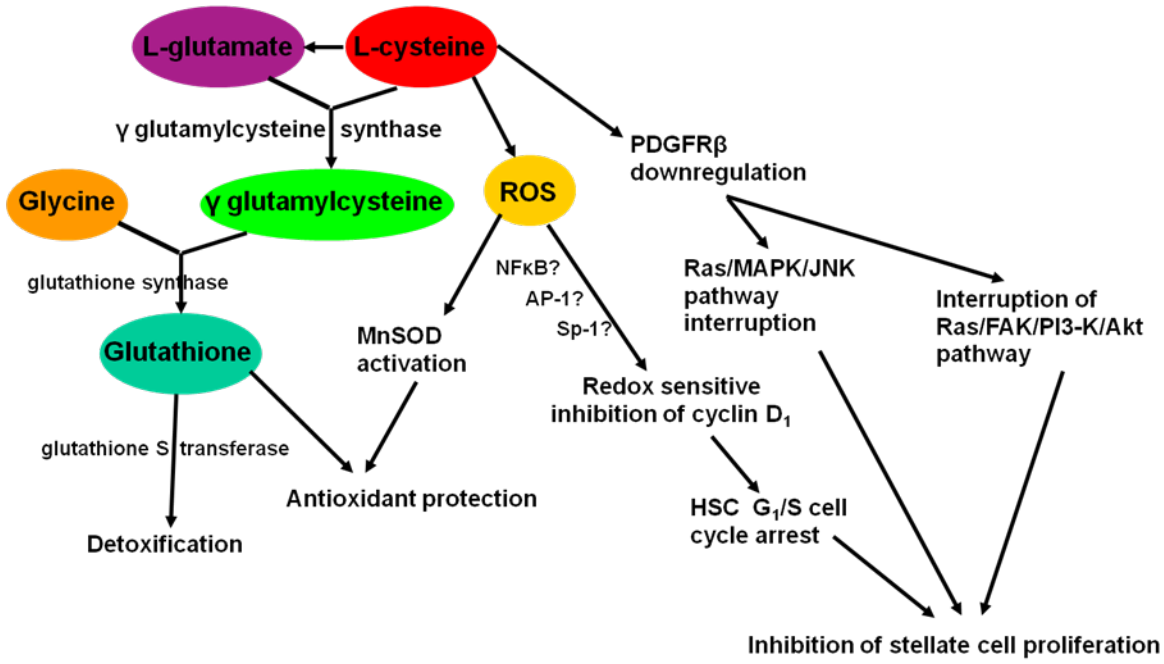

Figure 4-3. Proposed mechanisms for 2AAF inhibition of hepatic stellate cells: glutathione mediated, ROS mediated G1/S cell cycle arrest, PDGFR-beta downregulation with proliferation inhibiting effects; ROS – reactive oxygen species, MnSOD – manganese superoxide dismutase, NFkB – Nuclear factor kappa-light-chain-enhancer of activated B cells, AP-1- activator protein 1, Sp-1 – transcription factor, PDGFR-β – platelet derived growth factor receptor beta, Ras small GTPase involved in signal transduction, MAPK – Mitogen-activated protein kinase, JNK – c-Jun N-terminal kinase, FAK – focal adhesion kinase, PI3-K – Phosphatidylinositol 3 – kinase, Akt – protein kinases B family.

Table 4-1. Animals subjected to the stellate cell inhibition – oval cell activation L-cysteine/2-AAF/PHx protocol.

Time point	Number of animals	Experimental protocol
Control normal	3	No experimental procedure performed
Control diet	3	L-cysteine diet alone
Control 2AAF	3	2AAF ip implanted
Control diet/2AAF	3	L-cysteine diet, 2AAF ip implanted
Control diet/PHx	3	L-cysteine diet, 70% PH
Control 2-AAF/PHx	3 per time point	2AAFip implanted, 70% PH
Diet/2AAF/PHx day 1	3	L-cysteine, 2AAF ip implanted, 70% PH
Diet/2AAF/PHx day 3	3	L-cysteine, 2AAF ip implanted, 70% PH
Diet/2AAF/PHx day 5	3	L-cysteine, 2AAF ip implanted, 70% PH
Diet/2AAF/PHx day 7	3	L-cysteine, 2AAF ip implanted, 70% PH
Diet/2AAF/PHx day 9	3	L-cysteine, 2AAF ip implanted, 70% PH
Diet/2AAF/PHx day11	3	L-cysteine, 2AAF ip implanted, 70% PH
Diet/2AAF/PHx day13	3	L-cysteine, 2AAF ip implanted, 70% PH
Diet/2AAF/PHx day15	3	L-cysteine, 2AAF ip implanted, 70% PH
Diet/2AAF/PHx day20	3	L-cysteine, 2AAF ip implanted, 70% PH

Table 4-2. Antibodies and antigen retrieval methods used for immunohistochemistry

Protein	Animal	Retrieval	Concentration	Manufacturer	Cat. #
BrdU	mouse	10mM Na-citrate pH6	1:50	Dako	M0744
Ki67	mouse	10mM Na-citrate pH6	1:300	BD Pharmingen	556003
AFP	rabbit	Trilogy	1:600	Dako	A0008
OV6	mouse	N/A	1:150	Dr. Stuart Sell laboratory	N/A
Desmin		Dako Target Retrieval 1x	1:50	Dako	M0760
Ki67	Rabbit	Dako Target retrieval	1:2000	Novocastra-Leica	NCL-Ki67p

CHAPTER 5
RESULTS

Previous studies conducted by our laboratory have demonstrated that chemical suppression of transforming growth factor–beta (TGFβ) mediated up-regulation of connective tissue growth factor (CTGF) resulted in a greatly diminished oval cell response to 2-acetylaminofluorene/partial hepatectomy (2AAF/PHx) in rats. We hypothesized that this effect is due to decreased activation of hepatic stellate cells. In order to test this hypothesis, we maintained rats on a diet supplemented with 2% L-cysteine as a means of inhibiting stellate cell activation during the oval cell response to 2AAF/PHx.

In vitro experiments demonstrate that L-cysteine did, indeed, inhibit the activation of stellate cells. Desmin immunostaining of liver sections from 2AAF/PHx animals indicated that maintenance on the L-cysteine diet resulted in an 11.1-fold decrease in the number of activated stellate cells within the periportal zones. No direct effects on oval cells, regarding the proliferation index or phenotypical chages were observed.

The total number of cells proliferating in the periportal zones of livers from animals treated with L-cysteine was drastically reduced. Further quantitative analyses using immunostaining for both OV6 and AFP demonstrated a greater than four-fold decrease in the magnitude of the oval cell response in animals maintained on the L-cysteine diet. Global liver expression of AFP as measured by real-time PCR was shown to be decreased 4.7-fold in the L-cysteine treated animals. These data indicate that the activation of hepatic stellate cells is required for an appropriate oval cell response to 2AAF/PHx.

5.1 Evaluation of *in vitro* Response to L-cysteine of Selected Hepatic Cell Populations

Since the direct effects of L-cysteine on hepatic stem cells hasn't been explored yet, before starting the *in vivo* model we evaluated its *in vitro* effects on the oval cells, quiescent stellate cells and portal fibroblasts. WB-F344 cells, the only oval cell line currently available, were maintained on RPMI-1640 medium Primary isolated portal fibroblasts are a hepatic population rich in myofibroblasts exhibiting a phenotype very similar to the activated stellate cells. HSC T6 cells are the only available quiescent hepatic stellate cell line and were maintained under the same conditions in DMEM F12 50/50 medium.

When the desired confluence was achieved, the cells were synchronized with Demecolcine and then treated with L-cysteine for three days. The choice of L-cysteine was dictated by its proven capacity of inhibiting the hepatic stellate cell activation both *in* vivo and *in vitro* in murine liver fibrosis models. The cells undergoing the S-phase were identified by BrdU incorporation into newly synthesized DNA and immunostaining with anti BrdU antibodies.

Less is known about the L-cysteine effects on oval cells. In order to exclude a potential direct interference with their phenotype and proliferation attributable to L-cysteine, the hepatic progenitor cell line WB F344 was cultured both with and without L-cysteine in the culture medium. We weren't able to identify any visible changes in the WB F344 morphology under any of these circumstances examined (Figure 5-1 A and B). We determined that the BrdU incorporation index was similar for both L-cysteine treated and untreated cells. Figure 5-4 suggests that L-cysteine has no effect on the proliferation rate of these cells.

We next examined primary portal myofibroblast cultures (Figures 5-2 A and B), as well as the hepatic stellate cell line HSC-T6 (Figures 5-3 A and B). In contrast to the progenitor cell line, both of the mesenchymal cell cultures demonstrated a significant reduction in proliferation rates when culture media was supplemented with 100 µM L-cysteine. It's worth mentioning that HSC T6 cells are non activated stellate cells, whilst portal fibroblasts are terminally differentiated mesenchymal cells thought to derive, at least in part, from activated stellate cells.

Quantitative image analysis was performed in order to determine the BrdU incorporation index which reflects the comparative proliferative capacity of the examined hepatic cell populations. A 3.56-fold decrease in BrdU incorporation for HSC T6 and a 5.6-fold reduction for portal fibroblasts were observed (Figure 5-4). Taken together, quantitative image analysis data suggest that L-cysteine acts selectively on the mesenchymal cell populations examined. L-cysteine appears to be a selective in vitro inhibitor of hepatic mesenchymal populations examined.

5.2. Evaluation of *in vivo* Response of Hepatic Stellate Cells to L-cysteine Diet

Desmin immunofluorescent staining was performed on liver samples collected 9 days after acute injury during the 2AAF/PHx protocol as a preliminary step in assessing the stellate cell activation *in vivo.* The deliberate choice of day 9 post hepatectomy as a reference time point in our study is dictated by the peak of oval cell activation observed constantly at this particular time in the animals subjected to the 2AAF/PHx protocol. We have observed a global reduction of desmin expression in animals exposed to L-cysteine (Figure 5-5). Since tissue morphology is not visible on IF (Immunofluorescence) labeled cryosections, it was difficult at this stage to discern which cells are responsible for the noted difference in hepatic desmin expression. Further

immunostaining of paraffin sections was performed in order to reveal the phenotype of desmin positive cells.

Normal liver tissue expresses desmin in endothelial cells, myofibroblast-like cells which surround the arteries in the portal space and in activated stellate cells scatered throughout the hepatic parenchyma, as Figure 5-6 shows. In the areas located outside the periportal zones, the presence of desmin positive cells is very seldom. Under pathological circumstances generated by any form of liver injury, desmin positive cells are present in higher numbers in close proximity to the necrotic cells, being observed among the early post injury changes[128].

As a consequence of the hepatectomy injury in our model, numerous desmin positive hepatic stellate cells are present in the acinar zone one, in close proximity to the small oval-shaped cells which are the regenerating phenotype in the 2AAF/PHx model. Interestingly, the radiating pattern of oval cell migration toward the centrolobular area is followed by the stellate cells which seem to extend projections around the progenitors, as Figure 5-7 A) and B) shows. When L-cysteine exposure was added, a considerable lower number of desmin positive stellate cells were present in the periportal areas. Not restricted to the perivascular structures, these cells are in higher number than in the normal liver and are also spatially associated with the same oval shaped phenotype, as seen in Figure 5-7 C) and D).

For a more accurate assessment of the stellate cell activation status, a quantitative computer image analysis was performed. A significant 11.1-fold reduction in hepatic pericyte presence on the entire liver section was observed when the animals were exposed to L-cysteine, as opposed to the situation when only the oval cell activation

protocol was performed (Figure 5-8). Taken together, these data suggest that L-cysteine has an inhibitory effect on the hepatic stellate cell population *in vivo*.

5.3. Evaluation of Cell Morphology in L-cysteine/2AAF/PHx Treated Rats

Histological characterization of liver regeneration in the 2-AAF/PHx model for rat oval cell activation demonstrated the expected robust proliferation of smaller oval-shaped cells emanating from the portal zone (Figure 5-10 A and B). These cells were not present in untreated rat liver (Figure 5-9 A and B). In animals that were maintained on the 2% L-cysteine diet the small oval cell response in the portal zone remained quite modest (Figure 5-10 C and D).

The disparity between the amplitude of the small oval cell response in the two groups is most evident on days 9 post partial hepatectomy. This time point is known to coincide with the peak of oval cell proliferation following 2AAF/PHx in rats. Aside from the reduced oval cell presence in L-cysteine treated animals, there is also a notable difference in cell morphology. In the L-cysteine treated group, the cells tended to be larger (over 10μm diameter) with a slightly reduced nucleus to cytoplasm ratio, more rounded nuclei and basophilic or vacuolar cytoplasm (Figure 5-10 C and D).

The comparative analysis of liver morphology for the two animal groups studied was further performed for all time points. The histological exam of liver samples from animals kept on hepatic stellate cell inhibitory diet revealed a delayed onset of oval cell response after 2-AAF/PHx injury. By day 3 post hepatectomy very few portal spaces had isolated cells (1-2/field) with morphology suggestive for the oval cell phenotype (Figure 5-11 B). The control group which was submitted only to the 2-AAF/PHx treatment displayed by day 3 a robust onset of progenitor-like oval cell presence in the peri portal spaces (Figure 5-11 A), spreading into the acinar zone I by day 5 (Figure 5-

11 C). The oval cell response remains very modest during the first week in the diet group (Figure 5-11 D) and the individual cell morphology observed in both groups is suggestive for oval cells in Roskams[90] classification (Figures 5-11 and 5-12 A and B).

The disparity between the amplitude of the regenerative response in the two groups persists on days 9 and 11, the peak of oval cell activation in 2-AAF/PHx model, as shown in Figures 5-10 and 5-12 B and D. The newly observed cells on day 9 sections are more numerous by day 11, as seen in Figure 5-12 D). Their morphology is closer in appearance to the small hepatocyte-like phenotype, named by Roskams[50] intermediate hepatocyte-like cells and is the center of a controversy over being considered an intermediary differentiating stage of oval cells or a distinct immature progenitor population, as Best and Coleman[126] suggest. Unfortunately, because of the lack of reliable markers, it is hard to discern at this stage if they are indeed the progenitor subset described by the above mentioned authors, or oval cells which already made the commitment toward the hepatocyte lineage.

In the end of the second week and during the third week post hepatectomy the oval cell response gradually decreases in the 2-AAF/PHx group (Figure 5-13 A and C). In these animals, by day 20 most of the oval cells have undergone differentiation and only few cells with morphology suggestive for the oval cell phenotype are visible in the periportal space (Figure 5-13. C). The regenerating response is still vigorous in the L-cysteine exposed group and interestingly, most of the cells exhibiting small hepatocyte-like phenotype start having clear vacuoles in their cytoplasm (Figure 5-13 B and D). The presence of vacuoles is indicative of intense metabolic activity and metabolite storage in these small hepatocyte-like cells. They appear clear on Hematoxylin and Eosin stained

sections suggesting that they might hold a lipidic material. In the end of the third week posthepatectomy almost the entire zone I of the acinus is occupied by cells with small hepatocyte-like morphology and clear vacuoles in the cytoplasm, but small islands of oval cells are still visible among the small hepatocyte-like cells (Figure 5-13 D).

Although L-cysteine and 2-AAF by themselves could be incriminated for inducing this particular phenotype, our control images show that neither L-cysteine alone (Figure 5-14 D), nor in combination with 2AAF (Figure 5-14 B), administered to animals kept under identical conditions induce clear vacuole formation in hepatocytes' cytoplasm. The presence of these vacuoles could be the result of either increased liponeogenesis from glucose, or a form of lipid storage. Periodic acid Schiff (PAS) staining was performed in order to identify if glycogen, the storage form of glucose is present, as a substrate for increased liponeogenesis in small hepatocyte-like cells. Normal liver has few glycogen in the periportal area, due to the acinar zone I hepatocytes' propensity to glycogenolysis, as Figure 5-15 shows. Day 11 post hepatectomy was chosen as timepoint for this staining, due to the presence at this stage of a larger number of small hepatocyte-like cells. On images from animals subjected only to the 2AAF/PHx protocol, we haven't noticed glycogen inside the cytoplasm of oval cells or periportal hepatocytes, as expected (Figure 5-16 A and B). Interestingly, the animals kept on diet had glycogen only in the cytoplasm of zone III mature hepatocytes, but not in the vacuolated small hepatocyte-like cells (Figure 5-16 C and D). It is possible that the content of cytoplamic vacuoles in transitional hepatocytes to be of lipid origin. PAS staining results suggest that lipid presence might be the result of increased storage and not of active liponeogenesis from glucose.

5.4. Evaluation of Cell Proliferation in Regenerating Liver under L-cysteine Exposure

We next sought to determine the proliferation status of the cells within the periportal zones of livers from 2AAF/PHx treated animals both with, and without the L-cysteine diet. Immunostaining for Ki67 nuclear antigen was performed on samples collected on day 9 following PHx. Ki67 identifies all cells that have exited the quiescent state, G_0, and have entered the cell cycle .

Hepatocytes are the cell population which normally proliferates after hepatic injury. In the absence of any lesion, hepatocytes only divide to replace the aged cells which suffer apoptosis. Thus, in the normal liver very few hepatocytes, mainly localized in the periportal zone proliferate, as Figure 5-17 shows. A large number of proliferating cells were present in the periportal zones of rat liver subjected to the 2AAF/PHx protocol, as seen in Figure 5-18 A) and B). Considerably fewer cells were Ki67 positive on the sections collected from animals kept on L-cysteine diet (Figure 5-18 C) and D). The quantitative image analysis performed on these sections showed a 3.96 fold reduction in the number of proliferating cells in the periportal zones of the liver from rats maintained on the L-cysteine diet, as seen in Figure 5-19. These data suggest that L-cysteine exposure is associated with reduced cell proliferation in periportal areas. They also indicate a significant reduction of oval cell contribution to hepatic mass recovery.

A double IF (immunofluorescent) staining was performed to investigate if the reduced proliferation correlates with low levels of stellate cell activation in the L-cysteine treated liver. Sections were stained for Ki67 and desmin and in normal liver very few hepatocytes, mainly located in the limiting plate, are proliferating (Figure 5-20). Desmin is an intermediary filament which is present in the activated stellate cells and the

vascular wall. In the normal liver is very hard to identify the activated stellate cells located in the normal hepatic parenchyma because of their scarcity, but the myofibroblasts, their active form, are present around the portal triad, as shown in Figure 5-20.

The liver exposed to 2AAF and PHx has a very robust population of cells with ovoid nuclei positive for Ki67. Numerous desmin positive activated stellate cells are seen in the periportal areas, in close proximity to the Ki67 positive cells. The stellate cell projections are wrapped around the proliferating oval cells, as seen in Figure 5-21 A and B. In contrast, on sections collected from animals maintained on L-cysteine diet considerably fewer Ki67 positive proliferating oval cells are present. The desmin presence is reduced too, confirming the effectiveness of L-cysteine inhibition of stellate cell activation. The spatial distribution of Ki67 and desmin positive cells is similar to the pattern observed in the 2AAF/PHx group (Figure 5-21 C and D). Taken together, these results suggest that the observed reduction in the oval cell proliferation is associated with decreased stellate cell activation induced by L-cysteine diet.

5.5. AFP Expression in Periportal Regions of Regenerating Liver

Alpha-feto protein (AFP) is a fetal globulin found in adult liver only in hepatocellular carcinoma, rarely in cholangiocarcinoma, but constantly in the oval stem cells. Known as a marker of their non-terminally differentiated status, it is currently used to identify the oval cell population. As expected, on the normal liver sections used as controls no AFP positive cells were apparent, as Figure 5-22 shows. Under normal circumstances very few oval cells are present in the canals of Hering and they are rarely seen on light microscopy sections.

Sections collected from animals subjected to the 2AAF/PHx protocol alone, or in association with L-cysteine diet were examined for AFP positive cells. As expected, the portal zones of livers from 2AAF/PHx treated animals contained a large population of AFP positive cells (Figure 5-23 A and B). They exhibit the characteristic radiary migration from the periportal space towards the centrolobular vein. The phenotype of these positive cells correlates with Roskams description of oval cells, having an oval-shaped nucleus and reduced nucleus to cytoplasm ratio.

A sensibly lower presence of AFP positive cells was observed on the sections from L- cysteine treated group. Some cells exhibited oval cell phenotype. It is worth noting though, that a greater percentage of the cells within the portal zones of livers from animals maintained on the L-cysteine diet appeared to be transitional hepatocytes (small hepatocyte-like cells). Morphologically, they are larger than the average diameter of an oval cell (5-10 µm), but smaller than a mature hepatocyte (20-30 µm). On Hematoxylin and Eosin stained sections their cytoplasm is basophilic (Figures 5-12 D and 5-13 B) and they express weakly AFP, as shown in Figure 5-23 C) and D).

Quantitative image analysis of scanned liver samples revealed that in the animals exposed to L-cysteine there was present a 4.3-fold decrease in AFP positive areas (Figure 5-24).

Global AFP expression in the livers of animals subjected to 2AAF/PHx was determined by quantitative real-time PCR (Figure 5-25). AFP message was measured relative to the normal liver and normalized to beta actin. Animals that were exposed to L-cysteine demonstrated a 4.7-fold decrease in total liver expression of AFP as

compared to animals that were fed the normal diet. These results suggest a significant reduction of oval cell contribution to hepatic mass recovery.

5.6 Immunohistochemical Identification of Progenitor Cell Population

An alternative oval cell marker was used to confirm the findings of the AFP immunostaining. OV6 is a well characterized marker for oval cells and bile duct cells, binding to both CK 14 and CK 19 (cytokeratins 14 and 19) present in the oval cells. In normal liver, only the bile ducts within the portal triad were positive for OV6, due to their characteristic expression of CK 19 in the cytoskeleton (Figures 5-26) and to a reduced presence of oval cells under physiological circumstances.

Cryosections collected from animals subjected to 2AAF/PHx contained a large population of OV6 positive cells within the periportal zone that radiated out toward the central vein (Figure 5-27 A and B), which correlates with AFP findings. This is consistent with a normal oval cell response at day 9 following PHx in the 2AAF/PHx model. In contrast to this, the liver sections from animals maintained on the L-cysteine diet displayed a very modest oval cell response at day 9 following PHx (Figure 5-27 C and D), mostly confined to the periportal areas. The reduced contribution of oval cells to the regeneration process is confirmed by the OV6 immunostaining. Since cell morphology is not so well conserved on cryosections, we scanned the slides for quantitative image analysis of the OV6 positive cells on our samples. Computer image analysis of scanned slides confirmed the 3.5-fold disparity in the magnitude of oval cell response in animals that were fed the normal rat food, as compared to animals that were administered L-cysteine (Figure 5-28). Taken together, all these observations strongly suggest that the L-cysteine associated to the 2-AAF/PHx model of hepatic injury induces a diminished and delayed regenerative response in rat liver.

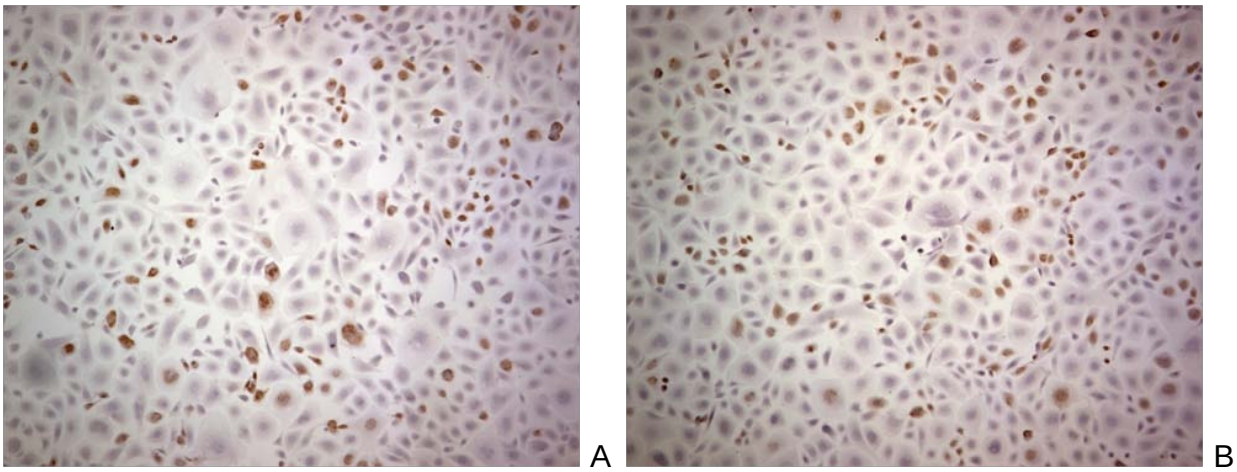

Figure 5-1. L-cysteine effects on WB F344 ovall cell line. Representative pictures of BrdU stained chamber slides taken during an experiment done in triplicate. A) L-cysteine untreated control vs. B) 100µM L-cysteine exposed cells, showing no significant changes in morphology and BrdU uptake.

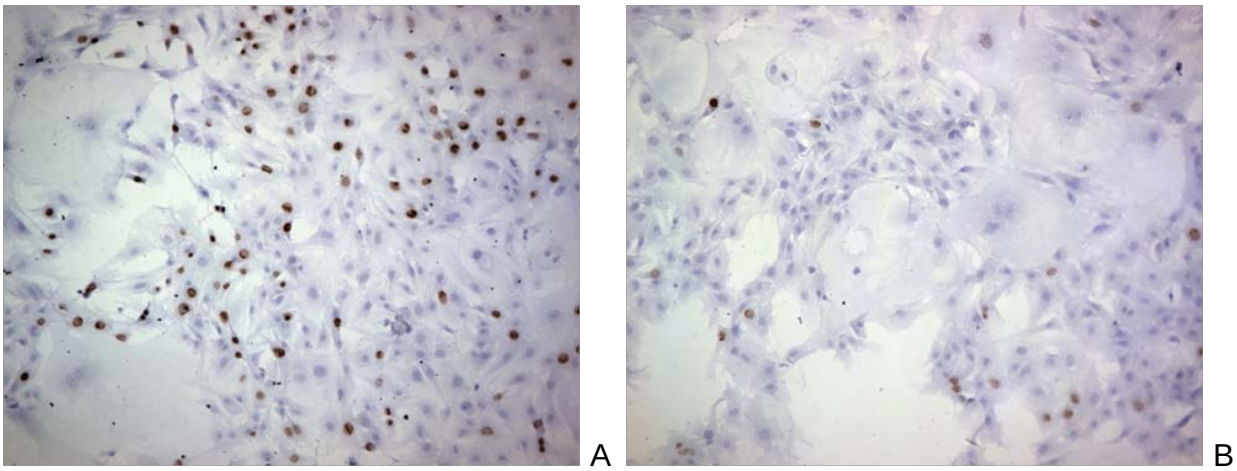

Figure 5-2. L-cysteine effects on portal myofibroblasts. Representative pictures of BrdU stained chamber slides taken during an experiment done in triplicate. A) L-cysteine untreated control vs. B) 100 µM L-cysteine exposed cells displaying a marked reduction in BrdU incorporation.

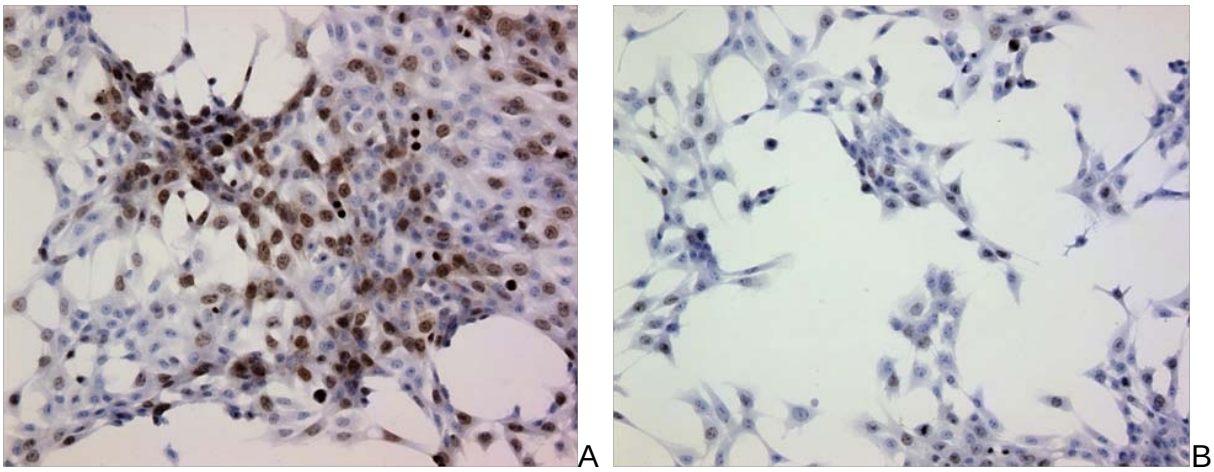

Figure 5-3. L-cysteine effects on HSC T6 hepatic stellate cell line. Representative pictures of BrdU stained chamber slides taken during an experiment done in triplicate. A) L-cysteine untreated control vs. B) 100µM L-cysteine exposed cells showing reduced number of cells undergoing S phase

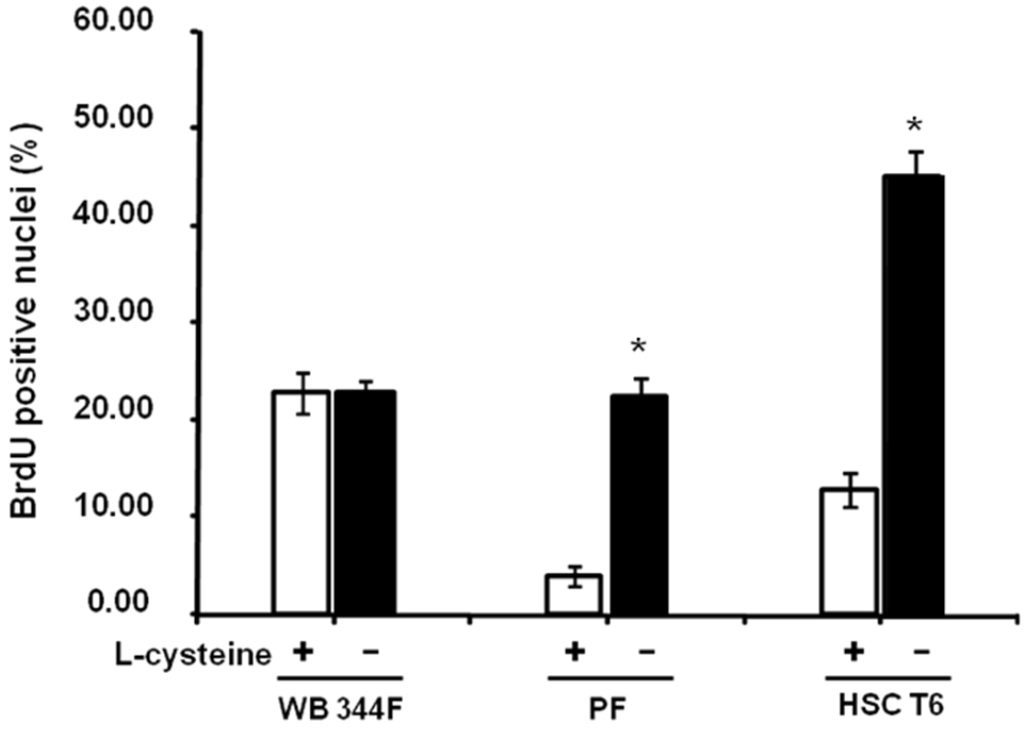

Figure 5-4. Comparative image analysis of Brdu incorporation index in WB 344F oval cell line, PF portal fibroblasts and HSC T6 stellate cell line; white columns - L-cysteine exposed cells, black columns controls maintained on regular culture media. Data represent the mean +/- SD of three independent experiments, $p<0.05$.

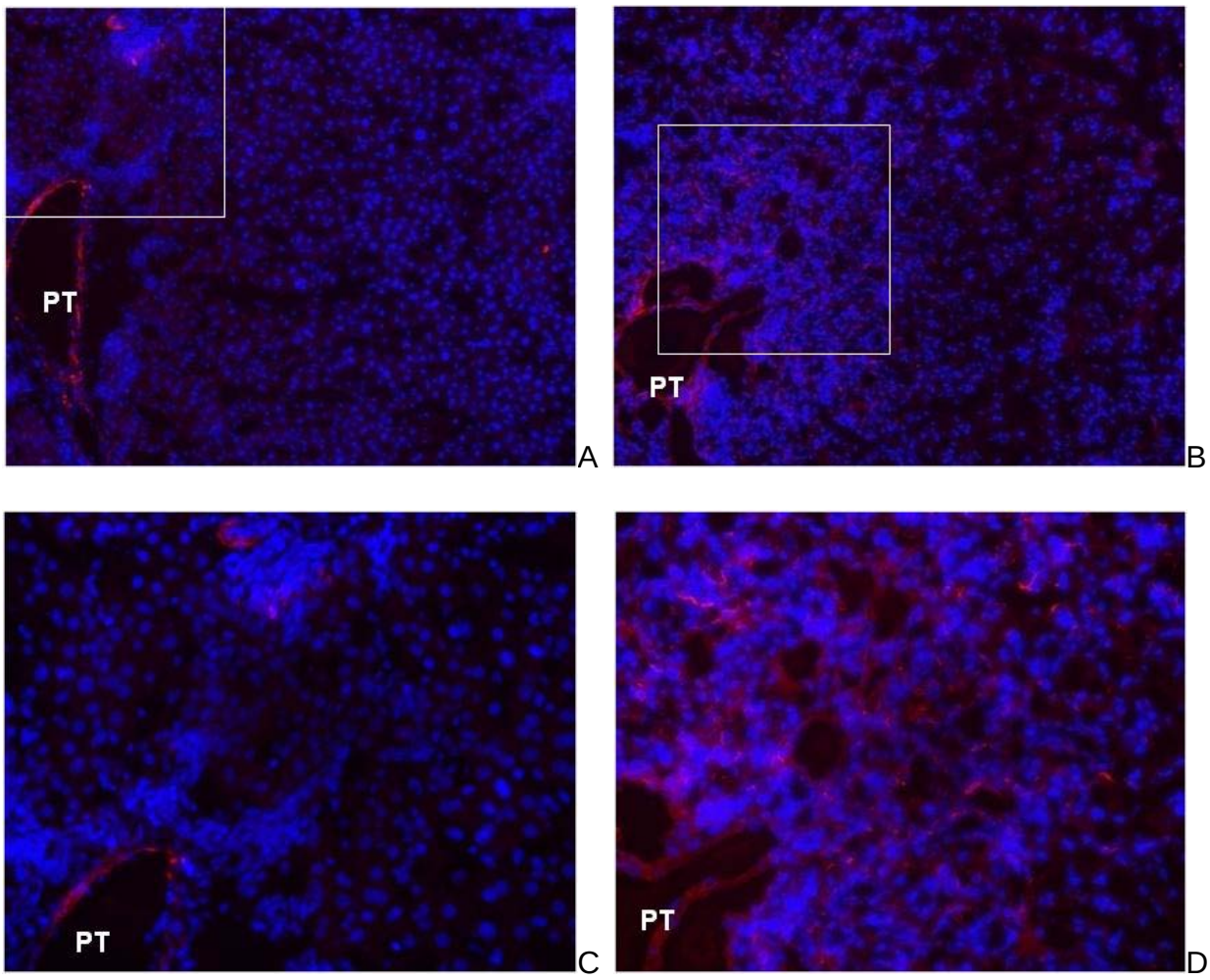

Figure 5-5. Comparative image analysis of desmin positive areas on liver sections from animals sacrificed 9 days post hepatectomy; representative pictures of desmin immunofluoresce stained cryosections were taken during an experiment done in triplicate. A) L-cysteine exposed animals (n = 3), 20X magnification B) control animals (n = 3) subjected only to the 2AAF/PHx protocol, 20X magnification C) same group (n = 3) as A) 40X magnification and D) same group (n = 3) as B) 40X magnification; PT – portal triad.

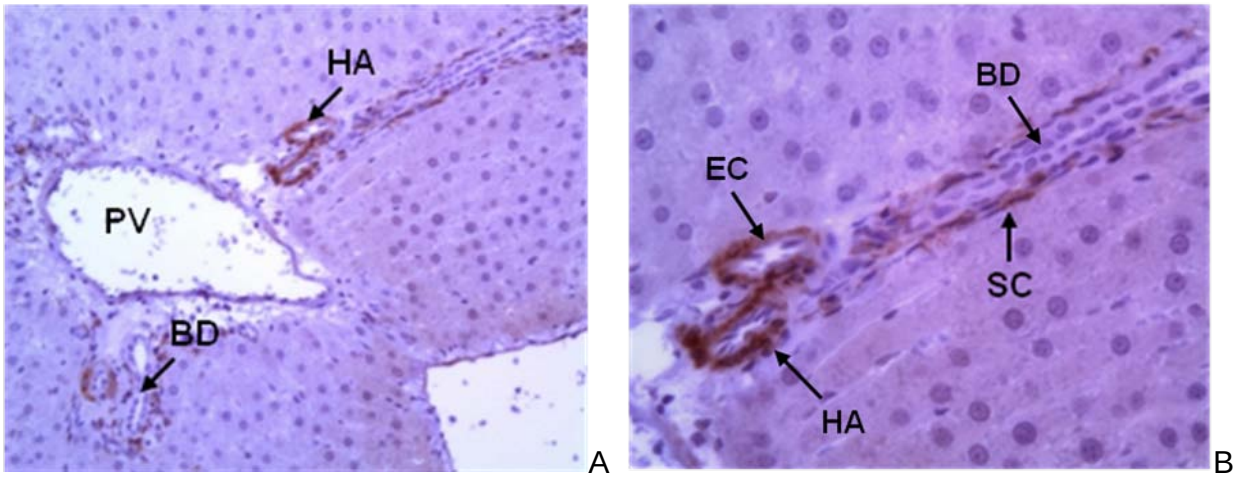

Figure 5-6. Desmin immunostaining of normal rat liver; representative pictures taken during an experiment done in triplicate. Samples collected from three different animals (n = 3) were used each time. A) 20X magnification, B) 40X magnification showing positive vascular walls and rare hepatic stellate cells/myofibroblasts in the periportal areas. HA – hepatic artery branch, PV – portal vein branch, BD – bile duct branch, SC – stellate cell, EC – endothelial cell.

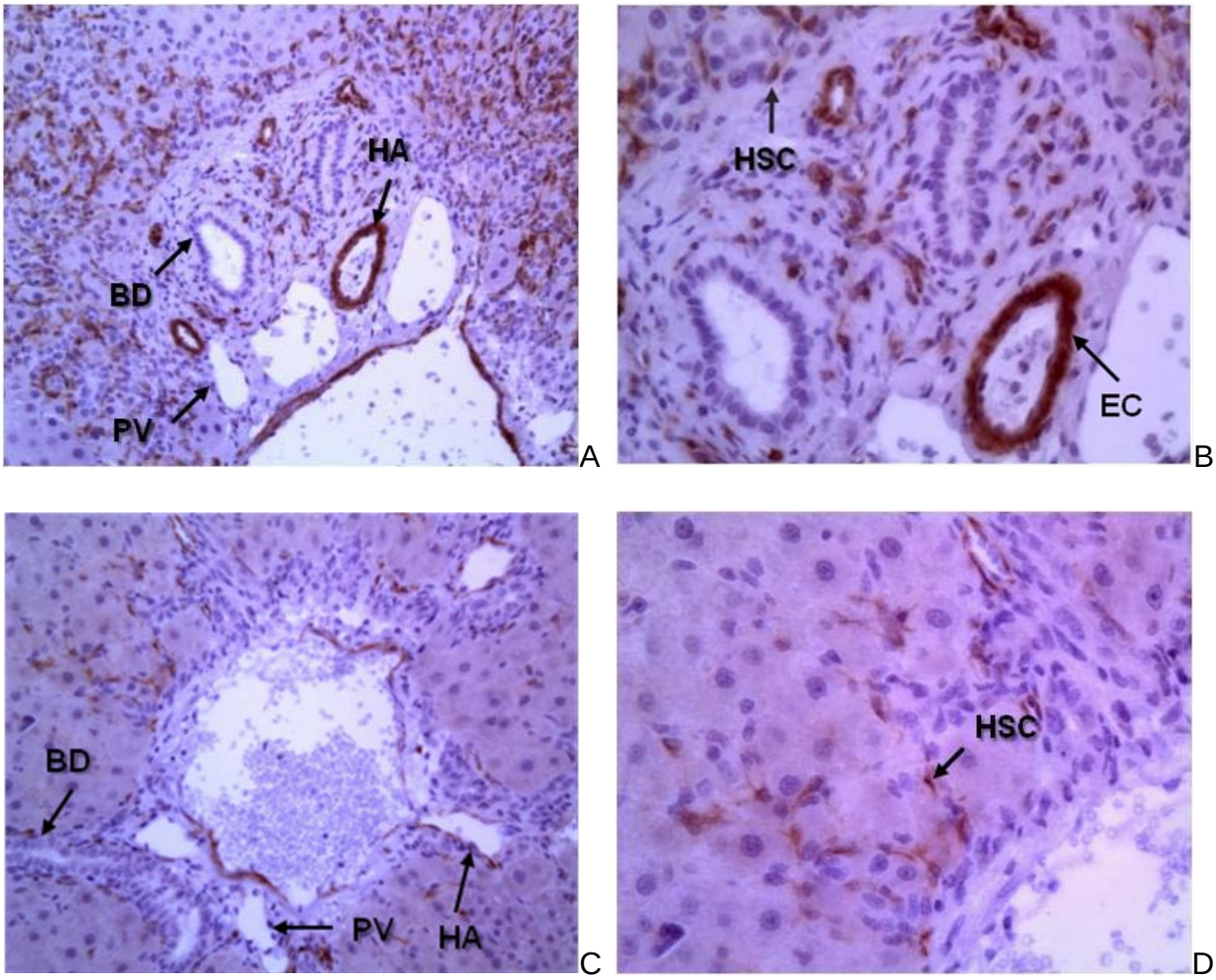

Figure 5-7. Desmin immunostaining of rat liver sections collected on day 9 post hepatectomy from animals (n = 3) exposed to L-cysteine C) 20X magnification, D) 40X magnification, as opposed to 2AAF/PHx treated rats (n = 3) A) 20X magnification, D) 40X magnification, showing positive vascular walls and reduced hepatic stellate cells in the diet exposed animals. Representative pictures were taken during an experiment done in triplicate. HA – hepatic artery branch, PV – portal vein branch, BD – bile duct branch, HSC – hepatic stellate cell, EC – endothelial cell.

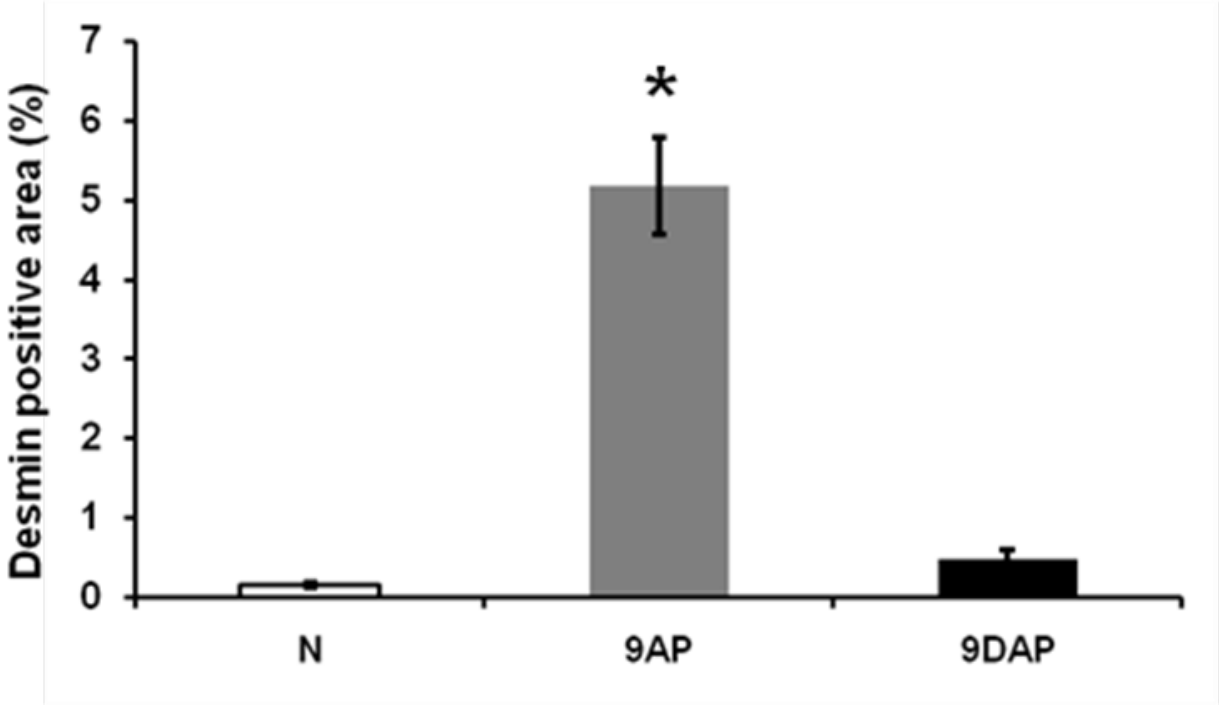

Figure 5-8. Comparative quantitative image analysis of desmin positive areas reflecting decreased activated stellate cell presence on sections from animals exposed to L-cysteine diet: N – normal rat liver, 9AP – samples collected on day 9 post acute liver injury in animals under 2AAF/PHx protocol, 9DAP – liver sections from animals kept on L-cysteine diet associated to 2AAF/PHx (timepoint day 9 post hepatectomy). Data represent the mean +/- SD of three independent experiments, $p<0.05$.

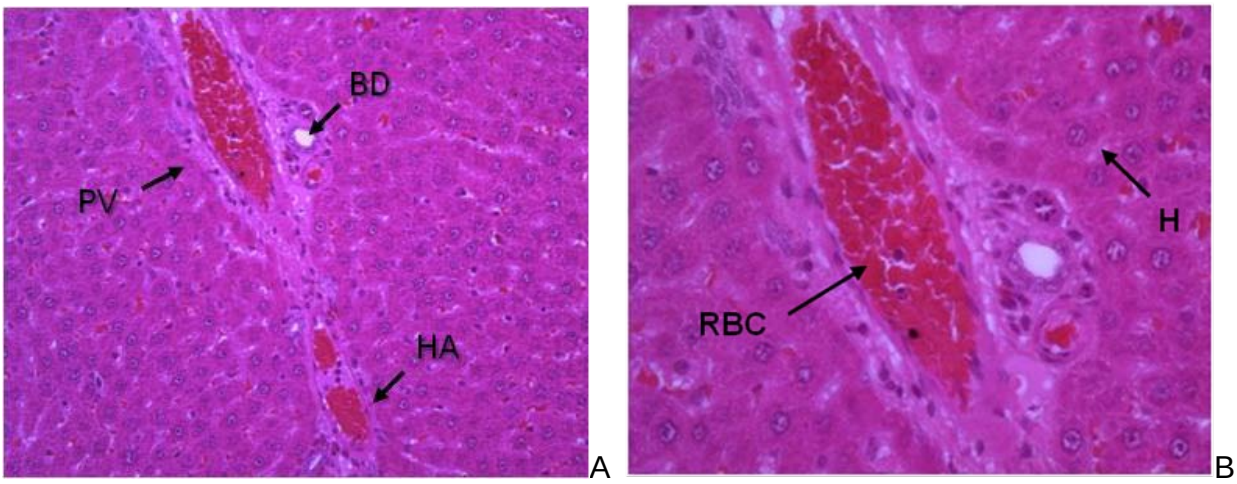

Figure 5-9. Hematoxylin and Eosin staining of normal rat liver shows that the periportal areas are devoid of oval cell presence. Representative pictures were taken during an experiment done in triplicate, using sections collected from three different animals (n = 3) each time. A) 20X magnification, B) 40X magnification. HA – hepatic artery branch, PV – portal vein branch, BD – bile duct branch, H – hepatocyte, RBC – red blood cell.

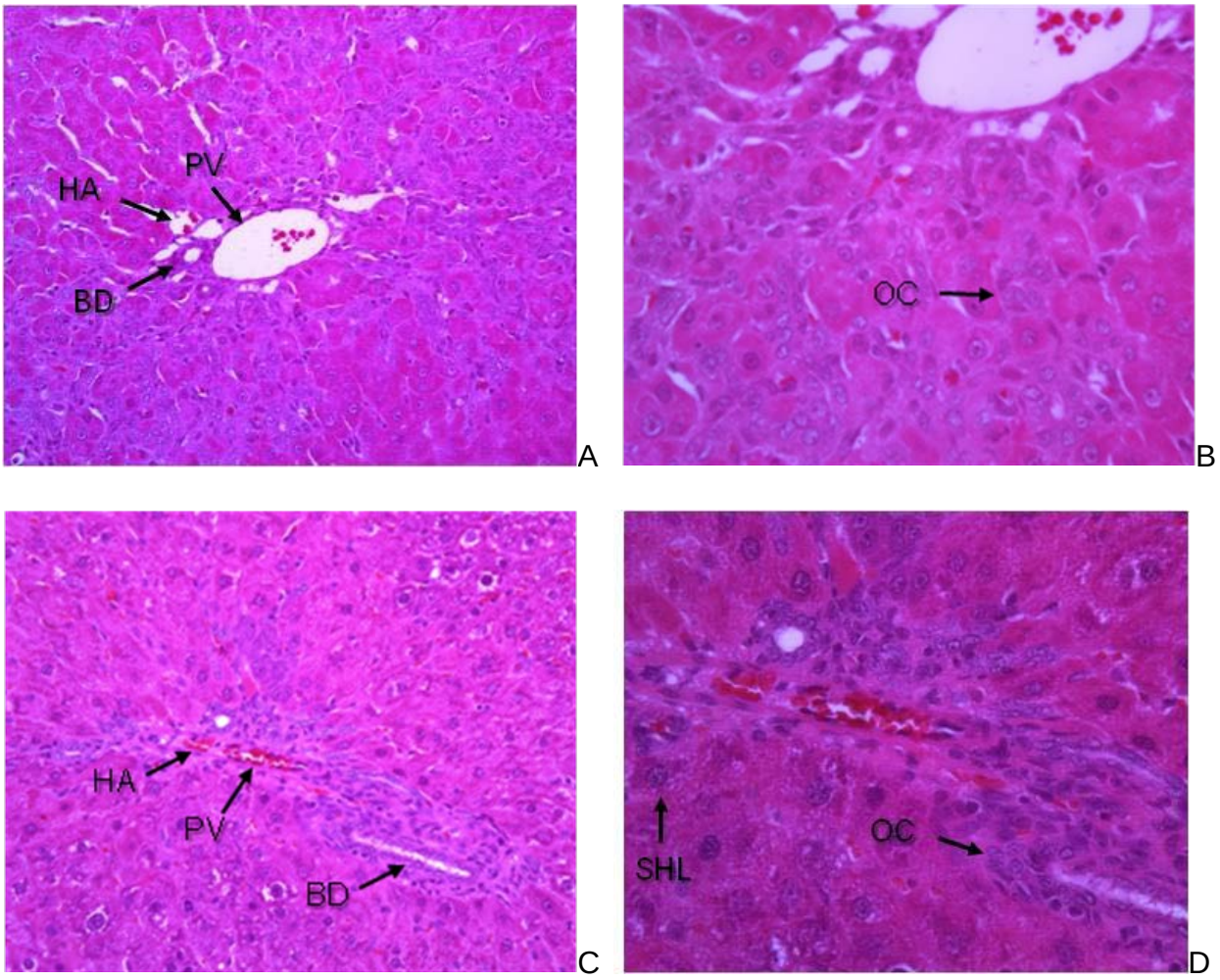

Figure 5-10. Comparative histological exam of H&E stained liver samples collected on day 9 post acute liver injury from: animals (n = 3) on 2AAF/PHx protocol A) 20X magnification, B) 40X magnification and from rats (n = 3) maintained on L-cysteine diet and 2AAF/PHx C) 20X magnification, D) 40X magnification. Representative pictures were taken during an experiment done in triplicate; HA – hepatic artery branch, PV – portal vein branch, BD – bile duct branch OC – oval cell, SHL – small hepatocyte-like cell.

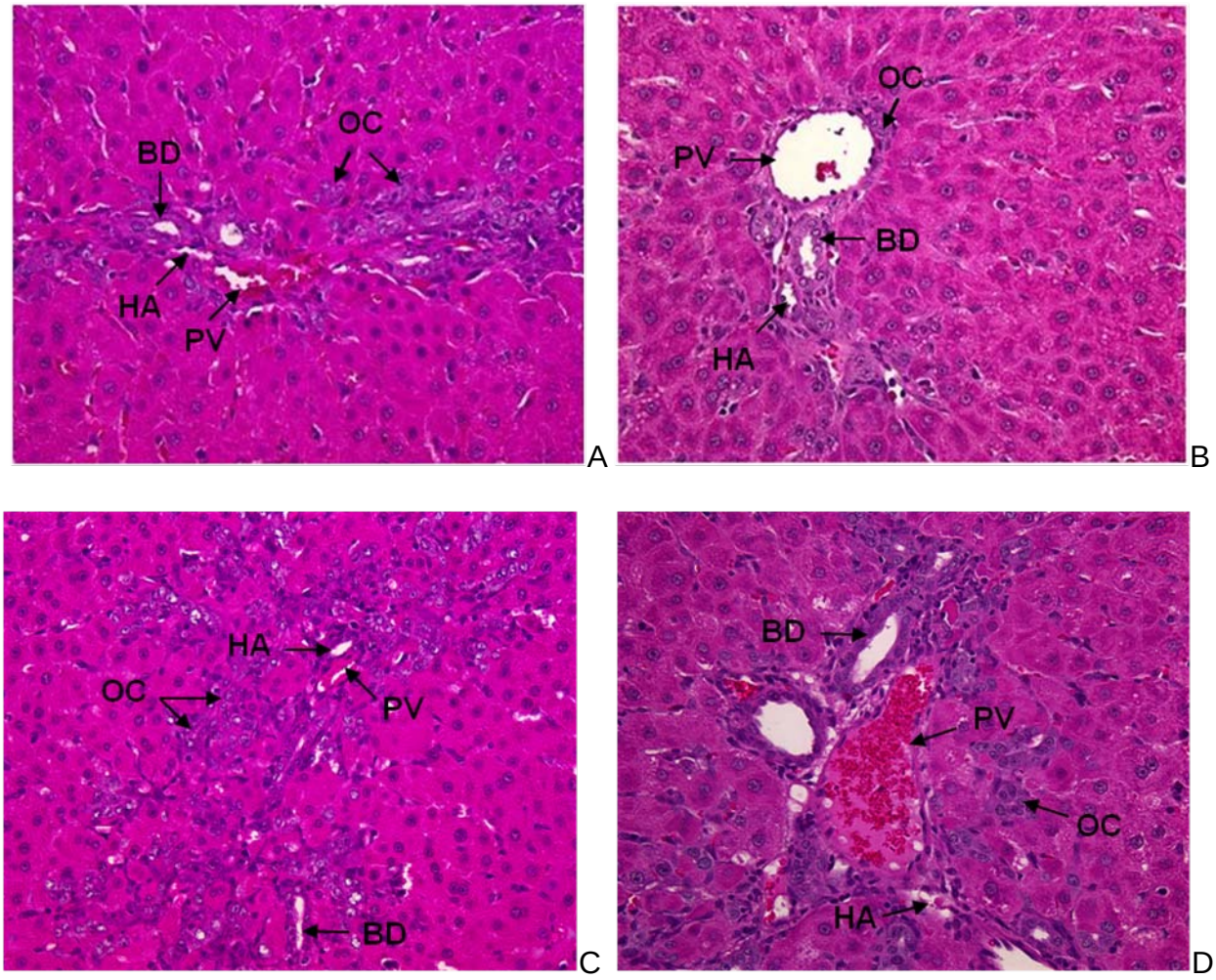

Figure 5-11. Comparative histological exam of liver sections; H&E staining of samples collected on days 3 (A and B) and 5 (C and D) post acute liver injury: from animals (n = 3) on 2AAF/PHx protocol (panels A and C) and from rats 9n = 3) maintained on L-cysteine diet and 2AAF/PHx (panels B and D). 20X magnification. Representative pictures were taken during an experiment done in triplicate and samples collected from three different animals (n = 3) were examined each time. OV – oval cell, HA – hepatic artery branch, BD – bile duct branch, PV – portal vein branch.

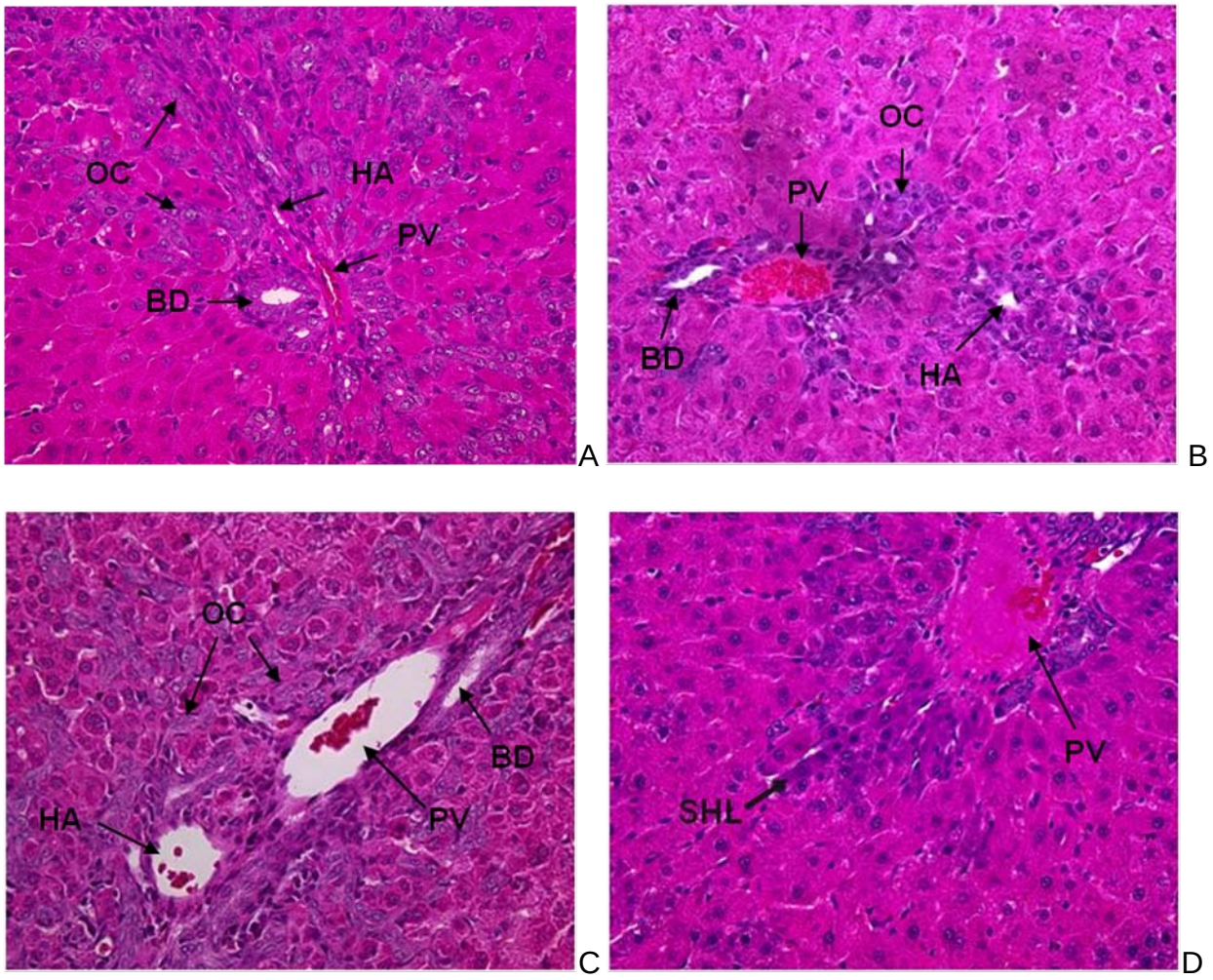

Figure 5-12. Comparative histological exam of H&E stained liver samples collected on days 7 (A and B) and 11 (C and D) post acute liver injury: from animals (n = 3) on 2AAF/PHx protocol (panels A and C) and from rats (n = 3) maintained on L-cysteine diet and 2AAF/PHx (panels B and D). 20X magnification. Representative pictures were taken during an experiment done in triplicate. SHL – small hepatocyte-like cell, OV – oval cell, HA – hepatic artery branch, BD – bile duct branch, PV – portal vein branch.

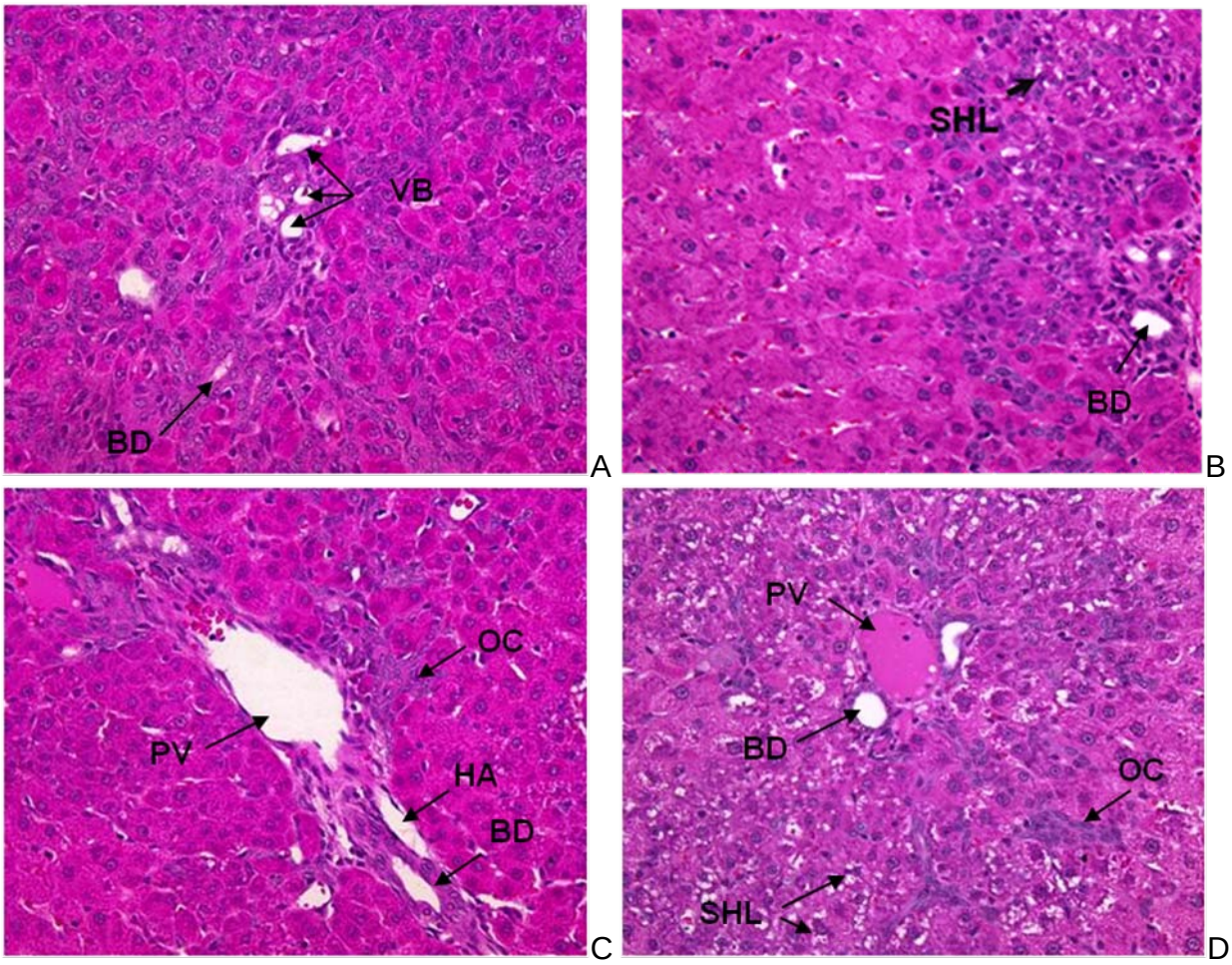

Figure 5-13. Comparative histological exam of H&E stained liver samples collected on days 15 (A and B) and 20 (C and D) post acute liver injury: from animals (n = 3) on 2AAF/PH protocol (panels A and C) and from rats (n = 3) maintained on L-cysteine diet and 2AAF/PH (panels B ad D). 20X magnification. Representative pictures were taken during an experiment done in triplicate. HA – hepatic artery branch, PV – portal vein branch, BD – bile duct branch, SHL – small hepatocyte-like cell starting to form vacuoles in the cytoplasm, OC – oval cell.

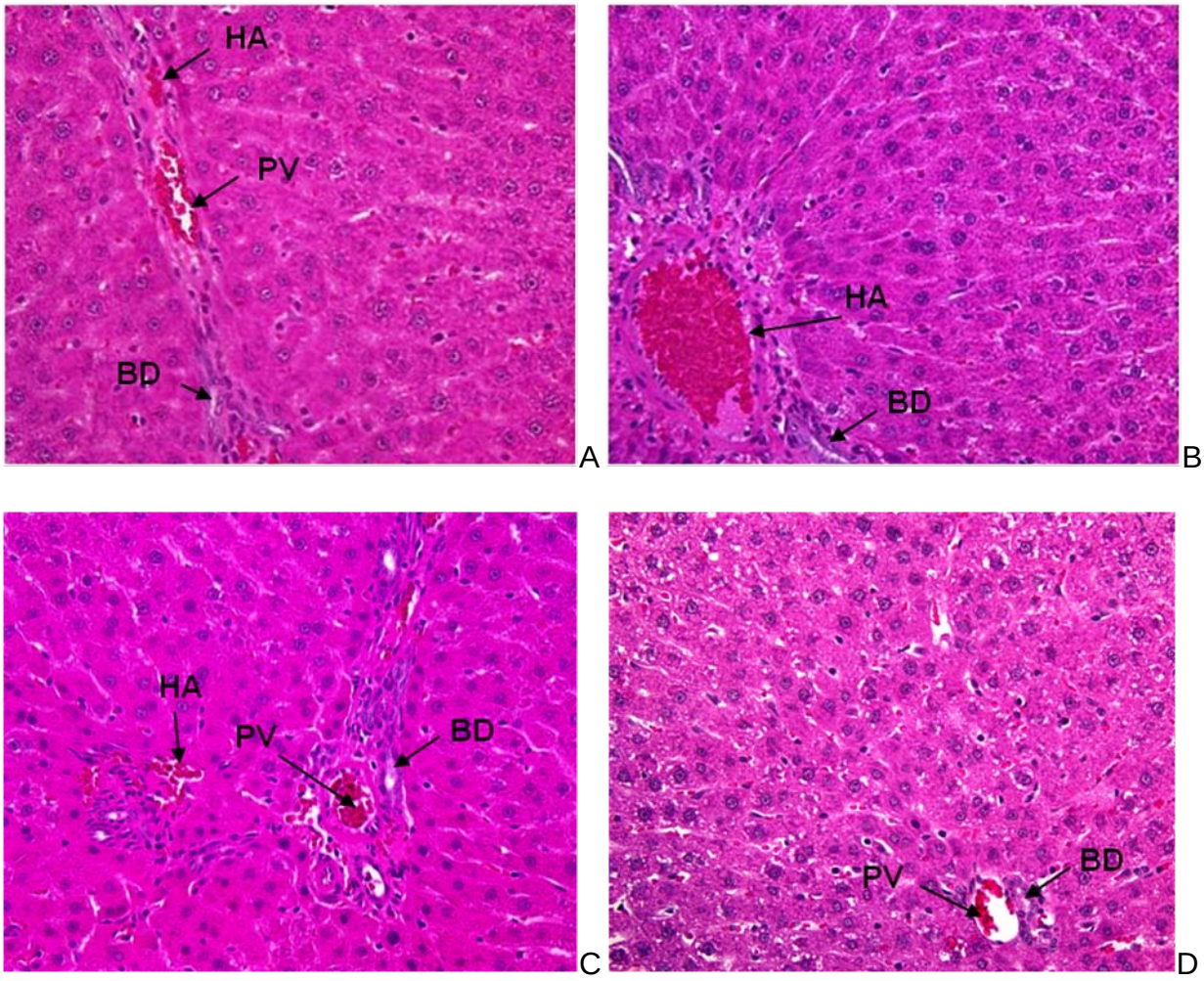

Figure 5-14. Comparative histological exam of Hematoxylin and Eosin stained control samples. A) normal liver, B) L-cysteine diet and 2AAF, C) 2AAF alone, D) L-cysteine diet alone. Representative pictures were taken during an experiment done in triplicate. Sections from three animals in each group (n = 3) were examined. HA – hepatic artery branch, PV – portal vein branch, BD – bile duct branch, 20x magnification.

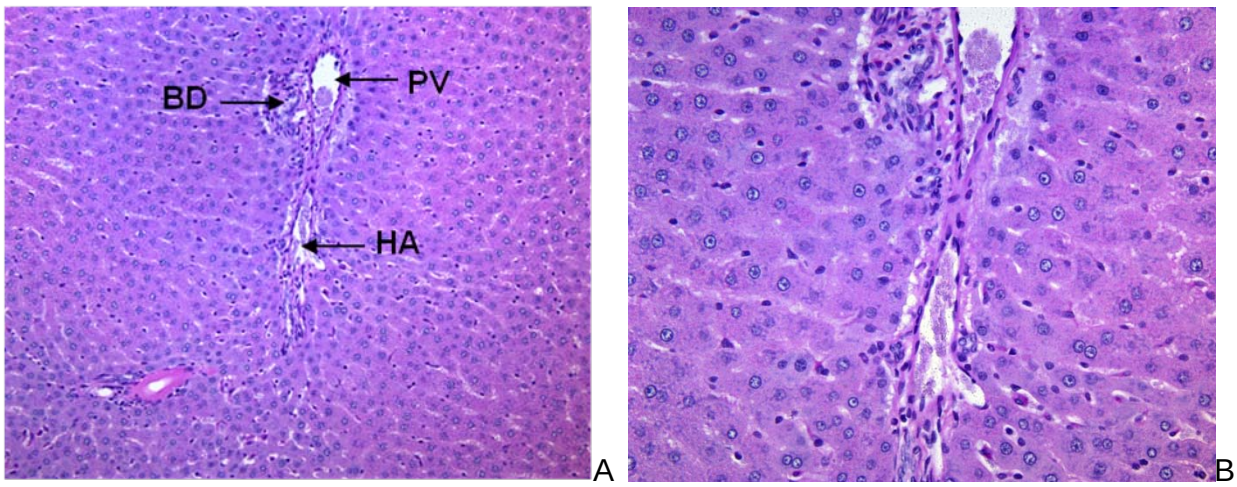

Figure 5-15. Normal rat liver: the low levels of cytoplasmic glycogen are not visible by PAS staining as distinct cytoplasmic granules in periportal hepatocytes. A) 20X magnification, B) 40X magnification. Representative pictures were taken during an experiment done in triplicate and sections from three different animals (n = 3) were examined each time. HA – hepatic artery branch, PV – portal vein branch, BD – bile duct branch.

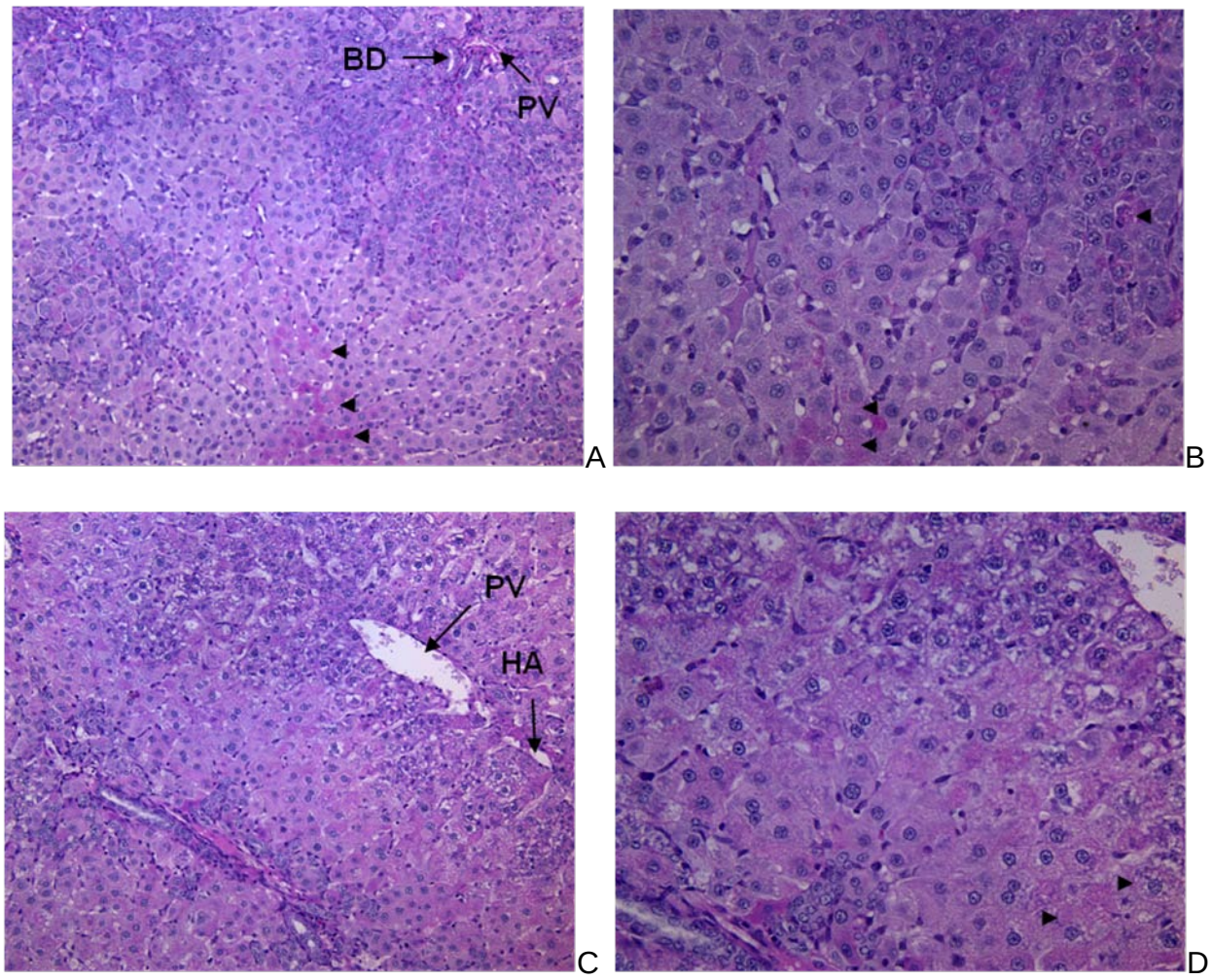

Figure 5-16. Comparative histological exam of PAS stained liver samples collected on day 11 post acute liver injury from animals (n = 3) exposed to 2AAF/PHx protocol (panels A and B) and rats (n = 3) kept on L-cysteine diet (panels C and D). 20X magnification (panels A and C) and 40X magnification (panels B and D). Representative pictures of glycogen loaded hepatocytes (pink) were taken during an experiment done in triplicate. HA – hepatic artery branch, PV – portal vein branch, BD – bile duct branch, arrowheads indicate PAS positive mature hepatocytes.

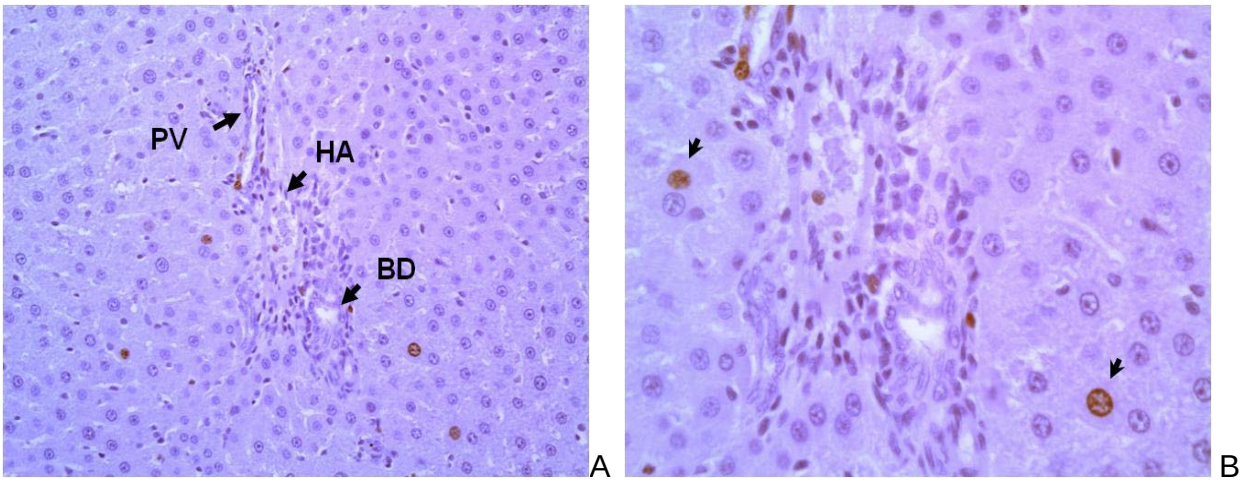

Figure 5-17. Ki67 immunostaining of normal rat liver; representative pictures were taken during an experiment done in triplicate and tissue samples collected from three animals (n = 3) were examined each time. A) 20X magnification, B) 40X magnification showing very few, periportally scattered hepatocytes which exit G_0 and enter the cell cycle. HA – hepatic artery branch, PV – portal vein branch, BD – bile duct branch, arrowheads indicate hepatocytes undergoing the cell cycle.

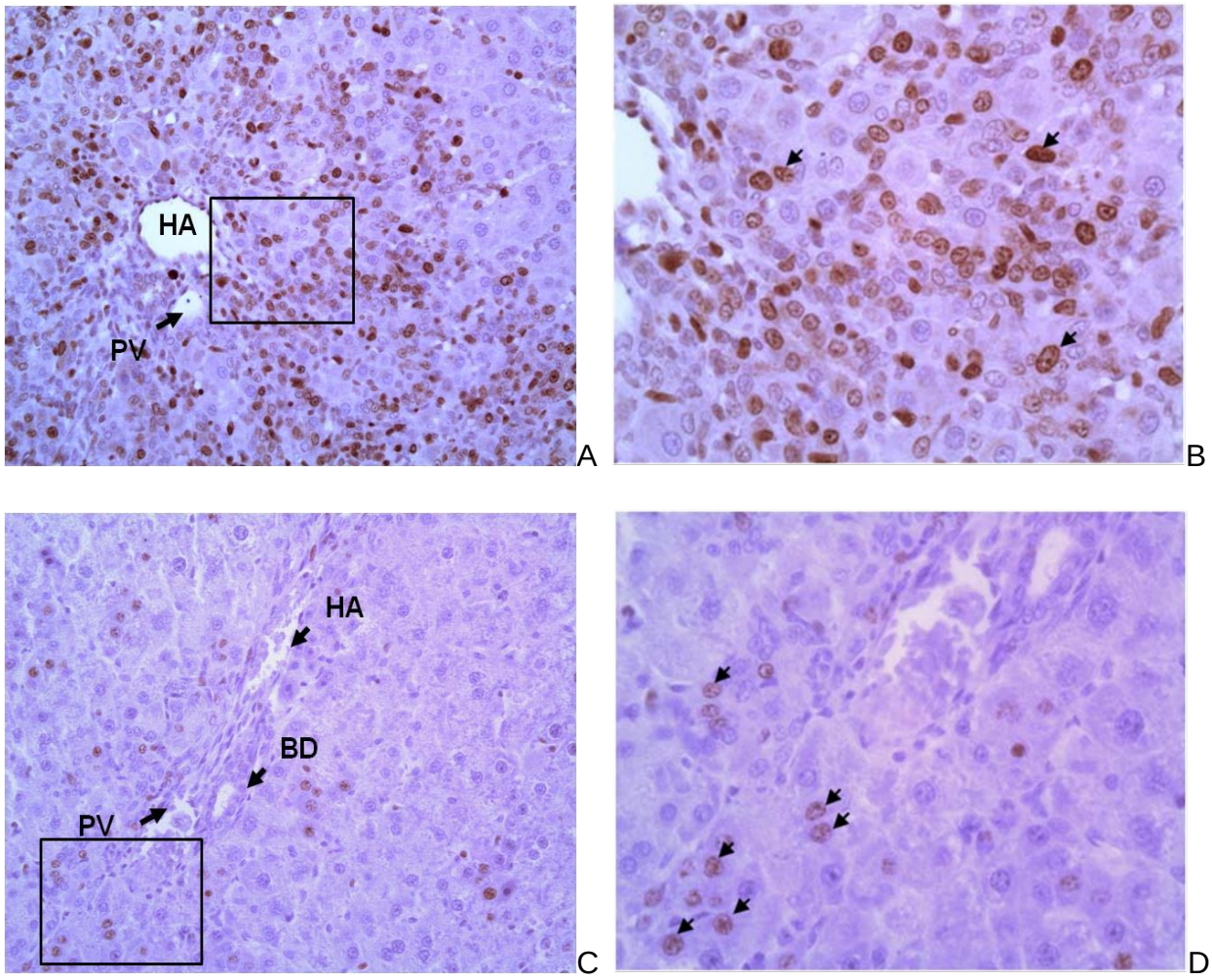

Figure 5-18. Ki67 immunostaining of rat liver sections collected on day 9 post hepatectomy from control animals (n = 3) undergoing 2AAF/PHx protocol A) 20X magnification and B) 40X magnification and same time point rats (n = 3) exposed to L-cysteine and 2AAF/PHx oval cell activation C) 20X magnification, D) 40X magnification. Representative pictures were taken during an experiment done in triplicate. HA – hepatic artery branch, PV – portal vein branch, BD – bile duct branch, arrowheads indicate Ki67 positive nuclei.

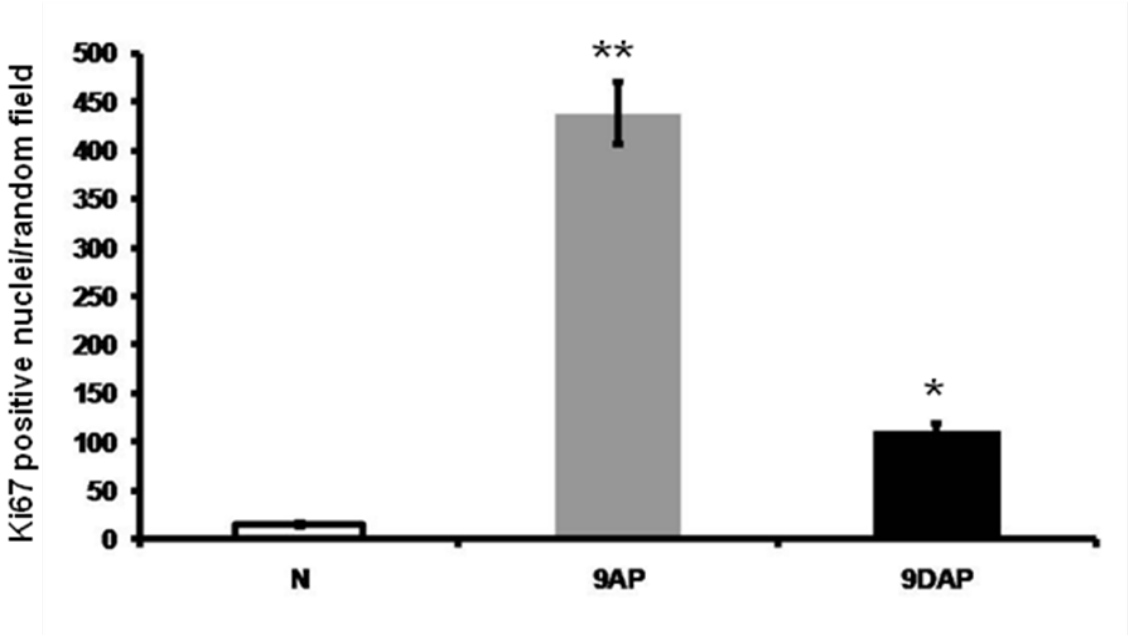

Figure 5-19. Comparative quantitative image analysis of hepatic proliferation potential during compensatory hyperplasia; Ki67 immunostaining of liver sections collected from normal rats (n = 3) – N and, on day 9 post hepatectomy, from control animals (n = 3) undergoing 2AAF/PHx protocol – 9AP and rats (n = 3) exposed to L-cysteine associated with 2AAF/PHx oval cell activation – 9DAP. Data represent the mean +/- SD of three independent experiments, * $p<0.05$ and ** $p<0.005$.

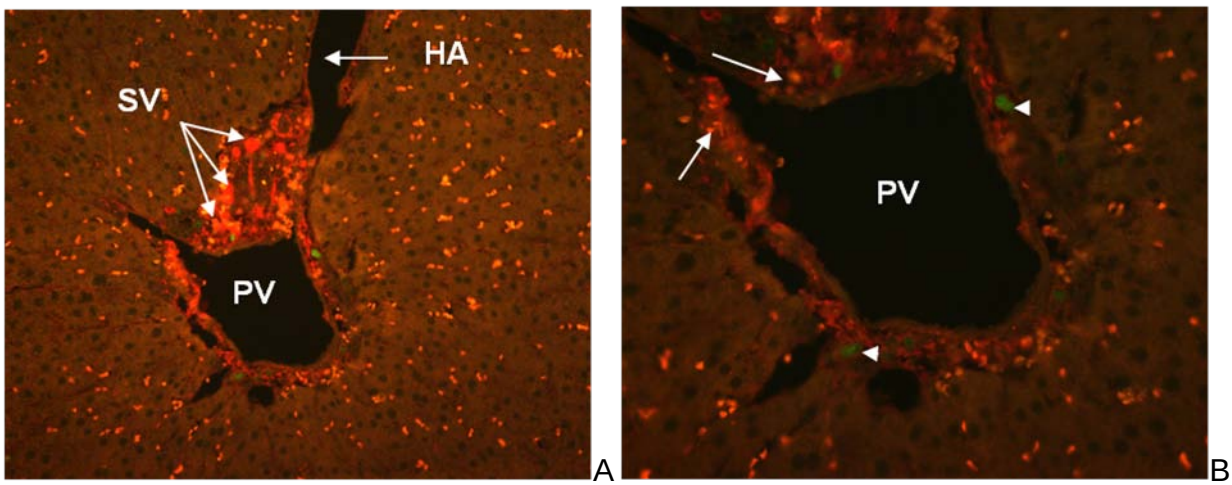

Figure 5-20. Double IF for Ki67 and desmin on normal liver sections showing very few hepatocytes located in the limiting plate which exit G0 and enter the cell cycle. Representative pictures were taken during an experiment done in triplicate, using liver samples from three animals (n = 3) each time. A) 20X magnification, B) 40X magnification. HA – hepatic artery branch, PV – portal vein branch, SV – small vessels, branches of hepatic artery, arrowheads indicate hepatocytes undergoing the cell cycle (nuclai stained green with FITC – fluorescein isothiocyanate) and arrows indicate desmin positive myofibroblasts and endothelial cells in the vascular wall (stained red with Texas red).

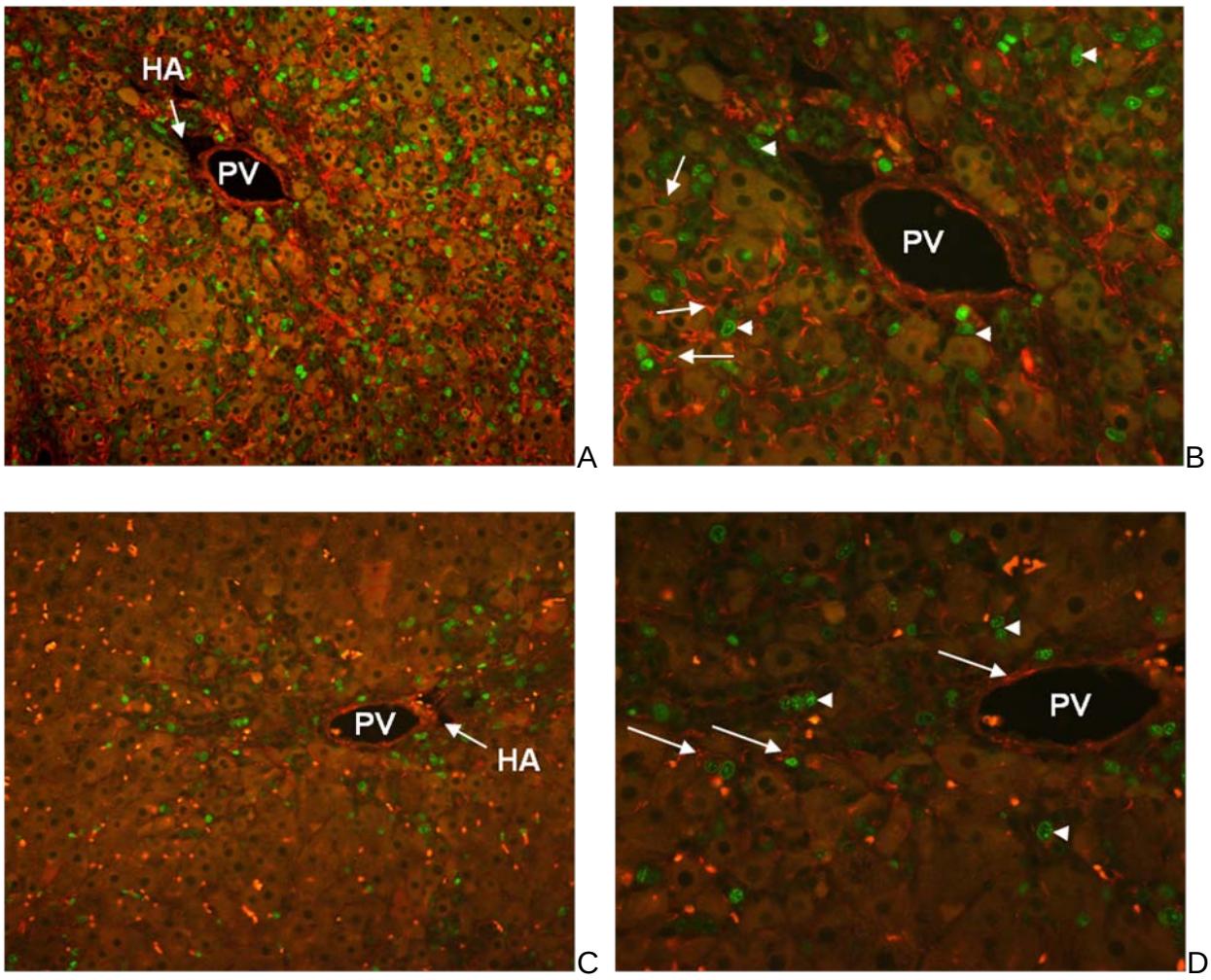

Figure 5-21. Double IF for Ki67 and desmin on liver sections collected 9 days post acute hepatic injury.from animals (n = 3) exposed to the 2AAF/PHx protocol A) 20X magnification, B) 40X magnification and from animals (n = 3) kept on L-cysteine diet associated to the 2AAF/PHx protocol C) 20X magnification, D) 40X magnification. Representative pictures were taken during an experiment done in triplicate. HA – hepatic artery branch, PV – portal vein branch, arrowheads indicate hepatocytes undergoing the cell cycle (nuclei stained green with FITC) and arrows indicate desmin positive activated stellate cells and endothelial cells (stained red with Texas red).

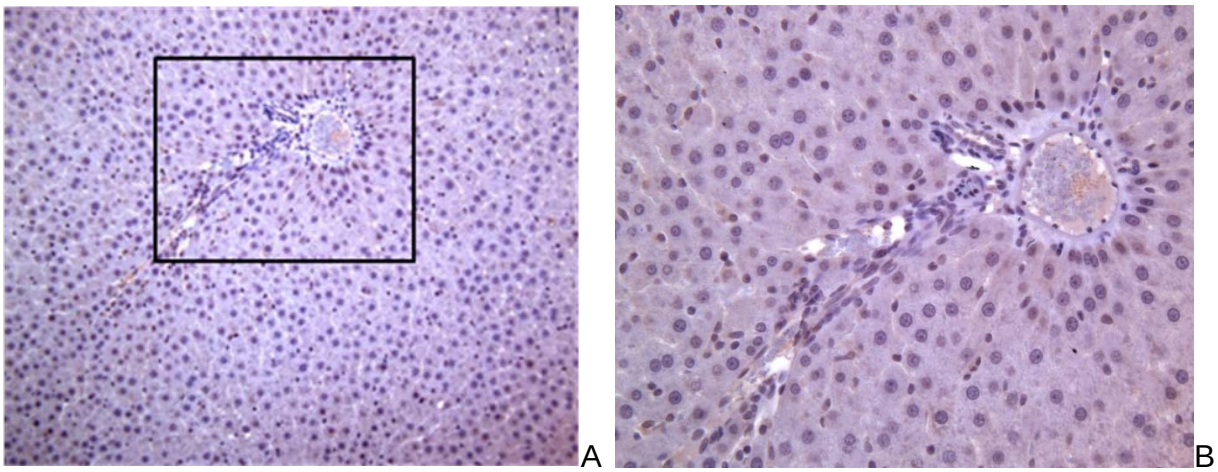

Figure 5-22. AFP immunostaining of normal rat liver; representative pictures were taken during an experiment done in triplicate and samples from three different animals (n = 3) were examined each time. A) 20X magnification, B) 40X magnification, showing the absence of AFP positive cells in animals with normal hepatocyte mediated regeneration.

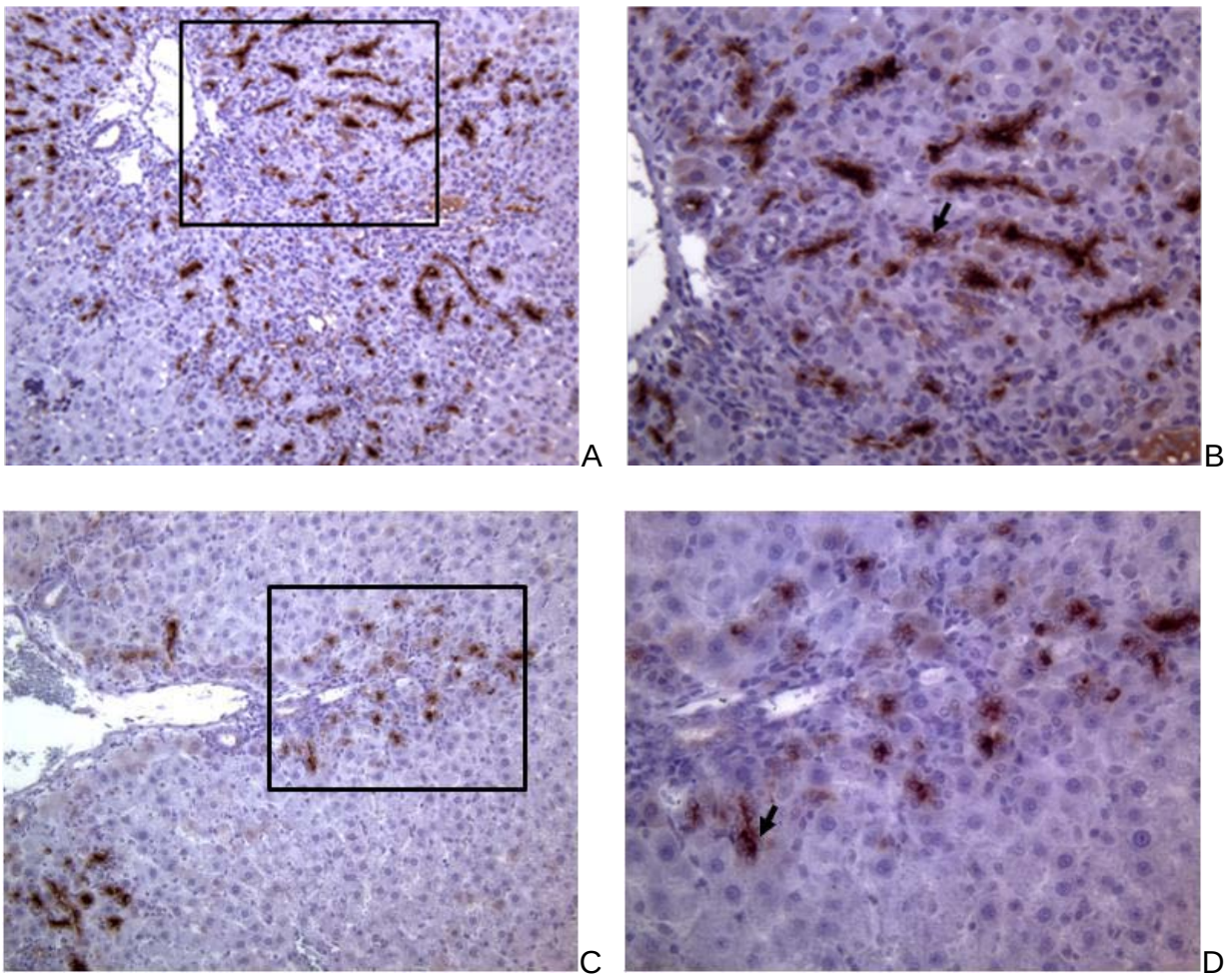

Figure 5-23. AFP immunostaining of rat liver sections collected on day 9 post hepatectomy from 2AAF/PHx treated rats (A – 20X magnification, B – 40X magnification), as opposed to animals exposed to L-cysteineand 2AAF/PHx (C – 20X magnification, D – 40X magnification), showing reduced numbers of oval cells and few small hepatocyte-like cells in the diet exposed animals. Arrows indicate AFP positive oval cells. Representative pictures were taken during an experiment done in triplicate and samples from three different animals (n = 3) were examined each time.

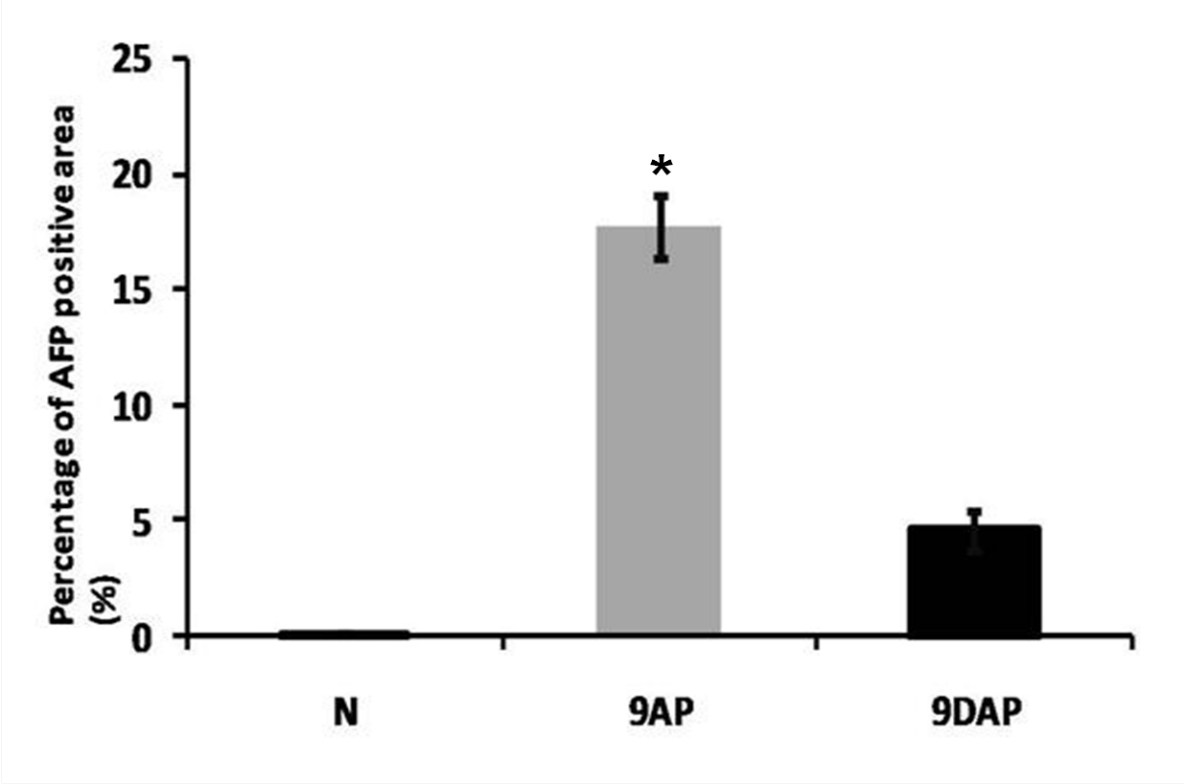

Figure 5-24. Comparative quantitative image analysis of AFP positive cell presence reflected by immunostaining. Liver sections were collected from: normal rats (n = 3) – N; on day 9 post hepatectomy, from control animals (n = 3) undergoing 2AAF/PH protocol – 9AP; at the same timepoint, rats (n = 3) exposed to L-cysteine and 2AAF/PHx oval cell activation protocol – 9DAP. Data represent the mean +/- SD of three independent experiments, $p<0.05$.

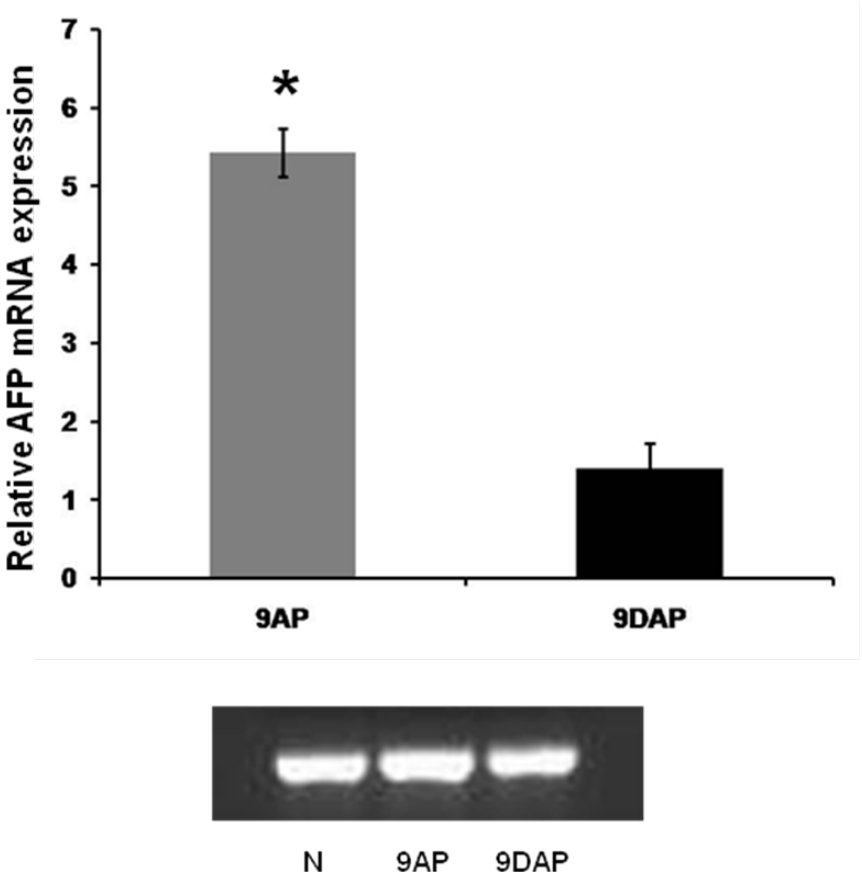

Figure 5-25. Real time PCR analysis – comparative expression of AFP reflecting the regeneration process on samples collected on day 9 post hepatectomy from animals (n = 3) subjected to the 2AAF/PHx protocol (9AP), respectively rats (n = 3) treated with L-cysteine during the same protocol (9DAP); values normalized to beta actin and normal liver tissue (N) expression of AFP; GAPDH was used as a loading control. Data represent the mean +/- SD of three independent experiments, $p<0.05$.

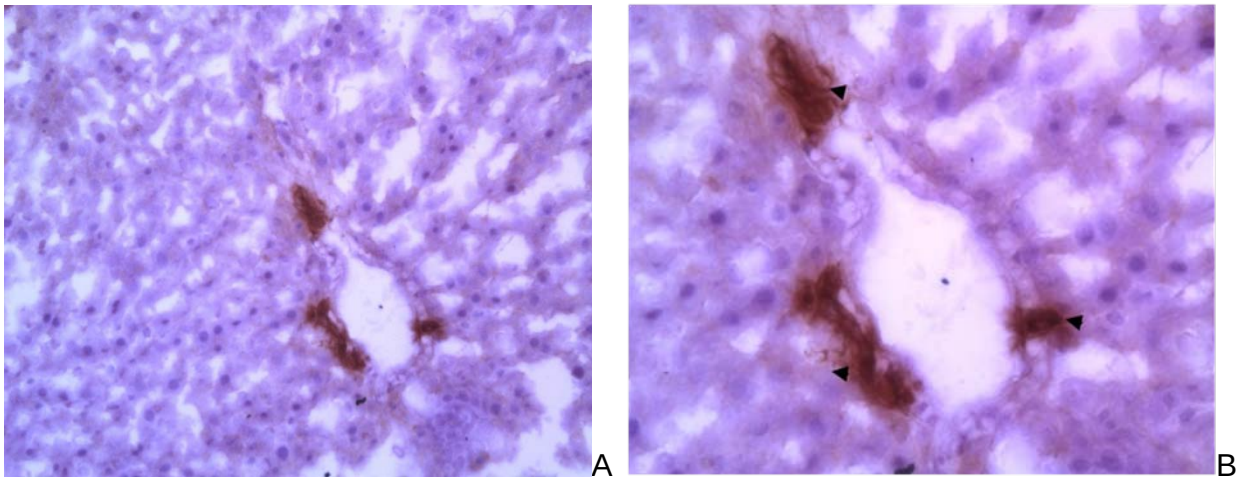

Figure 5-26. OV6 immunostaining of normal rat liver, showing the presence of positive bile duct cells in animals with normal hepatocyte mediated regeneration. Representative pictures were taken during an experiment done in triplicate. Samples collected from three different animals (n = 3) were analyzed each time. A) 20X magnification, B) 40X magnification,

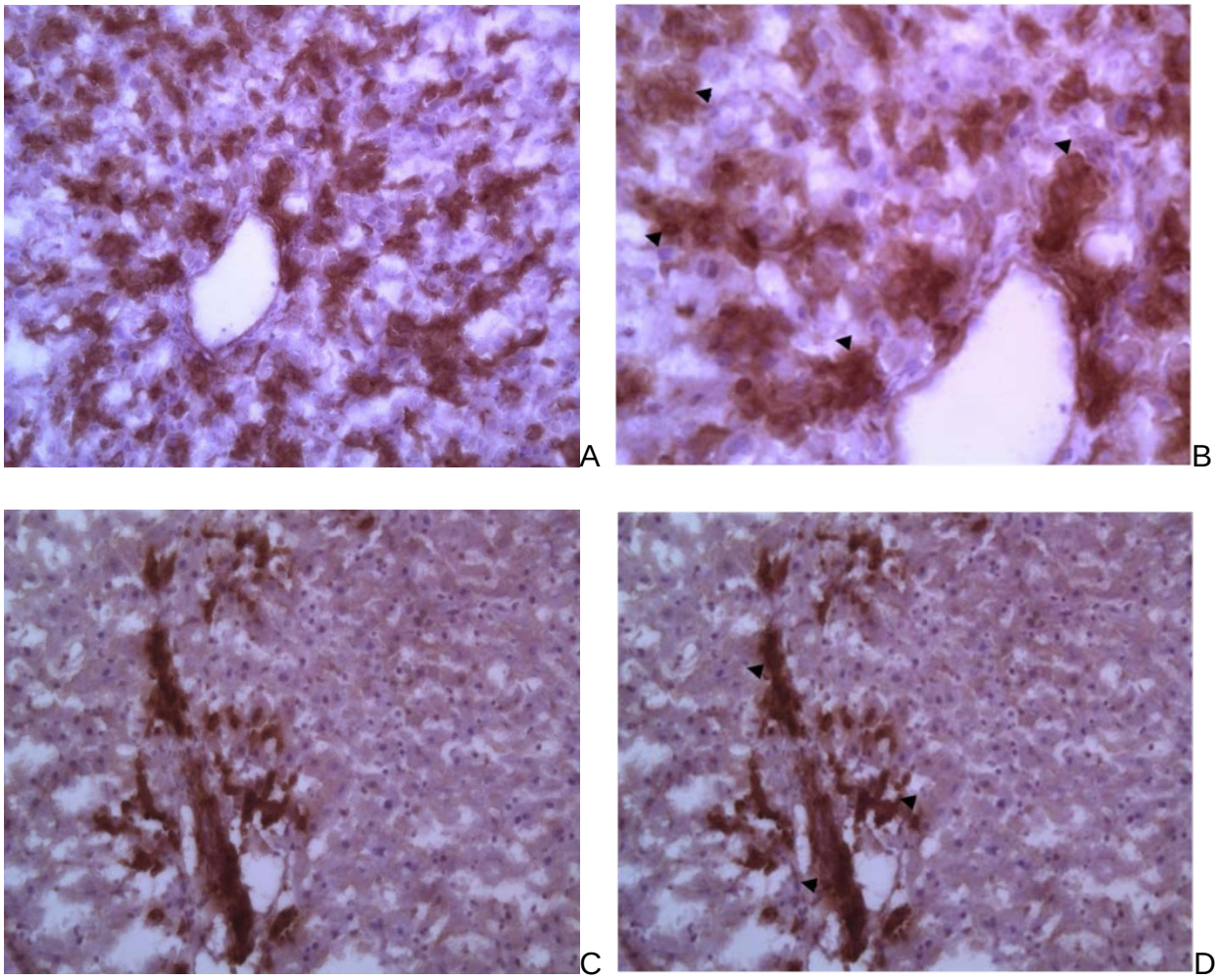

Figure 5-27. OV6 immunostaining of rat liver sections collected on day 9 post hepatectomy from: 2AAF/PH treated animals (A – 20X magnification, B – 40X magnification), as opposed to rats exposed to L-cysteine and 2AAF/PHx (C – 20X magnification, D – 40X magnification), showing reduced numbers of oval cells in the diet exposed animals. Representative pictures were taken during an experiment done in triplicate. Samples collected from three different animals (n = 3) were analyzed each time. Arrowheads indicate clusters of OV6 positive oval cells.

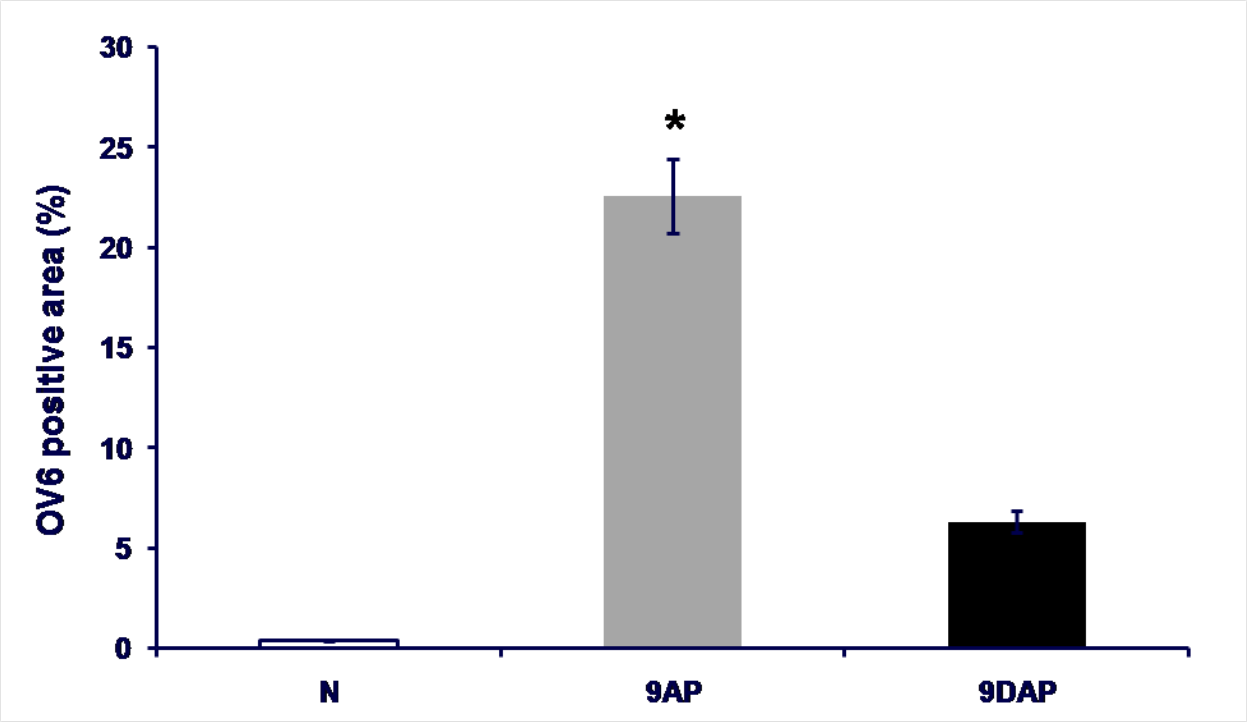

Figure 5-28. Comparative quantitative image analysis of OV6 positive cell presence reflected by immunostaining. Liver sections were collected from normal rats (n = 3) – N and, on day 9 post hepatectomy, from control animals (n = 3) undergoing 2AAF/PHx protocol – 9AP, and rats (n = 3) exposed to L-cysteine and 2AAF/PHx oval cell activation – 9DAP. Data represent the mean +/- SD of three independent experiments, $p<0.05$.

CHAPTER 6
DISCUSSIONS AND FUTURE DIRECTIONS OF STUDY

6.1 Interpretation of Results

Progenitor cell mediated liver regeneration is an alternative compensatory hyperplasia, able to restore hepatic mass when hepatocyte proliferation is severely impaired by massive liver necrosis or chronic cirrhogenic conditions[127]. It involves sequential waves of cytokine secretion and remodeling of the extracellular matrix. These two processes are intimately coupled, as the matrix can liberate chemical signals when degraded, and concentrate chemical signals[132] that bind to the matrix within specific regions[38, 133]. Thus ECM functions as a primary reservoir of biologically active molecules in the liver[132]. Hepatic stellate cells are the resident hepatic pericyte responsible for secreting cytokines and growth factors, but also for matrix remodeling. During hepatic regeneration the presence of increased numbers of hepatic stellate cells was noted in close proximity to the oval cells and direct contact between stellate cell projection and oval cell membranes was reported[18]. Activated hepatic stellate cells are the main source of MMPs and TIMPS that participate in matrix remodeling and release of bound cytokines[17, 128]. Matrix remodeling results in the establishment of a unique microenvironment, conducive for the proliferation and migration of cells within the regenerating zone. This renders the activation of hepatic stellate cells an important component of progenitor cell mediated regeneration process.

Previous research conducted by our group demonstrated that during progenitor cell mediated liver regeneration, a fibronectin rich provisional matrix is synthesized in the periportal zone[132]. We feel that it is likely that this provisional matrix contributes to the oval cell response, acting as a required substrate on which oval cells may proliferate

and providing binding sites for signaling molecules that regulate oval cell phenotype. One such example is CTGF which binds to the fibronectin rich provisional matrix of the periportal zone, where it is concentrated and made available to the oval cells which are known to express CTGF receptors[38].

Given these complex direct and indirect interactions between stellate and oval cells during regeneration, it is of great interest to understand to which extent is the regeneration process affected in the absence of stellate cell contribution. Knowing that parenchymal mass recovery in a timely manner is crucial for maintaining a normal hepatic function, we decided to inhibit the stellate cell activation. Oval cells and stellate cells are among the first cells to enter the cell cycle following injury in the 2AAF/PHx progenitor activation protocol[128]. Less is known regarding the exact temporal relationship between oval and stellate cell activation in the regenerating liver. It is for this reason that we chose to begin the L-cysteine diet well before initiation of the 2AAF/PHx protocol (Figure 4–1). The daily food intake and the body weight of all animals were monitored for the duration of the study in order to identify any potential effects attributable to the diet, and no significant differences were seen between animals fed the experimental and control diets.

Before establishing the animal model we tested the inhibitory effects of L-cysteine *in vitro*. Our study demonstrated that L-cysteine *per se* does not directly affect WB F344 oval cell proliferation in culture; nor does it induce any alterations of their phenotype. We opted to use two different mesenchymal cell populations for this assay. HSC T6 cells are the only available quiescent stellate cell line and they are demonstrated to maintain their non activated status for a minimum of one week in culture. The second

population examined, improperly named portal fibroblasts is composed mostly of myofibroblast cells believed to result from the activation of stellate cells. They exhibit the contractile properties necessary to modulate the blood influx into the hepatic lobule, one of the main functional characteristics of the activated stellate cell. Either in activated (portal fibroblasts) or quiescent state (HSC T6 stellate cells), both mesenchymal cells included in this study were sensitive to L-cysteine inhibiting effects. Their reduced proliferation was reflected by a sensibly diminished BrdU index. Interestingly, portal myofibroblasts have proved to be more sensitive to the inhibiting effects of L-cysteine, exhibiting a 5.6-fold reduction of their proliferation index, as opposed to 3.56-fold reduction in HSC T6 cells. This observation correlates with previous reports about L-cysteine reversing chemically induced fibrosis in DMN (Dimethylnitrosamine) fed rats, by directly inhibiting the proliferation of activated hepatic stellate cells[124].

The hepatocyte proliferation inhibitor used in our study (2-AAF) is activated and detoxified by the liver through rounds of hydroxylation and conjugation[129] which lead to renal excretion of water-soluble derivatives[130, 131]. Being a precursor for glutathione synthesis, it is reasonable to consider the possibility that L-cysteine could increase the rate of 2AAF detoxification. This would potentially lead to incomplete suppression of hepatocyte proliferation in the 2AAF/PHx model. However, examination of Ki67 stained liver sections from the L-cysteine treated group showed no signs of mature hepatocyte proliferation, the only Ki67 positive cells exhibiting oval cell and small hepatocyte-like phenotype (Figures 5-14, 5-15). This would seem to exclude differential 2AAF metabolism as a complicating factor in these studies. This finding is explained in part by glutathione's lack of effectiveness in competing with macromolecules for trapping the

reactive metabolites of 2-AAF, and also by its inability to interfere with DNA adduct formation[135].

Since the ECM fibers, enzymes and growth factors are secreted in the extracellular environment, the most used marker for oval cell activation is desmin, an intermediate filament wich is present in the activated Ito cell's cytoskeleton. Our immunostaining for desmin showed that the presence of activated stellate cells is significantly reduced during L-cysteine exposure, although their distribution in the vicinity of oval cells is conserved. No changes have been noticed in the characteristic pattern of stellate cell extensions wrapping around the regenerating cells. It is reported that due to the direct membrane contacts Ito cells are able to exert their "nourishing" function during oval cell proliferation[18]. The parallel reduction of stellate and oval cell presence in the regenerating liver (Figure 5-21) seems to be associated with a direct inhibition of their activation and not with an anomaly of migration or disruption of cell-to-cell interactions.

The human conditions associated with oval cell activation are characterized by exhaustion of hepatocyte function and proliferation capacity. The resulting hepatic failure would potentially benefit from an oval stem cell therapy able to recover the liver function before the onset of end-stage MODS (multiple organ dysfunction syndrome). For these reasons, any delay in the oval cell mediated liver regeneration can have fatal consequences. Comparative monitoring of oval cell activation revealed differences in regards to the onset and progression of liver regeneration. When stellate cells are inhibited the onset of regeneration is delayed. Only 1-2 cells/field exhibit morphology suggestive for the oval cell phenotype 3 days post hepatectomy (Figure 5-11 B) and a

robust oval cell response onset is observed only in the end of the first week (Figure 5-12 B). In contrast, the group exposed only to 2AAF/PHx exhibits a robust onset of regeneration starting with day 3 post acute injury (Figure 5-11A). This disparity between the responses at corresponding time points is persistent during the whole course of hepatic regeneration in our model. The hepatic mass would eventually be restored, but not exclusively by oval cell contribution. Once the oval cell differentiation is complete and the 2AAF release is over, the resulting hepatocytes would take over and start divide. However, it would take considerably more time for the liver mass to be restored. A combined oval and stellate cell therapy might accelerate the regeneration and overcome the time constraints imposed by the onset of fatal MODS.

Another interesting feature of the L-cysteine treated livers is the apparent accumulation of small hepatocyte-like cells, also known as transitional hepatocytes (Figure 5-12 D). These cells are morphologically similar to hepatocytes, but are much smaller and weakly express AFP. They have been observed in retrorsine hepatic injury models and are considered by some authors an intermediary stage in normal differentiatiation towards hepatocyte, whilst others see them as an independent progenitor cell[126]. In our model, we speculate that in the absence of an adequate stellate support, oval cells might take two pathways. If the differentiaton cues are missing, they might fail to complete the differentiation program and the intermediary hepatocytes we have seen are a developmental arrested phenotype. Conversely, if during regeneration the coupling between cytokine mediated priming phase and growth factor promoted proliferation fails, oval cells might start differentiation towards hepatocytes earlier than expected and the small hepatocyte-like cells are just a normal

differentiating phenotype. This would suggest that inhibition of stellate cell activation following 2AAF/PHx not only affects oval cell proliferation, but also oval cell differentiation. Once again, this would most likely result from the lack of an appropriate microenvironment within the regenerating zone.

One recently published study demonstrates that stellate cells within the liver may, through a process of mesenchymal to epithelial transition, give rise to hepatocytes[89]. It is possible that this phenomenon involves an intermediate cell type with oval cell properties. It is impossible though, to determine if decreased mesenchymal to epithelial transition contributes to the reduction in oval cell proliferation seen in our model. However, this possibility deserves mention.

Two distinct cellular markers, AFP and OV6, were used to identify the oval cell population in our study. Quantitative image analyses and real time PCR analysis showed a disparity in oval cell presence at corresponding time points between the two animal groups. Overall, the blunted oval cell response in animals fed the L-cysteine diet is likely due to a combination of the loss of a major cytokine and growth factor source (i.e. activated stellate cells), coupled with the loss of an appropriate microenvironment for expansion of the oval cell population (i.e. the fibronectin rich provisional matrix). The end result of L-cysteine treatment is a delayed restoration of liver mass following the 2AAF/PHx protocol. Because the injury does eventually resolve in the L-cysteine treated group, redundant pathways for the regulation of oval cell phenotype likely exist. However, the significant reduction in oval cells seen at what would normally be considered the time of maximal oval cell proliferation proves, for the first time, the critical role of stellate cells in oval cell mediated liver regeneration.

6.2 Clinical Applications

Terminal cirrhosis is a medical challenge in the sense that to this date it has no effective cure and irreversibly progresses to decompensated liver failure. A fairly significant number of hepatic conditions progress toward cirrhosis. Despite their various pathophysiological mechanisms – ranging from autoimmune disorders like primary billiary cirrhosis to genetic mutations (seen in Wilson disease or hemochromatosis) and chronic hepatitis C infection – they are all accompanied by persistent activation of stellate cells which results in cirrhosis.

In an ideal outcome, the oval cell hepatic regeneration which takes place in the cirrhotic nodules would restore the liver mass and the fibrosis would decrease to a point where the neovascularization would reestablish functional connections with the indemn hepatocytes inside the nodules. The common denominator for these ideal outcome is the hepatic stellate cell which is able to influence the amplitude of regeneration and synthesize the fibrotic tracts in cirrhotic liver. The more we know about stellate cell's involvement and interactions with the other resident cell populations, the more chances of developing a strategy for dissociating these two functions and inhibiting the fibrogenic outcome.

Due to their remarkable capacity of proliferation, pluripotency and engraftment in various tissues, stem cells have shown great promise as a potential candidate for cell therapy. Ideally, stem cells isolated from an individual would be expanded *in vitro,* primed towards a certain differentiation path and reinjected into the desired organ. It is known that hepatocyte transplantation is followed only by transient engraftment, thus limiting its potential of being used in cell therapy. Researchers and clinicians turned to exploring the oval cells' potential of being used as an alternative cell therapy. Since at

least one subpopulation of oval cells is bone marrow derived, there is a chance of isolating them from blood.

In various experimental models oval cells have been implanted into mammalian liver and subsequent presence of donor derived tissue has been demonstrated. Over the years the engraftment potential of oval cell has been thoroughly documented. Unfortunately, very few hepatocytes derived from donor oval cells have been identified in the recipient liver. Increasing the numbers of donor derived cells might be achieved by priming the local environment to become more conducive for oval cell proliferation, migration and differentiation. Perhaps chemically induced, a transient activation of stellate cells might be the boost that injected oval cells need to proliferate in higher numbers. Or, injecting oval and stellate cells concomitantly would result in a better outcome in terms of graft size.

Using cell therapy as an alternative for transplantation in patients with cirrhosis requires a very thorough characterization of the interactions between the oval and stellate cells. The hyperactivated stellate cells, already existing in the cirrhotic liver at the moment of progenitor cell injection might induce a hyperproliferation of progenitors, or conversely, might keep them in a nondifferentiated state. The prior administration of L-cysteine, can inhibit stellate cell proliferation and reduce the fibrotic tracts to an extent which might allow the vessel formation and migration of oval cells into the adjacent areas of hepatic lobules.

6.3 Future Directions of Study

This present research opens the door for two main directions of study which would shed more light on the complex interactions between the hepatic stellate cells and oval cells in the liver. One direction might be the characterization of the hepatic extracellular

matrix in terms of the delicate balance between MMPs and TIMPs during the L-cysteine inhibition of stellate cells. It is reasonable to assume that certain variations in MMPs expression would result in matrix degradation which would favor deposition of new fibers produced by stellate cells. ECM profile is very important at each step of oval cell migration from the periportal space towards the pericentral zone, ensuring the adequate supply with regenerative cells at the site of injury.

Also, MMP mediated cleavage liberates and activates growth factors necessary for oval cell proliferation and differentiation. During liver regeneration, after the priming step, the recovery is not possible without an adequate supply of growth factors produced by existing hepatocytes, Kupffer cells and hepatic stellate cells. Some of these necessary growth factors are produced in an inactive form and are bound to the ECM. Without the MMP degradation, they would never be available for the matricrine regulation of liver regeneration.

An alternative avenue would be represented by the characterization of cytokine production of stellate cells when their activation is inhibited by L-cysteine. It is possible that the delayed regenerative response is at least in part the consequence of a reduced cytokine and growth factor stimulation by the stellate cells. Corroborated with the study of ECM profile under L-cysteine exposure this new research avenue would shed light on the significant contributors to oval cell proliferation, migration and differentiation.

An unexpected finding in our study was the presence of small hepatocyte-like cells at time points during regeneration when they are usually absent in the 2AAF/PHx model. Whether they are the result of an accelerated differentiation of the oval cells, a differentiation arrested cell, or are an alternative progenitor recruited when the oval cell

response is weak it is still to be found. Exploring this new regenerative cell player in the context of stellate cell inhibition represents a new direction for future research.

CHAPTER 7
SUMMARY AND CONCLUSIONS

The aim of this study was to gain a better insight into the cellular interactions between the stellate cells and the oval cells in the liver regeneration process by chemically blocking the Ito cell activation. In summary, our results suggest that L-cysteine, the non-essential amino acid used for this purpose, is an effective inhibitor of hepatic stellate cells in our model of liver regeneration.

The blunted oval cell response in animals fed the L-cysteine diet results in a significant delay of the regeneration process following 2AAF/PHx. The significant reduction in oval cells seen at corresponding time points throughout the oval cell mediated regeneration proves the critical role of stellate cells in oval cell mediated liver regeneration. We believe that by influencing the proliferation rate of oval cells and, as other studies have shown[38], changing the ECM profile in the regenerating liver, the stellate cells do play a necessary role in facilitating oval cell proliferation in the liver. Our data also indicate that when the stellate cells are not able to contribute effectively to the oval cell mediated regeneration, the liver mass recovery takes place at a considerably lower pace. Compared to the 2AAF/PHx regeneration model, the regeneration at identical time points post acute injury is reduced and the whole process is delayed.

The presence of small hepatocyte-like cells is a novel finding. It indicates the existence of redundant pathways which are activated in the injured liver when the oval cell mediated regeneration is blunted. The transitional small hepatocyte-like cells might also be the result of premature or arrested differentiation of oval cells in the absence of an adequate support from the inhibited stellate cells.

Chemical inhibition of stellate cell activation resulted in an abnormal profile of the regenerative process, delayed and blunted, involving phenotypic changes of regenerating cells. Considering all our findings, this study concludes that the activation of hepatic stellate cells is required for an appropriate oval cell response to 2AAF/PHx hepatic injury.

LIST OF REFERENCES

1. Desmet VJ. The liver: biology and pathobiology. Arias IM and Boyer JL (eds.), pp. 3-15, Raven Press, New York (2001).

2. Kierszembaum AL. Histology and cell biology: an introduction to pathology. Chapter 17 Digestive glands. Mosby, Inc, 2002; 457-474.

3. Crawford JM. Robbins and Cotran: Pathologic Basis of Disease. Kumar,V., Abbas,A. & Fausto N. (eds.), pp. 877-938, Elsevier Saunders, Philadelphia (2005).

4. Floch MH, Floch NR, Kowdley KV. Netter's Gastroenterology. Chapter: Vessel and duct distributions and liver segments. W B Saunders Book Company, 2004; 674.

5. Kogure K, Ishizaki M, Nemoto M, Kuwano H, Makuuchi M. A comparative study of the anatomy of rat and human livers. J Hepatobiliary Pancreat Surg 1999; 6:171-175.

6. Fausto N. The Liver biology and pathobiology. Arias,I.M. & Boyer,J.L. (eds.), pp. 1501-1518, Raven Press, New York (1994).

7. Fausto N, Campbell JS. The role of hepatocytes and oval cells in liver regeneration and repopulation. Mech Dev. 2003; 120(1):117-30.

8. Overturf K, al-Dhalimy M, Ou CN, Finegold M, Grompe M. Serial transplantation reveals the stem cell-like potential of adult mouse hepatocytes. Am J Pathol. 1997; 151(5):1273-80.

9. Tateno C, Yoshizato K. Growth potential and differentiation capacity of adult rat hepatocytes in vitro. Wound Repair and Regeneration 1999; 7(1):36-44.

10. Lynch T, Price A. The effect of cytochrome P450 on drug response, interactions and adverse effects. American family physician 2007; 76 (3): 391-6.

11. Sleyster EC and Knook DL. Relation between localization and function of rat liver Kupffer cells. Laboratory investigation 1982; 47:4Laboratory investigation 1982. 47: 484-490.

12. Wisse E, Braet F, Luo D, De Zanger R, Jans D, Crabbe E, Vermoesen A. Structure and function of sinusoidal lining cells in the liver. Toxicology and Pathology 1996; 24: 100-111.

13. Knolle PA and Gerken G. Local control of the immune response in the liver. Immunological Reviews 2000; 174: 21-34.

14. Decker K. The response of liver macrophages to inflammatory stimulation. Keio Journal of Medicine 1998; 47:1-9.

15. Roth S, Gong W, Gressner AM. Expression of different isoforms of TGF-beta and the latent TGFbeta binding protein (LTBP) by rat Kupffer cells. Journal of Hepatology 1998; 29(6): 915-922.

16. Iredale JP, Benyon RC, Arthur MJ, Ferris WF, Alcolado R, Winwood PJ, Clark N, Murphy G. Tissue inhibitor of metalloproteinase-1 messenger RNA expression is enhanced relative to interstitial collagenase messenger RNA in experimental liver injury and fibrosis. Hepatology 1996; 24(1): 176-184.

17. Knittel T, Mehde M, Kobold D, Saile B, Dinter C, Ramadori G. Knittel T, Mehde M, Kobold D, Saile B, Dinter C, Ramadori G. Expression patterns of matrix metalloproteinases and their inhibitors in parenchymal and non-parenchymal cells of rat liver: regulation by TNF-alpha and TGF-beta1. Journal of Hepatology 1999; 30(1): 48-60.

18. Paku S, Schnur J, Nagy P, Thorgeirsson SS. Origin and structural evolution of the early proliferating oval cells in rat liver. Am J Pathol 2001; 158:313-323.

19. Rockey DC. Hepatic blood flow regulation by stellate cells in normal and injured liver. Seminars in Liver Disease 2001; 21(3): 337-349.

20. Sato M, Suzuki S, Senoo H. Hepatic stellate cell. Unique characteristics in cell biology and phenotype. Cell Structure and Function 2003; 28:105-112.

21. Jezequel AM, Novelli G, Venturini C. Quantitative analysis of the perisinusoidal cells in human liver; the lipocytes. Front Gastrointest Res. 1984; 8:85-90.

22. Friedman SL, Wei S, and Blaner WS. Retinol release by activated rat hepatic lipocytes: regulation by Kupffer cell-conditioned medium and PDGF. Am. J. Physiol. 1993; 264:G947-G952.

23. Niki T, De Bleser PJ, Xu G., Van den B.K., Wisse E. and Geerts A. Comparison of glial fibrillary acidic protein and desmin staining in normal and CCl4-induced fibrotic rat livers. Hepatology 1996; 23: 23(6):1538-45.

24. Niki T., Pekny M., Hellemans K., Bleser PD, Berg KV, Vaeyens F, Quartier E, Schuit F and Geerts A. Class VI intermediate filament protein nestin is induced during activation of rat hepatic stellate cells. Hepatology 1999; 2:520-527, 1538-1545.

25. Cassiman D, Barlow A, Vander Borght S, Libbrecht L, Pachnis V. Hepatic stellate cells do not derive from the neural crest. Journal of Hepatology 2006; 44: 1098-1104.

26. Liu XJ, Yang L, Luo FM, Wu HB, Qiang Q. Association of differentially expressed genes with activation of mouse hepatic stellate cells by high-density cDNA microarray. World J Gastroenterol. 2004; 10(11):1600-1607.

27. Hata J, Ikeda I, Uno H, Asano S. Expression of hepatocyte growth factor mRNA in rat liver cirrhosis induced by N-nitrosodimethylamine as evidenced by in situ RT-PCR. Journal of Histochemistry Cytochemistry 2002; 50(11): 1461-1468.

28. Ozaki I, Zhao G, Mizuta T, Ogawa Y, Hara T, Kajihara Z, Hisatomi A, Sakai T, Yamamoto K. Hepatocyte growth factor induces collagenase (matrix metalloproteinase-1) via the transcription factor Ets-1 in human hepatic stellate cell line. Journal of Hepatology 2002; 36(2): 169-178.

29. Fujito K, Evarts RP, Hu Z, Marsden ER, Thorgeirsson SS.Expression of stem cell factor and its receptor, c-kit, during liver regeneration from putative stem cells in adult rat. Laboratory Investigation 1994; 70(4): 511-516.

30. Win KM, Charlotte F, Mallat A, Cherqui D, Martin N, Mavier P, Preaux AM, Dhumeaux D, Rosenbaum J. Mitogenic effect of transforming growth factor-beta 1 on human Ito cells in culture: evidence for mediation by endogenous platelet-derived growth factor. Hepatology 1993; 18(1): 137-145.

31. Mangasser-Stephan K, Gartung C, Lahme B, Gressner AM. Expression of isoforms and splice variants of the latent transforming growth factor beta binding protein (LTBP) in cultured human liver myofibroblasts. Liver 2001; 21(2): 105-113.

32. Friedman SL, Roll FJ, Boyles J, Bissell DM. Hepatic lipocytes: the principal collagen-producing cells of normal rat liver. Proceedings of the National Academy of Sciences (USA) 1985; 82(24):8681-8685.

33. Schäfer S, Zerbe O, Gressner AM. The synthesis of proteoglycans in fat-storing cells of rat liver. Hepatology 1987; 7(4): 680-687.

34. Knittel T, Janneck T, Müller L, Fellmer P, Ramadori G. Transforming growth factor beta 1-regulated gene expression of Ito cells. Hepatology 1996; 24(2): 352-360.

35. Han YP, Zhou L, Wang J, Xiong S, Garner WL, French SW, Tsukamoto H. Essential role of matrix metalloproteinases in interleukin-1-induced myofibroblastic activation of hepatic stellate cell in collagen. Journal of Biological Chemistry 2004; 279(6): 4820-4828.

36. Wang DR, Sato M, Li LN, Miura M, Kojima N, Senoo H. Stimulation of Pro-MMP-2 Production and Activation by Native Form of Extracellular Type I Collagen in Cultured hepatic stellate cells. Cell Structure and Function 2003; 28(6): 505-513.

37. Kim T-H, Mars WM, Stolz, DB, Petersen BE, Michalopoulos GK. Extracellular matrix remodeling at the early stages of liver regeneration in the rat. Hepatology 1997; 26(4):896-904.

38. Pi L, Ding X, Jorgensen M, Pan JJ, Oh SH, Pintilie D, Brown A, Song WY, Petersen BE. Connective tissue growth factor with a novel fibronectin binding site promotes cell adhesion and migration during rat oval cell activation. Hepatology. 2008; 47(3):996-1004.

39. Ross MH, Kaye GI. & Pawlina W. Histology: a text and atlas. Lippincott Williams & Wilkins, Philadelphia, Pa (2003).

40. Columbano A and Shinozuka H. Liver regeneration versus direct hyperplasia. The FASEB Journal 1996; 10(10):1118-1128.

41. Fausto N, Campbell JS, Riehle KJ. Liver regeneration. Hepatology. 2006. 43(2 Suppl 1): S45-53.

42. Steer CJ. Liver regeneration. FASEB J 1995; 9:1396-1400.

43. Higgins GM and Anderson RM. Experimental pathology of the liver: Restoration of the liver of the white rat following partial surgical removal. Arch Pathol 1931; 12, 186-202.

44. Bucher NLR. Regeneration of Mammalian Liver. Int Rev Cytol 1963; 15:245.

45. Michalopoulos GK. Liver regeneration: molecular mechanisms of growth control. FASEB J. 4, 1990; 176-187.

46. Rabes HM. Kinetics of hepatocellular proliferation after partial resection of the liver. Prog. Liver Dis 1976; 5:83-99.

47. Badr MZ, Belinsky SA, Kauffman FC and Thurman RG. Mechanism of hepatotoxicity to periportal regions of the liver lobule due to allyl alcohol: role of oxygen and lipid peroxidation. J. Pharmacol. Exp. Ther. 1986; 238:1138-1142.

48. Edwards MJ, Keller BJ, Kauffman FC and Thurman RG. The involvement of Kupffer cells in carbon tetrachloride toxicity. Toxicol. Appl. Pharmacol. 1993; 119: 275-279.

49. Lombardi B and Ugazio G. Serum lipoproteins in rats with carbon tetrachloride-induced fatty liver. J. Lipid Res. 1965; 6:498-505.

50. Reid WD. Mechanism of allyl alcohol-induced hepatic necrosis. Experientia 1972; 28:1058-1061.

51. Maximow A. Der Lymphozyt als gemeinsame Stammzelle der verschiedenen Blutelemente in der embryonalen Entwicklung und im postfetalen Leben der Säugetiere. Folia Haematol. Int. Mag. Klin. Morphol. Blutforsch. 1909; 8:125-141.

52. Konstantinov IE. In search of Alexander A. Maximov: The man behind the unitarian theory of hematopoiesis. Perspectives in Biology and Medicine. 2000; 43(2): 269-276.

53. Till JE, McCulloch EA. A direct measurement of the radiation sensitivity of normal mouse bone marrow cells. Radiation Research 1961; 14:213-222.

54. McCulloch EA., Till JE. The radiation sensitivity of normal mouse bone marrow cells, determined by quantitative marrow transplantation into irradiated mice. Radiation Research 1960; 13(1):115-125.

55. Buckner CD, Epstein RB, Rudolph RH, Clift RA, Storb R, Thomas ED. Allogeneic marrow engraftment following whole body irradiation in a patient with leukemia. Blood 1970; 35:741-750.

56. Osawa M, Hanada K, Hamada H and Nakauchi H. Long-term lympho-hematopoietic reconstitution by a single CD34-low/negative hematopoietic stem cell. Science 1996; 273: 242-245.

57. Magnuson,T., Epstein,C.J., Silver,L.M. & Martin,G.R. Pluripotent embryonic stem cell lines can be derived from tw5/tw5 blastocysts. Nature 1982; 298:750-753.

58. Evans MJ and Kaufman MH. Establishment in culture of pluripotential cells from mouse embryos. Nature 1981; 292:154-156.

59. Keller GM. In vitro differentiation of embryonic stem cells. Curr. Opin. Cell Biol.1995; 7:862-869.

60. Martin GR. Isolation of a pluripotent cell line from early mouse embryos cultured in medium conditioned by teratocarcinoma stem cells. Proc. Natl. Acad. Sci. USA. 1981; 7634-7638.

61. Smith AG. Embryo-derived stem cells: of mice and men. Annu. Rev. Cell Dev. Biol. 2001; 17:435-462.

62. Kabrun N, Bühring HJ, Choi K, Ullrich A, Risau W, Keller G. Flk-1 expression defines a population of early embryonic hematopoietic precursors. Development 1997; 124: 2039-2048.

63. Nishikawa S.I, Nishikawa S, Hirashima M, Matsuyoshi N and Kodama H. Progressive lineage analysis by cell sorting and culture identifies FLK1+VE-cadherin+ cells at a diverging point of endothelial and hemopoietic lineages. Development 1998; 125:1747-1757.

64. Robertson SM, Kennedy M, Shannon JM and Keller G. A transitional stage in the commitment of mesoderm to hematopoiesis requiring the transcription factor SCL/tal-1. Development 2000; 127:2447-2459.

65. Schmitt RM, Bruyns E and Snodgrass HR. Hematopoietic development of embryonic stem cells in vitro: cytokine and receptor gene expression. Genes Dev. 1991; 5:728-740.

66. Faloon P, Arentson E, Kazarov A, Deng CX, Porcher C, Orkin S, Choi K. Basic fibroblast growth factor positively regulates hematopoietic development. Development 2000; 127:1931-1941.

67. Huber TL., Kouskoff V, Fehling HJ, Palis J and Keller G. Haemangioblast commitment is initiated in the primitive streak of the mouse embryo. Nature 2004; 432:625-630.

68. Bautch VL, Redick SD, Scalia A, Harmaty M, Carmeliet P, Rapoport R. Characterization of the vasculogenic block in the absence of vascular endothelial growth factor-A. Blood 2000; 95:1979-1987.

69. Kearney JB, Ambler CA, Monaco KA, Johnson N, Rapoport RG, Bautch VL. Vascular endothelial growth factor receptor Flt-1 negatively regulates developmental blood vessel formation by modulating endothelial cell division. Blood 2002; 99:2397-2407.

70. Roberts DM, Kearney JB, Johnson JH, Rosenberg MP, Kumar R, Bautch VL. The vascular endothelial growth factor (VEGF) receptor Flt-1(VEGFR-1) modulates Flk-1 (VEGFR-2) signaling during blood vessel formation. Am. J. Pathol. 2004; 164: 1531-1535.

71. Zippo A, De Robertis A, Bardelli M, Galvagni F, Oliviero S. Identification of Flk-1 target genes in vasculogenesis: Pim-1 is required for endothelial and mural cell differentiation in vitro. Blood. 2004; 103:4536-4544.

72. Asahara,T. Murohara T, Sullivan A, Silver M, van der Zee R, Li T, Witzenbichler B, Schatteman G, Isner JM. Isolation of putative progenitor endothelial cells for angiogenesis. Science 1997; 275:964-967.

73. Ferrari,G. Cusella-De Angelis G, Coletta M, Paolucci E, Stornaiuolo A, Cossu G, Mavilio F. Muscle regeneration by bone marrow-derived myogenic progenitors. Science 1998; 279:1528-1530.

74. Petersen BE, Bowen WC, Patrene KD, Mars WM, Sullivan AK, Murase N, Boggs SS, Greenberger JS, Goff JP. Bone marrow as a potential source of hepatic oval cells. Science 1999; 284:1168-1170.

75. Bjornson CR, Rietze RL, Reynolds BA, Magli MC and Vescovi AL. Turning brain into blood: a hematopoietic fate adopted by adult neural stem cells in vivo. Science 1999; 283:534-537.

76. Theise ND, Nimmakayalu M, Gardner R, Illei PB, Morgan G, Teperman L, Henegariu O, Krause DS. Liver from bone marrow in humans. Hepatology 2000; 32:11-16.

77. Alison MR, Poulsom R, Jeffery R, Dhillon AP, Quaglia A, Jacob J, Novelli M, Prentice G, Williamson J, Wright NA. Hepatocytes from non-hepatic adult stem cells. Nature. 2000; 406(6793):257.

78. Krause DS, Theise ND, Collector MI, Henegariu O, Hwang S, Gardner R, Neutzel S, Sharkis SJ. Multi-organ, multi-lineage engraftment by a single bone marrow-derived stem cell. Cell 2001; 105:369-377.

79. Herzog EL, Chai L and Krause DS. Plasticity of marrow-derived stem cells. Blood 2003; 102:3483-3493.

80. Ianus A., Holz GG, Theise ND, Hussain MA. In vivo derivation of glucose-competent pancreatic endocrine cells from bone marrow without evidence of cell fusion. J. Clin. Invest 2003; 111:843-850.

81. Jiang Y, Jahagirdar BN, Reinhardt RL, Schwartz RE, Keene CD, Ortiz-Gonzalez XR, Reyes M, Lenvik T, Lund T, Blackstad M, Du J, Aldrich S, Lisberg A, Low WC, Largaespada DA, Verfaillie CM. Pluripotency of mesenchymal stem cells derived from adult marrow. Nature 2002; 418:41-49.

82. Horwitz EM. Stem cell plasticity: a new image of the bone marrow stem cell. Curr. Opin. Pediatr. 2003; 15:32-37.

83. Petersen BE. Hepatic "stem" cells: coming full circle. Blood Cells Mol. Dis. 2001; 27:590-600.

84. Petersen BE, Terada N. Stem cells: a journey into a new frontier. J. Am. Soc. Nephrol. 2001; 12:1773-1780.

85. Farber E. Similarities in the sequence of early histological changes induced in the liver of the rat by ethionine, 2-acetylaminofluorene, and 3'-methyl-4-dimethylaminozbenzene. Cancer Res 1956; 16:142-151.

86. Weiss MC, Strick-Marchand H. Isolation and characterization of mouse hepatic stem cells in vitro. Seminars in Liver Diseases 2003; 23(4): 313-324.

87. Gualdi R, Bossard P, Zheng M, Hamada Y, Coleman JR, Zaret KSHepatic specification of the gut endoderm in vitro: cell signaling and transcriptional control. Genes and Development 1996; 10:1670-1682.

88. Lagasse E, Connors H, Al-Dhalimy M, Reitsma M, Dohse M, Osborne L, Wang X, Finegold M, Weissman IL, Grompe M. Purified hematopoietic stem cells can differentiate into hepatocytes in vivo. Nature Medicine 2000; 6: 1229-1234.

89. Yang L, Jung Y, Omenetti A, Witek RP, Choi S, Vandongen HM, Huang J, Alpini GD, Diehl AM. Fate-mapping evidence that hepatic stellate cells are epithelial progenitors in adult mouse livers. 2008; 26(8):2104-13.

90. Roskams T, De Vos R, Van Eyken P, Myazaki H, Van Damme B, Desmet V. Hepatic OV-6 expression in human liver disease and rat experiments: evidence for hepatic progenitor cells in man. J Hepatol 1998; 29: 455-463.

91. Sobaniec-Lotowska ME, Lotowska JM, Lebensztejn DM. Ultrastructure of oval cells in children with chronic hepatitis B, with special emphasis on the stage of liver fibrosis: the first pediatric study. World J Gastroenterol. 2007; 13(21):2918-2922.

92. He ZP, Tan WO, Tang YF, Feng MF. Differentiation of putative hepatic stem cells derived from adult rats into mature hepatocytes in the presence of epidermal growth factor and hepatocyte growth factor. Differentiation 2003; 71(4-5): 281-290.

93. Preisegger KH, Factor VM, Fuchsbichler A, Stumptner C, Denk H, Thorgeirsson SS. Atypical ductular proliferation and its inhibition by transforming growth factor beta1 in the 3,5-diethoxycarbonyl-1,4-dihydrocollidine mouse model for chronic alcoholic liver disease. Lab Invest 1999; 79:103-109.

94. Golding M, Sarraf C, Lalani E, Alison MR. Reactive biliary epithelium: The product of a pluripotential stem cell compartment? Human Pathology 1996; 27:872-884.

95. Solt DB and Farber E. New principle for the analysis of chemical carcino-genesis. Nature. 1976; 263:702-703.

96. Evarts RP, Nagy P, Marsden E, Thorgeirsson SS. A precursor-product relationship exists between oval cells and hepatocytes in rat liver. Carcinogenesis. 1987; 8:1737-1740.

97. Evarts RP, Nagy P, Nakatsukasa H, Marsden E, Thorgeirsson SS. *In vivo* differentiation of rat liver oval cells into hepatocytes. Cancer Res. 1989; 49:1541-1547.

98. Fausto N. Protooncogenes and growth factors associated with normal and abnormal liver growth. Dig. Dis. Sci. 1991; 36:653-658.

99. Kinosita R. Studies on the cancerogenic chemical substances. Transactions of the Japanese Pathological Society 1937; 665-727.

100. Leduc, EH, Wilson,J.W. Injury to liver cells in carbon tetrachloride poisoning; histochemical changes induced by carbon tetrachloride in mouse liver protected by sulfaguanidine. AMA. Arch. Pathol. 1958; 65: 147-157.

101. Lemire JM, Shiojiri N, Fausto N. Oval cell proliferation and the origin of small hepatocytes in liver injury induced by D-galactosamine. Am. J. Pathol. 1991; 139: 535-552.

102. Price JM, Harman JW, Miller EC, Miller JA. Progressive microscopic alterations in the livers of rats fed the hepatic carcinogens 3'-methyl-4-dimethylaminoazobenzene and 4'-fluoro-4-dimethylaminoazobenzene. Cancer Res. 1952; 12: 192-200.

103. Wilson JW and Leduc EH. Role of cholangioles in restoration of the liver of the mouse after dietary injury. J. Pathol. Bacteriol. 1958; 76: 441-449.

104. Williams JM. The role of the Wnt family of secreted proteins in oval “stem” cell based liver regeneration. 2007. College of Medicine, Department of Pathology, Immunology and Laboratory Medicine, University of Florida. Thesis/Dissertation.

105. Lowes KN, Croager EJ, Olynyk JK, Abraham LJ, Yeoh GC. Oval cell mediated liver regeneration: Role of cytokines and growth factors. J Gastroenterol Hepatol. 2003; 18(1):4-12.

106. Deng J, Steindler DA, Laywell ED, Petersen BE. Neural trans-differentiation potential of hepatic oval cells in the neonatal mouse brain. Exp. Neurol. 2003; 182: 373-382.

107. Petersen BE, Goff JP, Greenberger JS and Michalopoulos GK. Hepatic oval cells express the hematopoietic stem cell marker Thy-1 in the rat. Hepatology 1998; 27:433-445.

108. Petersen BE, Grossbard B, Hatch H, Pi L, Deng J, Scott EW.. Mouse A6-positive hepatic oval cells also express several hematopoietic stem cell markers. Hepatology 2003; 37:632-640.

109. Farber E. Hepatocyte proliferation in stepwise development of experimental liver cell cancer. Dig. Dis. Sci. 1991; 36:973-978.

110. Sell S and Pierce GB. Maturation arrest of stem cell differentiation is a common pathway for the cellular origin of teratocarcinomas and epithelial cancers. Lab Invest 1994; 70: 6-22.

111. Hixson DC and Allison JP. Monoclonal antibodies recognizing oval cells induced in the liver of rats by N-2-fluorenylacetamide or ethionine in a choline-deficient diet. Cancer Res. 1985; 45: 3750-3760.

112. Dunsford HA, Karnasuta C, Hunt JM, Sell S. Different lineages of chemically induced hepatocellular carcinoma in rats defined by monoclonal antibodies. Cancer Res. 1989; 49:4894-4900.

113. Dunsford HA and Sell S. Production of monoclonal antibodies to preneoplastic liver cell populations induced by chemical carcinogens in rats and to transplantable Morris hepatomas. Cancer Res. 1989; 49:4887-4893.

114. Hsia CC, Evarts RP, Nakatsukasa H, Marsden ER, Thorgeirsson SS. Occurrence of oval-type cells in hepatitis B virus-associated human hepatocarcinogenesis. Hepatology. 1992; 16(6):1327-33.

115. Vandersteenhoven AM, Burchette J, Michalopoulos G. Characterization of ductular hepatocytes in end-stage cirrhosis. Arch Pathol Lab Med. 1990; 114:403-406.

116. Fausto N. The Liver biology and pathobiology. Arias IM, Boyer JL (eds.). Raven Press. 1994; 1501-1518.

117. Garfield S, Huber BE, Nagy P, Cordingley MG and Thorgeirsson SS. Neoplastic transformation and lineage switching of rat liver epithelial cells by retrovirus-associated oncogenes. Mol. Carcinog. 1988; 1:189-195.

118. Marceau N. Cell lineages and differentiation programs in epidermal, urothelial and hepatic tissues and their neoplasms. Lab Invest 1990; 63:4-20.

119. Gordon MD and Nusse R. Wnt signaling: multiple pathways, multiple receptors, and multiple transcription factors. J. Biol. Chem. 2006; 281:22429-22433.

120. Farber E. Similarities in the sequence of early histologic changes induced in the liver of the rat by ethionine, 2-acetylaminoflouorene, and 3'-methyl-4-dimethylaminoazbenzene. Cancer Res. 1956; 16: 142.

121. Yin L, Lynch D, Sell S. Participation of different cell types in the restitutive response of the rat liver to periportal injury induced by allyl alcohol. J Hepatol 1999; 31:497–507.

122. Pi L, Oh SH, Shupe T, Petersen BE. Role of connective tissue growth factor in oval cell response during liver regeneration after 2-AAF/PHx in rats. Gastroenterology 2005; 128(7):2077-88.

123. Miyamoto S, Nakamura M, Yano K, Ishii G, Hasebe T, Endoh Y, Sangai T, Maeda H, Shi-chuang Z, Chiba T, Ochiai A. Matrix metalloproteinase-7 triggers the matricrine action of insulin-like growth factor-II via proteinase activity on insulin-like growth factor binding protein 2 in the extracellular matrix. Cancer Sci 2007; 98(5): 685-691.

124. Horie T, Sakaida I, Yokoya F, Nakajo M, Sonaka I, Okita K. L-cysteine administration prevents liver fibrosis by suppressing hepatic stellate cell proliferation and activation. Biochem Biophys Res Commun. 2003; 305(1):94-100.

125. Trautwein C, Will M, Kubicka S, Rakemann T, Flemming P, Manns MP. 2-Acetaminofluorene blocks cell cycle progression after hepatectomy by p21 induction and lack of cyclin E expression. Oncogene 1999;18:6443–53.

126. Best DH, Coleman WB. Bile duct destruction by 4,4'-diaminodiphenylmethane does not block the small hepatocyte-like progenitor cell response in retrorsine-exposed rats. Hepatology. 2007; 46(5):1611-9.

127. Lowes KN, Brennan BA, Yeoh GC, Olynyk JK. Oval cell numbers in human chronic liver diseases are directly related to disease severity. Am J Pathol. 1999; 154(2):537-41.

128. Evarts RP, Nakatsukasa H., Marsden ER, Hu Z., and Thorgeirsson SS. Expression of transforming growth factor-a in regenerating liver and during hepatic differentiation. Mol. Carcinog. 1992; 5: 25-31.

129. Miller EC, Miller JA, Hartmann HA. N-Hydroxy-2-acetylaminofluorene: a metabolite of 2-acetylaminofluorene with increased carcinogenic activity in the rat. Cancer Res. 1961; 21, 815-24.

130. Weisburger JH, Weisburger EK. Biochemical formation and pharmacological, toxicological, and pathological properties of hydroxylamines and hydroxamic acids. Pharmacol Rev. 1973; 25(1):1-66. Review.

131. Lotlikar PD, Hong YS. Microsomal N- and C-oxidations of carcinogenic aromatic amines and amides. Natl Cancer Inst Monogr. 1981; (58):101-7.

132. Ellerbroek, SM, Wu YI, Stack MS. Type I collagen stabilization of matrix metalloproteinase-2. Arch. Biochem. Biophys. 2001; 390, 51–56.

133. Freise C, Erben U, Muche M, Farndale R, Zeitz M, Somasundaram R, Ruehl M. The alpha 2 chain of collagen type VI sequesters latent proforms of matrix-metalloproteinases and modulates their activation and activity. Matrix Biol., print copy in press 2009 Aug. Available from URL: www.sciencedirect.com/science?_ob=ArticleURL&_udi=B6VPM-4X1SB84-2&_user=2139813&_rdoc=1&_fmt=&_orig=search&_sort=d&_docanchor=&view=c&_acct=C000054276&_version=1&_urlVersion=0&_userid=2139813&md5=f0621d8c889048dbf732074d8db11c6b

134. Bettzieche A, Brandsch C, Hirche F, Eder K, Stangl GI. L-cysteine down-regulates SREBP-1c-regulated lipogenic enzymes expression via glutathione in HepG2 cells. Ann Nutr Metab. 2008; 52(3):196-203.

135. Meerman JH, Tijdens RB. Effect of glutathione depletion on the hepatotoxicity and covalent binding rat liver macromolecules of N-hydroxy-2-acetylaminofluorene. Cancer Res. 1985; 45(3):1132-9.

BIOGRAPHICAL SKETCH

Dana Gabriela Pintilie was born in Suceava, Romania. She attended “George Bacovia’ High School, graduating the Mathematics and Physics program in 1986.

She obtained a medical doctor degree from the University of Medicine and Pharmacy “Gr. T. Popa” Iasi in 1992. Deciding to further her education, she enrolled in the graduate program at the same university and, under the mentorship of Dr. Mircea Chiriac she obtained a PhD in anatomy in 2003, with the thesis “A telomic and systemic interpretation of the celial trunk”.

Searching for an opportunity to learn new molecular techniques and better prepare for the complex approach modern research requires, Dana decided to come to the United States and enroll in the Interdisciplinary Program in Biomedical Sciences at the University of Florida, beginning the fall of 2005.

After four years and a half of diligent work under the mentorship of Dr. Bryon Petersen, Dana will receive her doctorate in molecular cell biology at the University of Florida College of Medicine. Her project consisted in elucidating the effects of stellate cell inhibition on oval cell proliferation.

Her scholastic accomplishments include being an Alumni fellow at the University of Florida during her Ph.D. studies. She received the Outstanding International Student Award 2009 from the University of Florida College of Medicine.